Elucidation of Functions of the AKAP GSKIP

DISSERTATION

Inaugural-Dissertation

to obtain the academic degree

Doctor rerum naturalium (Dr. rer. Nat.)

Submitted to the department of Biology, Chemistry and
Pharmacy of Freie Universität Berlin

by

Mohamed Mostafa Hassan Elkewedi

from Alexandria, Egypt

Berlin 2018

This work was conducted from August 2014 until July 2018 at the Max-Delbrück Center for Molecular Medicine in Berlin under the supervision of Priv.-Doz. Dr. Enno Klußmann

I hereby declare that the following work was performed by me alone, only with the use of literature and materials listed. I further declare that to the best of my knowledge this work is novel and does not conflict with any earlier published work.

Berlin, October 2018
Mohamed Elkewedi

Acknowledgments

1. Table of Contents

Abbreviations

AC: adenylyl cyclase

ADF: actin depolymerizing factor

AKAP: A-kinase anchoring protein

AKB: A-kinase binding

AJ: adherens junction

AMP: adenosine-5'-monophosphate

APC: adenomatosis polyposis coli

ATP: adenosine-5'-triphosphate

BSA: bovine serum albumin

cAMP: cyclic adenosine-3',5'-monophosphate

cNMP: cyclic nucleotide monophosphate

C: catalytic PKA subunit

Cdc42: cell division control protein 42

CFL: cofilin

CKI: casein kinase I

CNG: cyclic nucleotide-gated channels

D/D: dimerization and docking domain

DMEM: Dulbecco's modified eagle medium

DMSO: dimethyl sulphoxide

DNA: deoxyribonucleic acid

Drp1: dynamin related protein 1

DSP: desmoplakin

DTT: dithiothreitol

EDTA: ethylenediaminetetraacetic acid

EGTA: ethyleneglycoltetraacetic acid

EMT: epithelial-mesenchymal transition

EPAC: exchange proteins directly activated by cAMP

F-actin: filamentous actin

FBS: fetal bovine serum

FMP: Leibniz-Institut für Molekulare Pharmakologie

FSK: forskolin

$G\alpha_s$: stimulatory G protein alpha

$G\alpha_{i/o}$: G_i alpha subunit

Gα$_{q/11}$: G$_q$ alpha subunit

G-actin: globular actin

GAPDH: glyceraldehyde-3-phosphate dehydrogenase protein

GDI: guanosine nucleotide dissociation inhibitor

GDP: guanosine-5'-diphosphate

GEF: guanine nucleotide exchange factor

GFP: green fluorescent protein

GID: GSK3 interaction domain

GMP: guanosine-5'-monophosphate

GPCR: G protein-coupled receptor

GSK3β: glycogen synthase kinase 3 beta

GSKIP: GSK3β interaction protein

GTP: guanosine-5'-triphosphate

HCN: hyperpolarization-activated cyclic nucleotide–gated channels

Hrs: hours

HSP90: heat shock protein 90

IF: immunofluorescence

Ig: immunoglobulin

IP: immunoprecipitation

JAM: junctional adhesion molecule

KD: knockdown

KO: knockout

LIMK: LIM domain kinase

LSM: laser scanning microscope

MAP2D: microtubule-associated protein 2D

MAPK: mitogen-activated protein kinase

MAPKAPK2/MK2: MAP kinase-activated protein kinase-2

MDC: Max Delbrück Center for Molecular Medicine

MET: mesenchymal-epithelial transition

Min: minute(s)

MLC: myosin light chain

MLCP: myosin light chain phosphatase

MRLC: myosin regulatory light chains

MYLK: myosin light chain kinase

NT: non-targeting siRNA

OPA-1: dynamin-like 120 kDa protein

PAGE: polyacrylamide gel electrophoresis

PAK: p21-activated kinase

PBS: phosphate buffered saline

PDE: phosphodiesterase

PHF2: PHD finger protein 2

PKA: protein kinase A

PKC: protein kinase C

PKD: protein kinase D

PKG: protein kinase G

PMSF: phenylmethylsulphonyl fluoride

PP1: protein phosphatase 1

PP2B: protein phosphatase 2B

PVDF: polyvinylidene fluoride

R: regulatory PKA subunit

RIIBD: RII-binding domain

Rac-1: Ras-related C3 botulinum toxin substrate 1

Rap1: Ras-related protein 1

Rap2: Ras-related protein 2

RhoA: Ras homolog family member A

RhoGDI: Rho-GDP-dissociation inhibitor

RNA: ribonucleic acid

ROCK: Rho-associated kinase

RT: room temperature

S: serine

SDS: sodium dodecylsulfate

shRNA: short hairpin RNA

siRNA: short interfering RNA

SNAIL: zinc finger protein SNAI1

SSH: slingshot phosphatases

TBS: Tris buffered saline

TBS-T: TBS with Tween 20

TGF-β: transforming growth factor beta

Thr: threonine

TJ: tight junction

WT: wild-type

ZEB1: zinc finger E-box binding homeobox 1/2

ZO-1: zonula occludens protein 1

ZO-2: zonula occludens protein 2

ZO-3: zonula occludens protein 3

List of Tables

List of Figures

2. Introduction

2.1 cAMP signalling

Second messengers are ubiquitous small intracellular molecules and ions that transmit extracellular signals to downstream target effector proteins. The resting cellular levels of second messengers are low and are rapidly elevated as a response to extracellular stimuli. To enable specific cellular responses to each of a plethora of stimuli, precise temporal and spatial control of signal propagation is required. (Lodish *et al.* 2000, Newton *et al.* 2016, Ab Naafs, 2017).

Cyclic adenosine 3'5'- monophosphate (cAMP), the first second messenger to be discovered, plays an integral role in the intracellular responses to various hormones and neurotransmitters (Rall and Sutherland, 1958). The levels of cAMP are mainly regulated through two enzyme families, the adenylyl cyclases (ACs), which synthesize cAMP and the phosphodiesterases (PDEs), which degrade it. The generation of cAMP is induced through the binding of an extracellular first messenger to a G-protein coupled receptor (GPCR) (Fig. 1). GPCRs constitute a large group of exclusive eukaryotic receptors that interact with heterotrimeric G proteins. The heterotrimeric G protein family comprises membrane associated proteins, which possess three different subunits, an alpha (α) subunit, a beta (β) subunit, and a gamma (γ) one. The binding of on extracellular agonist elicits a conformational change in the G-protein complex, causing the receptor to act as a guanine nucleotide exchange factor (GEF) for the G protein and resulting in the exchange of GDP for GTP on the Gα subunit of the complex. The G-protein heterotrimer then dissociates and the liberated Gα subunit activates AC, which in turn converts ATP into cAMP and pyro-phosphate. The Gα subunit family comprises four members, Gα_s, G$\alpha_{i/o}$, G$\alpha_{q/11}$ and G$\alpha_{12/13}$ subunits, where each of these subunits has a unique modulatory function, for instance the Gα_s, G$\alpha_{i/o}$ subunits serve to regulate the activity of AC, with the former being a stimulatory subunit that enhances the cyclase activity and the latter being an inhibitory subunit that inhibits AC. The elevation of cAMP levels above a threshold results in the activation of cAMP downstream effectors, such as the exchange proteins directly activated by cAMP (EPACs), the cyclic nucleotide-gated channels (CNG)/hyperpolarization-activated cyclic nucleotide–gated channels (HCN), and the cAMP-dependent protein kinase A (PKA). All these effector proteins possess a cyclic nucleotide monophosphate (cNMP) binding domain comprising around 120 amino acids. (Seino and Shibasaki, 2005, Clapham and Neer, 1997, Albert and Robillard, 2002, McCormick and Baillie, 2014).
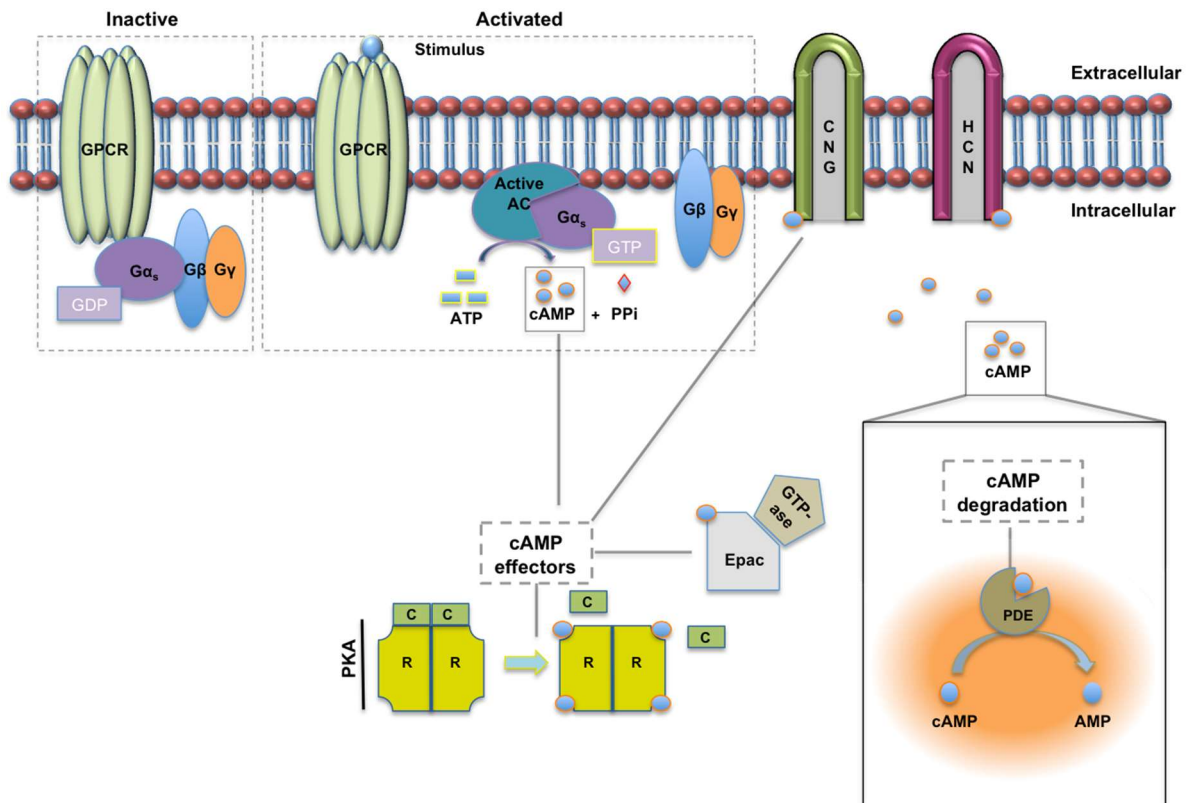
Figure 1. GPCR-dependent cAMP signalling cascade. The stimulation of GPCRs by first messengers/stimuli elicits a conformational change in the associated heterotrimeric Gs-protein complex, resulting in the activation of the enzyme AC. Active AC converts ATP into the second messenger cAMP, which proceeds to activate its downstream effectors, such as PKA, EPACs, and CNG/HCN. PDEs inhibit cAMP signalling by the hydrolysis of cAMP to AMP.

ACs comprise a family of enzymes, which catalyse the single step cyclization reaction converting ATP to cAMP. Ten different mammalian isoforms of AC have been identified and characterized, with AC(1-9) being transmembrane proteins, whereas AC10 is a soluble, cytosolic one. The various members of the AC family are divided into groups based on their structural homology and regulatory properties. Other than the soluble AC, which is activated by Ca^{2+} and bicarbonate, all the other transmembrane isoforms are activated by $G\alpha_s$ and the labdane diterpene, forskolin. Other activators of the transmembrane isoforms include calcium (Ca^{2+}), $G\beta\gamma$, and protein kinase C (PKC) (Hurley 1999, Motiani *et al.* 2018, Patel *et al.* 2010).

PDEs regulate the cAMP and cyclic guanosine monophosphate (cGMP) homeostasis by hydrolysing the phosphodiester bond in cAMP/cGMP, yielding AMP and GMP respectively. Mammalian PDEs are divided into 11 families comprising more than 100 isoforms. They share structural similarities, where all isoforms possess a conserved catalytic domain situated in the C-terminal region. They, however, vary in their biological functions, owing to the variable, isoform-specific regulatory domain situated in the N-terminal region. PDE isoforms 4, 7, and 8 hydrolyse cAMP only, whereas isoforms 5, 6, and 9 only catalyse the hydrolytic cGMP

conversion, and isoforms 1, 2, 3, 10, and 11 have dual specificity, hydrolysing both cAMP and cGMP. The binding affinity of PDEs varies greatly from one isoform to another (Rall and Sutherland, 1958, Vezzosi and Bertherat, 2011).

Epac proteins act as GEFs for Rap1 and Rap2, two small GTPases belonging to the Ras superfamily. These GTPases exist in two states, an inactive guanosine diphosphate (GDP)-bound state and an active guanosine triphosphate (GTP)-bound one, where GEFs mediate their activation through catalysing the exchange of GDP for GTP. There are two known isoforms of Epac, Epac1 and Epac2, both of which are mostly ubiquitously expressed. Structurally, the two isoforms are similar, being multidomain proteins with a C-terminal catalytic region that confers the exchange activity and an autoinhibitory N-terminal regulatory region, which possesses cNMP binding domains. Epac1 has one cNMP domain, while Epac2 has two cNMP domains (Gloerich and Bos, 2010, Schmidt *et al.* 2013).

CNG and HCN are voltage gated non-selective potassium (K^+) channels that regulate the membrane potential of the cells. The direct binding of cAMP to the channels results in their opening and consequently changes of membrane potential. CNG channels are present in photoreceptors and olfactory sensory neurons, where they play an integral role in signal propagation. HCN channels play a role in the regulation of cardiac rhythm and in conjunction with TRIP8b, an auxiliary accessory subunit of the channels, they modulate the neuronal firing rate (Craven and Zagotta, 2006, Wainger *et al.* 2001, Bankston *et al.* 2017).

2.1.1 cAMP dependent protein kinase; protein kinase A

cAMP dependent protein kinase, a serine/threonine kinase, commonly referred to as protein kinase A (PKA), is the major effector of cAMP. The origins of the discovery of PKA date back to the 1950s, when Nobel prize winner biochemists Edmond Fisher and Edwin Krebs hypothesized that glycogen metabolism is regulated by a cAMP dependent enzyme. Consequently, Krebs purified the enzyme from rabbit skeletal muscle in 1968 and named it cAMP-dependent protein kinase, a denotation to the complete dependence of the kinase on cAMP for its activity (Fischer *et al.* 1955, Walsh *et al.* 1968).

The structure of the inactive PKA holoenzyme was gradually uncovered as a tetramer, revealing PKA as only one of two kinases from around 540 human kinases, alongside casein kinase 2 to exhibit this unique structural arrangement. In the absence of cAMP, the intact holoenzyme exists as a dimeric regulatory subunit (R) bound to two catalytic ones (C). The binding of two molecules of cAMP to each of the R subunits triggers a conformational change on the holoenzyme, marked by the dissociation of the catalytic subunits and the subsequent phosphorylation of their targets. Four mammalian isoforms of the R subunit have been characterized, RIα, RIβ, RIIα and RIIβ, each of which is encoded by a separate gene. RIα and RIIα exhibit ubiquitous expression, whereas RIβ expression is mainly confined to the central

nervous system and RIIβ is found in multiple reproductive, fat, and endocrine tissues, as well as the brain. Three isoforms of the C subunit, Cα, Cβ, and Cγ have been identified in mammals, with the α and β isoforms being mostly ubiquitously expressed and the expression of the γ isoform being restricted to the testis. Depending on the isoform of the R subunit (RI or RII), the PKA holoenzyme is classified into PKA-I and PKA-II. The two PKA isoforms exhibit different characteristics, such as cAMP sensitivity, where PKA-I has a lower cAMP activation threshold than PKA-II. PKA-I exhibits mostly cytosolic distribution, whereas PKA-II is anchored to subcellular structures. The ability of any R subunit dimer to bind and restrain all C subunits, coupled with the presence of various splice variants for the RIα (two splice variants), Cα (two splice variants), and Cβ (six splice variants) subunits, constitute one of the main pillars of cAMP/PKA signalling diversity. (Corbin *et al*. 1977, Corbin *et al*. 1978, Zoller *et al.* 1979, Ringheim and Taylor, 1990, Turnham and Scott, 2016).

Each R subunit is made up of a dimerization and docking domain (D/D) situated at the N-terminus, followed by a largely disordered linker region comprising the C subunit auto-inhibitory sequence, a motif, which varies greatly between the various R subunits isoforms. Succeeding the linker region and located at the carboxy terminus of the R subunits, are two adjoining cAMP binding domains. The D/D domains of the R subunits dimer form an antiparallel X-type four helix bundle domain comprising a hydrophobic groove for docking the A-kinase anchoring proteins (AKAPs), referred to as the AKAP docking domain (Fig. 2A, Fig. 2B). The C subunits of PKA, the first protein kinase structures to be identified and characterized, harbour a catalytic core motif, which is common among all members of the broad protein kinase family. While the kinase core constitutes most of the PKA C subunit sequence (residues: 40-300), a characteristic variable A-helix N-terminus (residues: 1-39) and a C-terminus (residues: 301-350), shared among members of protein kinase A, C, and G families, comprise the rest of its structure. Whereas the C-terminus plays a role in interacting with the corresponding regulatory proteins, the N-terminus is capable of undergoing various posttranslational modifications, thereby modulating PKA action and localization.

Despite the activity of the C subunits being dependent on the local cAMP gradient, a cAMP independent regulator of the C subunit activity was uncovered and termed PKA inhibitor peptide (PKI). PKI acts a pseudo substrate for PKA, binding the free C subunits with high affinity following their cAMP-mediated dissociation from the R subunit dimer. All C subunits, other than Cγ, are capable of directly binding PKI. Upon the increase in PKI levels, PKI was found to accumulate in the nucleus and bind the free C subunits triggering their nuclear export to the cytoplasm through its nuclear export signal sequence. Moreover, Rho GTPase-activating protein 36 (ARHGAP36) was also recently uncovered as an antagonist of PKA signalling. In addition to directly binding and inhibiting the C subunit of PKA through a pseudo substrate motif, it enhances the ubiquitylation mediated endolysosomal degradation of the C

subunit (Manning *et al.* 2012, Taylor *et al.* 2012, Agustin *et al.* 2000, Di Benedetto *et al.* 2008, Skalhegg and Tasken, 2000, Pidoux and Tasken, 2010, Kinderman *et al.* 2006, Vigil *et al.* 2004, Bastidas *et al.* 2012, Chen *et al.* 2005, Eccles *et al.* 2016).
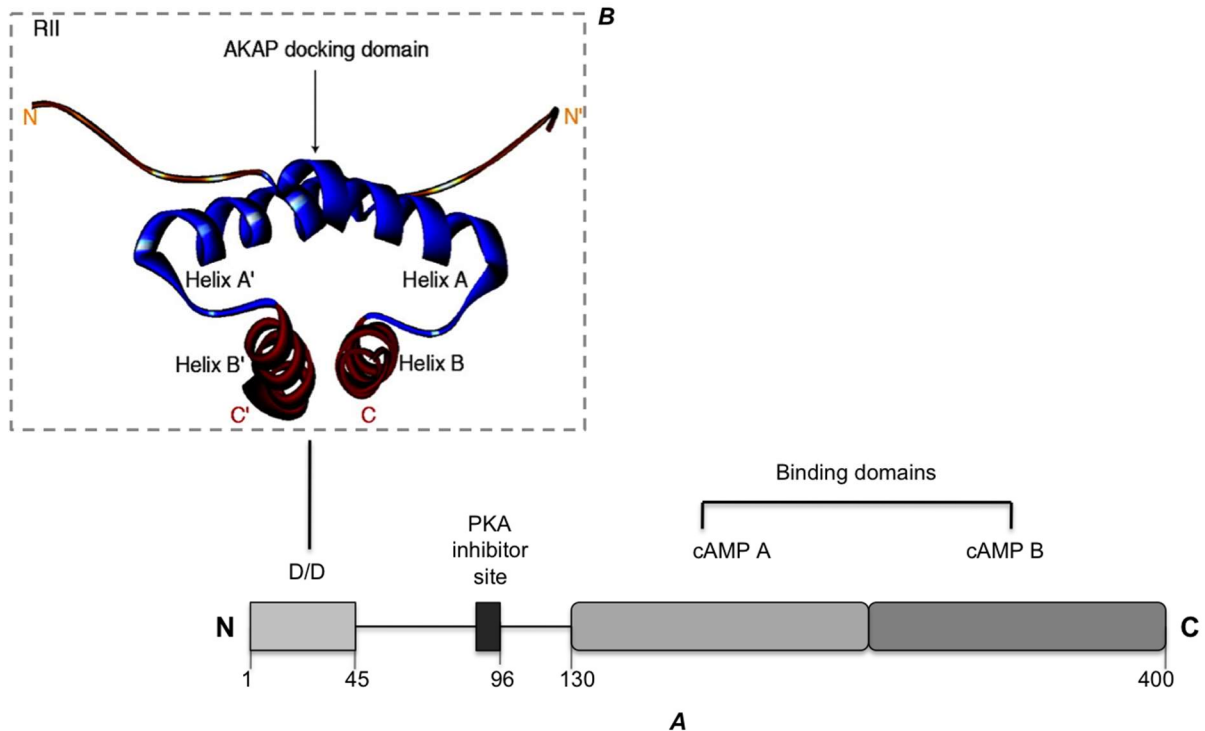
Figure 2A. RIIα subunit of PKA showing the N-terminally situated dimerization and docking domain (D/D), followed by the catalytic subunit binding PKA inhibitor site and two cAMP binding domains. Based on (Vigil *et al.* 2004). **Figure 2B. NMR structure of RIIα dimer D/D domain** (Pidoux *et al*. 2010) showing the anti-parallel X-type four helix bundle domain forming a hydrophobic AKAP docking groove. Based on (Newlon *et al*. 2001, Banky *et al*. 2003).

2.2 A-kinase anchoring proteins (AKAPs)

The spatial and temporal modulation of the cAMP/PKA signalling is achieved through A-kinase anchoring proteins (AKAPs), a family comprising more than 50 scaffolding proteins, sharing the ability to specifically bind cAMP-dependent PKA. AKAPs can be generally classified into canonical or non-canonical depending on their mode of interaction with the PKA R subunits. Canonical AKAPs, which comprise most of the known AKAPs, bind the D/D domain of R subunits of PKA through a structurally conserved A kinase binding (AKB) domain. The AKB domain spans 14-18 amino acids and forms an amphipathic α- helix that docks its hydrophobic face into the hydrophobic groove of the anti-parallel X-type four helix bundle D/D domain (Fig. 3). (Jarnaess *et al.* 2008, Götz *et al.* 2016, Newlon *et al.* 1999, Newlon *et al.* 2001, Gold *et al.* 2006, Kinderman *et al.* 2006, Calejo and Taskén, 2015).
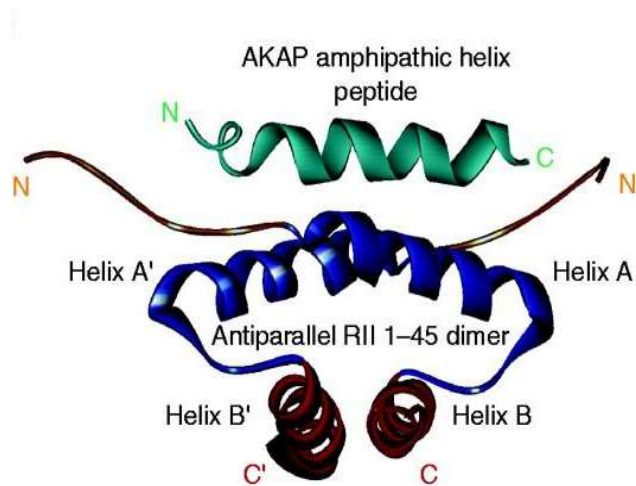
Figure 3. NMR structure of RIIα dimer D/D domain (Pidoux *et al*. 2010) and canonical AKAP helix peptide. (Newlon *et al*. 2001).

Due to the ubiquitous nature of PKA and the large number of its targets, very precise control of PKA activity has to be attained to allow for specific phosphorylation of the substrates. This specificity is brought about by AKAPs, which utilize their targeting domains to interact with the proteins or lipids of defined subcellular compartments such as the plasma membrane, the mitochondria, and the nucleus.

In addition to their direct interaction with PKA, AKAPs also bind other protein kinases (PKC, protein kinase D; PKD, and protein kinase G; PKG), as well as protein phosphatases (protein phosphatase 1; PP1 and protein phosphatase 2B; PP2B) and PDEs, hence creating confined signalosomes and allowing for high signal relay specificity (Fig. 4). Furthermore, some AKAPs possess an intrinsic catalytic activity, for example, AKAP-Lbc acts as a guanine nucleotide exchange factor and activates the small GTPase RhoA through its DHPH domain. (Schrade *et al.* 2018, Troger *et al.* 2012, Asirvatham *et al.* 2004, Schillace *et al.* 2001, Perkins *et al.* 2001, Diviani *et al.* 2001).

AKAPs tend to have different affinities for the different isoforms of the R subunits of PKA. Most AKAPs mainly bind the RII subunits, explaining why the AKB domain is commonly referred to as the RII-binding domain (RIIBD). Several AKAPs only bind RI subunits (SKIP and smAKAP) and some AKAPs, generally referred to as dual specific (D)AKAPs, bind both R subunit isoforms (Opa1, ezrin, and D-AKAP1) (Skroblin *et al.* 2010).
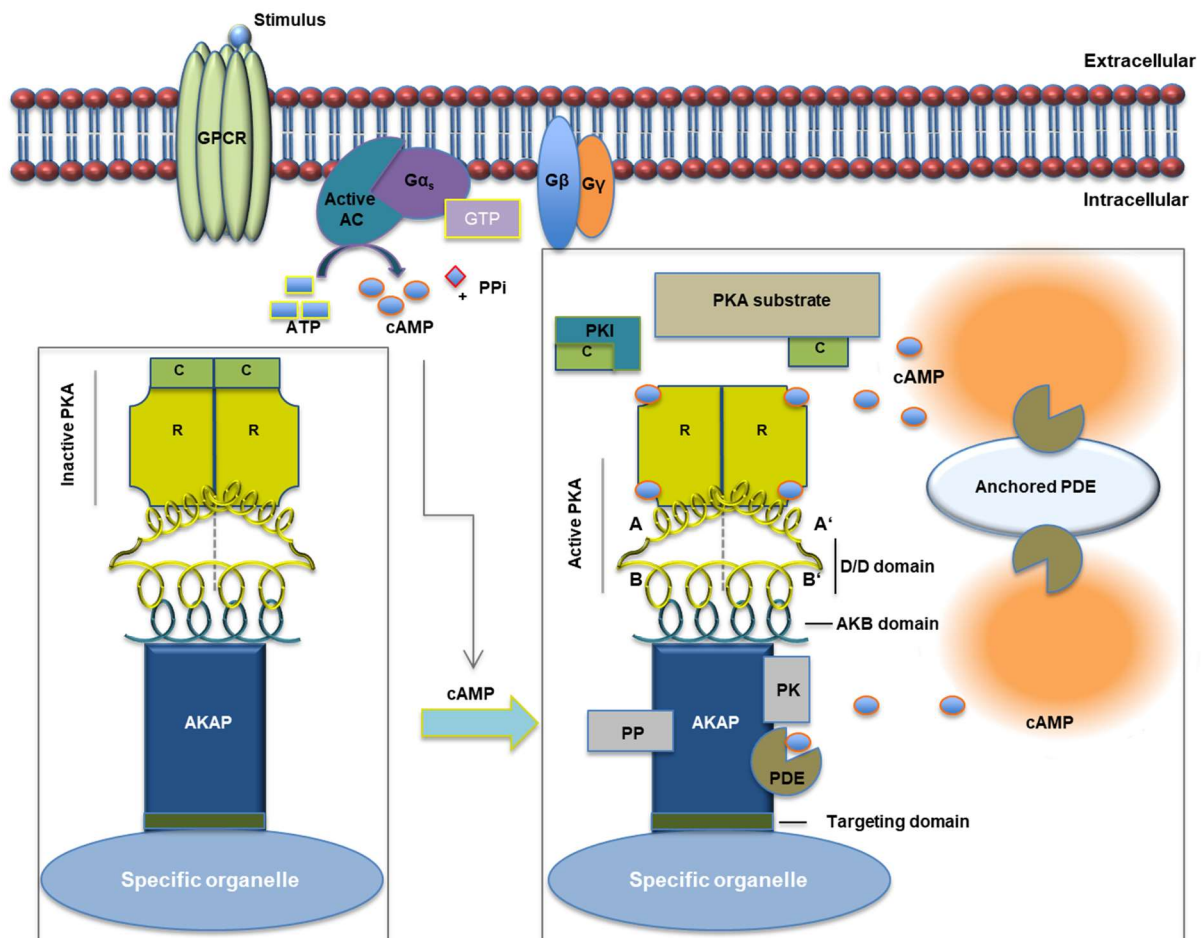
Figure 4. AKAP compartmentalized cAMP signalling. Through their targeting domains, AKAPs tether PKA to specific subcellular organelles, bringing it into close proximity of its substrates to facilitate their phosphorylation. The four helix bundle of the D/D domain of PKA R subunits interacts with the AKB amphipathic helix of AKAPs. AKAPs also bind other proteins, such as protein phosphatases (PPs), protein kinases (PKs) and phosphodiesterases (PDEs), hence facilitating the integration of different signalling systems.

The disruption in AKAP maintained compartmentalized signalling has been implicated in various widespread diseases, which necessitates the characterization of novel AKAPs at a molecular level, to allow for better pharmacological intervention. One of the major kinases, whose compartmentalization has been implicated with newly identified AKAPs, is the constitutively active glycogen synthase kinase 3 beta GSK3β.

2.2.1 Glycogen synthase kinase 3β (GSK3β)

The conserved Glycogen synthase kinase 3 (GSK3) family of ubiquitous serine/threonine kinases was originally discovered in the late 1970s as modulators of glucose metabolism, owing to their ability to negatively regulate the enzyme glycogen synthase (Cohen *et al.* 1979, Embi *et al.* 1980). The vast majority of eukaryotes express two isoforms of GSK3, namely GSK3α (51 kDa) and GSK3β (47 kDa), with GSK3α possessing an extra 63 amino residues at its N-terminus. Both isoforms are encoded by two highly homologous separate genes (Woodgett *et al.* 1990). However, despite their high structural similarity, they are non-redundant, since it was found that GSK3β deficient mice suffer from embryonic lethality

triggered by enhanced hepatocyte apoptosis, despite these embryos retaining normal expression levels of the α isoform (Hoeflich *et al.* 2000; Pandey *et al.* 2016).

The mode of action of GSK3β can vary. The kinase can directly phosphorylate some of its substrates, such as the microtubule protein Tau, and the scaffold protein Axin (Cho *et al.* 2002; Hart *et al.* 1988), or it requires a priming phosphorylation of its substrate by another kinase prior to acting, such as the β-catenin-priming phosphorylation at serine 45 by CKIα (Liu *et al.* 2002). Thomas *et al.* demonstrated that the GSK3-mediated phosphorylation in the absence of priming takes place 100-1000 folds slower compared to the phosphorylation succeeding priming, indicating that priming greatly increases the efficiency of the subsequent phosphorylations (Thomas *et al.* 1999).

Other than its role in glycogen metabolism, GSK3β has been implicated in the phosphorylation of more than 50 substrates in various signalling pathways (Serretti *et al.* 2012), among which are cell cycle regulators (cyclin D1; Diehl *et al.* 1998), microtubule-associated proteins (tau and kinesin light chain; Cho *et al.* 2002, Morfini *et al.* 2002), cellular metabolism regulators (pyruvate dehydrogenase; Hoshi *et al.* 1996), and transcription factors and their regulators (CREB and β-catenin; Rubinfeld *et al.* 1996, Ilouz *et al.* 2006).

β-catenin is a crucial structural and signalling molecule, which has been implicated in the maintenance of epithelial integrity, as well as the regulation of gene expression in canonical Wnt signalling. Upon synthesis, β-catenin is integrated into a complex with E-cadherin at the adherens junction (AJ), one of the major epithelial cell junctions, where it also interacts with α-catenin and influences the associated junctional actin dynamics. Protein kinases or E-cadherin downregulation were found to liberate β-catenin from the junctional complex, where it is readily phosphorylated and marked for proteasomal degradation by a multiprotein destruction complex. The destruction complex comprises the scaffold proteins Axin and adenomatous polyposis coli (APC), as well as the kinases GSK3β and casein kinase I (CKI). The activation of Wnt signalling is marked by the disassembly of the destruction complex and the inactivation of GSK3β, hence β-catenin is not degraded, accumulates in the cytosol and translocates to the nucleus, where it acts as a transcriptional co-activator and activates Wnt target genes (Caspi *et al.* 2008, Valenta *et al.* 2012, Stamos and Weis, 2013).

One of the defining unique features of GSK3β, is that it exists in a constitutively active state. The modulation of its activity is attained by the inhibitory phosphorylation on serine 9 (Sutherland *et al.* 1993). Various kinases have been shown to impose negative regulation on the activity of GSK3β, among which is PKA (Fang *et al.* 2000; Li *et al.* 2000). The ubiquitous nature of both PKA and GSK3β and their well-documented roles in various signalling systems, hint towards potential inclusion of AKAPs in complexes comprising both kinases. Thus far three AKAPs sharing the ability to bind both PKA and GSK3β have been identified, the microtubule-associated protein 2D (MAP2D), which binds type II PKA (Flynn *et al.* 2008), AKAP220, which

is capable of binding both PKA types, at two different sites, with site 1 (residues 610–623) interacting with RII PKA subunits and site 2 (residues 1633–1646) showing dual specificity for both R isoforms, albeit showing a clear preference to binding the RII isoform (Tanji *et al.* 2002; Whiting *et al.* 2015), and GSK3β interaction protein (GSKIP), the most recently identified member of the trio.

2.2.2 GSK3β interaction protein (GSKIP)

GSK3β interaction protein (GSKIP) is also known as C14orf129/CN129, a denotation to the chromosomal location of the encoding gene. In 2004, the NMR structure of GSKIP, back then a protein without a known function was uncovered through the Northeast Structural Genomics Consortium (Ramelot *et al.* 2004). It was revealed that the protein is made up of 139 amino acid residues and comprises four distinct parts, an unstructured N-terminus, followed by an α-helix, a central β-sheet and finally a second α-helix at the C-terminus part.

GSKIP was identified as a GSK3β interaction protein (Chou et al. 2006) by screening a human testis cDNA library and a yeast two hybrid system. It was found to contain a 25 amino acid region, homologous to the GSK3β interaction domain (GID) of Axin, residing in the C-terminus (Fig. 5). It was suggested that GSKIP may play a role in GSK3β inhibition and that it is involved in GSK3β- Axin-β-catenin complex, which is central to the Wnt signalling.
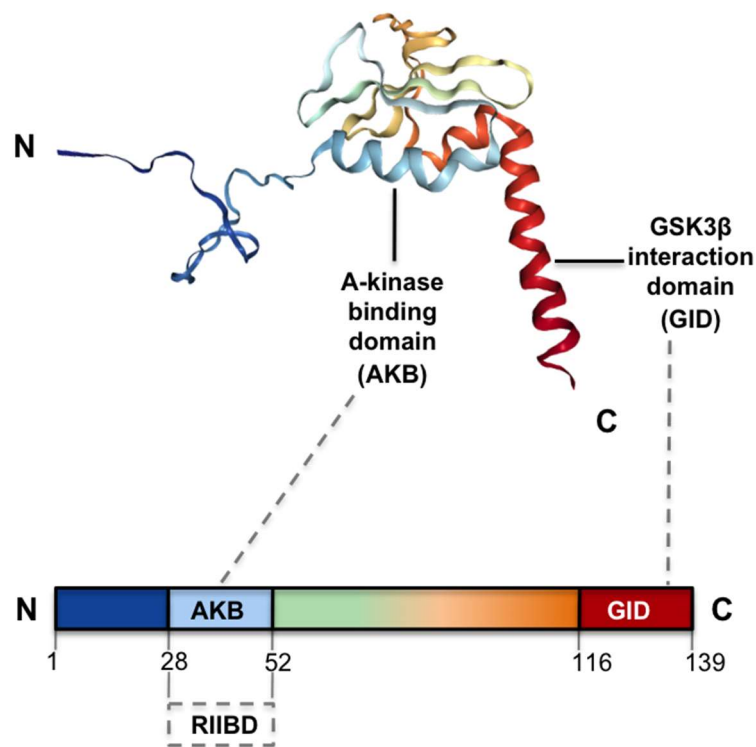
Figure 5. Tertiary and domain structure of the human GSKIP. The NMR-based structure of GSKIP as obtained from Protein Data Bank (PDB; ID: 1SGO).

GSKIP was identified as an AKAP by our group (Hundsrucker *et al*. 2010). An AKAP consensus sequence, representing the hydrophobic amino acids shared among all canonical AKAPs, was determined through aligning the RII-binding domains (RIIBDs) of known canonical AKAPs. By employing a bioinformatics approach utilizing the signature AKAP consensus sequence and the RIIBD characteristic isoelectric point range of AKAPs as a search tool on the SwissProt database, followed by peptide array screens, GSKIP was identified. Being capable of directly binding GSK3β and the RII subunits of PKA, GSKIP was found to mediate the inhibitory phosphorylation of GSK3β on serine 9 (S9) by PKA (Hundsrucker *et al*. 2010). In the canonical Wnt signalling, GSKIP was found to modulate the stability of β-catenin and consequently its transcriptional activity, through its ability to directly interact with PKA and GSK3β. GSKIP facilitates the GSK3β-mediated degradative phosphorylation of β-catenin at serines 33 (S33) and 37 (S37), and threonine 41 (Thr41), as well as the PKA-mediated protective phosphorylation at serine 675 (S675), thus implicating GSKIP in the fine-tuning of the canonical Wnt signalling (Dema *et al.* 2016).

Insight into the *in vivo* role of GSKIP was provided by studies of a conditional GSKIP knockout (KO) mouse model. E18.5 GSKIP-deficient embryos suffered from perinatal lethality, lung inflation failure, and incomplete closure of the palatal shelves, causing a craniofacial disorder known as cleft palate. Spanning embryonic days 10.5 through 14.5, GSKIP KO embryos exhibited decreased phosphorylation of GSK3β at S9, which translates to increased activity, hence pointing towards a potential role of GSKIP in modulating the GSK3β-mediated palatal shelf fusion (Deák *et al*. 2016).

A potential mitochondrial fission role of GSKIP in HEK293 cells was suggested by Chou *et al*. , where the PKA-mediated inhibitory phosphorylation of dynamin-related protein 1 (Drp1), a promoter of mitochondrial fission, was found to be dependent on both GSK3β and GSKIP. While the exact mechanism of action through which GSKIP contributes to the associated Drp1 complex was not elucidated, the data suggest that GSKIP is integral for the inhibitory Drp1 phosphorylation at serine 637 (S637) (Chou *et al.* 2015),.

The Human Protein Atlas (Uhlén *et al.* 2015) demonstrates that GSKIP is ubiquitously expressed in all cancer types (Fig. 6), with the highest abundance recorded in melanoma, urothelial, stomach, colorectal, and ovarian cancers, and the lowest in skin cancer. This expression pattern suggests a role for GSKIP in cancer. GSKIP was recently uncovered as a direct interacting partner of hepatocellular carcinoma-associated long non-coding RNA (HANR) in hepatoma cells (*Xiao et al.* 2017). It was suggested that HANR plays a role in cancer cell proliferation and hinders apoptosis, partly through regulating GSK3β phosphorylation and hence activity, through its ability to directly associate with GSKIP.
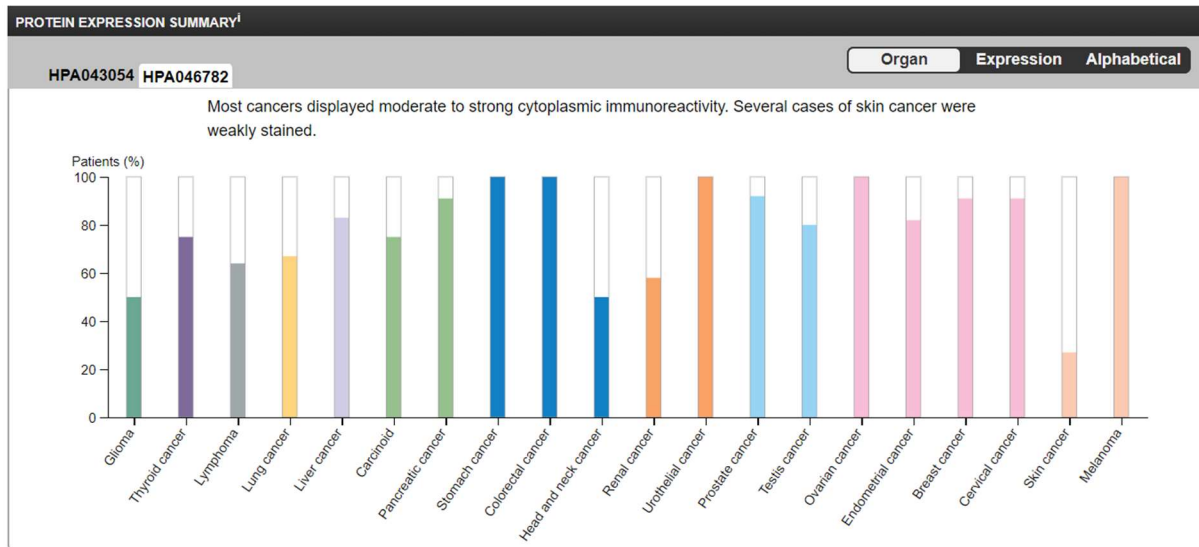
Figure 6. GSKIP protein expression in 20 different cancers. The expression level is determined by immunohistochemical analysis. The results were manually scored according to the staining intensity (negative, weak, moderate, and strong), and the percentage of the stained cells (<25%, 25-75% or >75%). Adapted from The Human Protein Atlas.

2.3 Epithelial cells

Epithelial cells are structurally similar but differ greatly in their functions, ranging from lining the body surfaces, such as the skin and gut to forming glandular structures, including the salivary gland and pancreas. One of the most distinct characteristics of epithelial cells is their ability to stack together forming continuous cohesive sheets known as epithelia. The individual cells making up the epithelium are linked together forming a functional unit and such adhesive linkage maintains the structural integrity through specialized portions of the cell membrane, known as cellular junctions (Lowe *et al.* 2015).

2.3.1 Epithelial cellular junctions

Cellular junctions are multiprotein complex structures that are crucial for various physiological and pathological processes. They are subdivided according to their functional roles into the occluding junctions and the anchoring junctions. The occluding junctions include the tight junctions (TJ), which maintain the outline of the epithelium to avoid the leakage of small molecules from one side to the other and the anchoring junctions. The anchoring junctions comprise the adherens junctions (AJ) and desmosomes, both of which serve to attach the cells and their cytoskeletal components to their neighbours. Alberts *et al.* 2002, Giepmans and Ijzendoorn, 2009, Garcia *et al.* 2017).

The TJ of epithelial cells serves a dual purpose, as a gate and as a fence. The gate function of the TJ is attributed to its role in regulating the paracellular permeability and transport, whereas the fence function is based on maintaining the cell polarity through separating the apical and basolateral membrane molecules. Unlike the AJ and desmosomes, which are situated at the basal side of the lateral membrane, the TJ is present at the apical side. The TJ is made up of both integral and peripheral membrane proteins, where the number of the transmembrane domains in the integral proteins varies from one to four, with the junctional adhesion molecule (JAM) being a single pass protein and the occludins and claudins being multi-pass ones. The integral transmembrane proteins of neighbouring cells form intercellular complexes comprising proteins of the same family, such as occludin-occludin, JAM-JAM, and claudin-claudin complexes (Fig. 7). These proteins are linked to the actin cytoskeleton by peripheral membrane proteins such as the zonula occludin proteins, ZO1, ZO2, ZO3, and the actin binding protein, cingulin (Shin *et al.* 2006; Steed *et al.* 2010; Raya-Sandino *et al.* 2017).

The AJs are essential for the maintenance of cellular adhesion, as well as the infrastructure of the associated actin cytoskeleton of the adjoining cells. The main proteins making up the AJs include cadherins, with E-cadherin being the most common one. The extracellular domain of E-cadherin protrudes from the cell surface to bind other cadherins located on neighbouring cells. While the intracellular cytoplasmic domain is integrated in a cadherin-catenin complex with the canonical Wnt signalling regulator protein, β-catenin and the actin filament binding protein, α-catenin (Fig. 7). Both catenins are critical for the integrity of the AJ, since their absence disrupts the interaction between the actin filaments and the cadherin-complex, resulting in the disorganization of the entire junction (Tian *et al.* 2011; Yonemura *et al.* 2010).

Desmosomes also play an integral role in cell-cell contacts and cellular adhesion, since they confer resistance to shearing stress. The desmosomes comprise the transmembrane proteins known as the desmosomal cadherins, desmoglein and desmocollin, which similarly to cadherins in the AJ, mediate the interactions between adjacent cells through the association of their extracellular domains. The cytoplasmic tails of the cadherins form a complex with the intermediate filaments, which is mediated by the desmosomal plaque proteins, desmoplakin (DSP), plakoglobin, and plakophilin (Fig. 7). The interaction between the intermediate filament binding protein DSP, and the corresponding intermediate filaments is essential for the formation of the functional desmosome unit, since it anchors the filament network to the cadherin-plakoglobin/plakophilin complex (Kowalczyk and Green, 2013; Neuber *et al.* 2010).
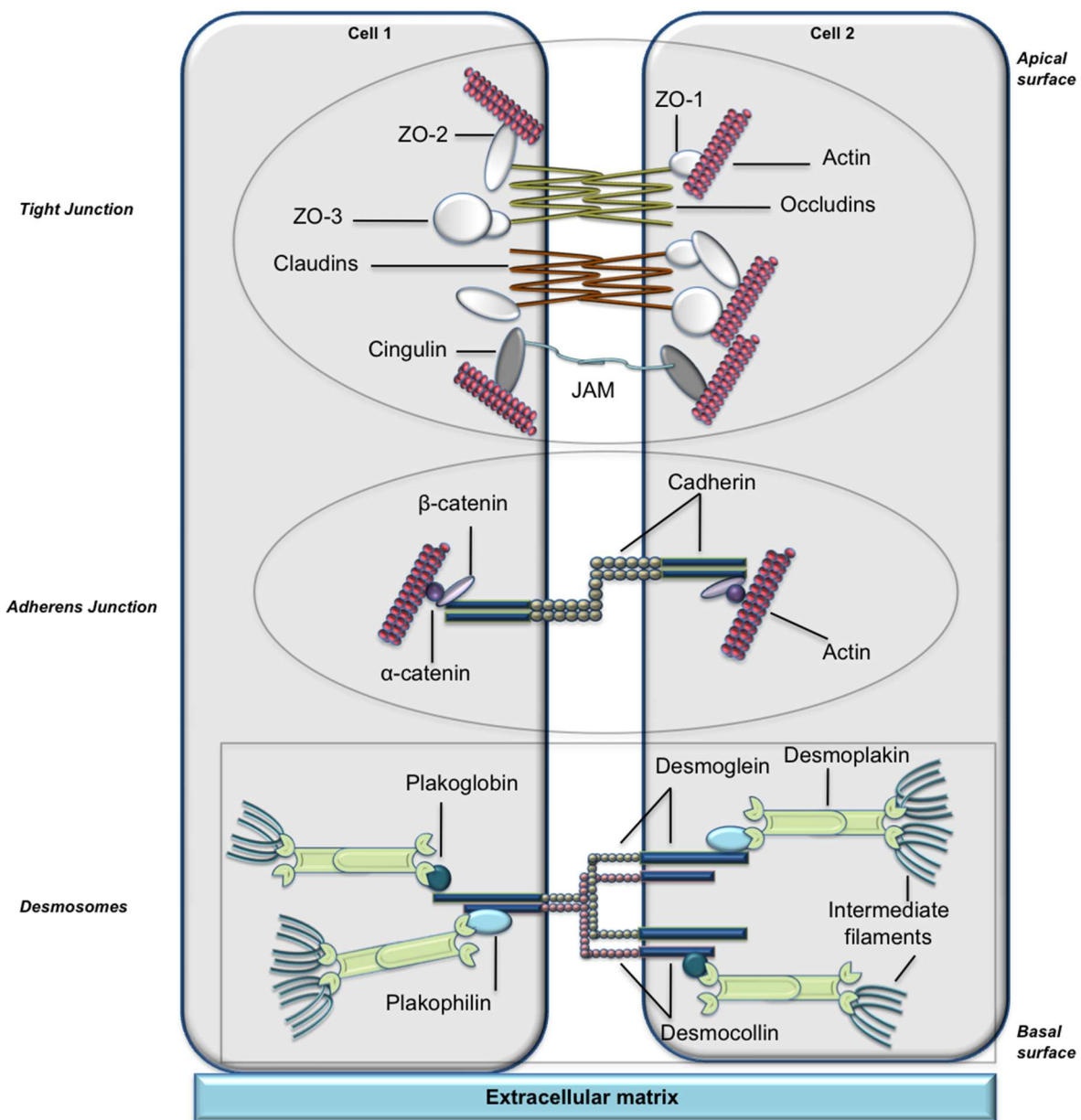
Figure 7. Epithelial cell junction distribution and composition. TJs are the most apical junctions, followed by the AJs and the desmosomes. ZO : zonula occludens, JAM : Junctional adhesion molecules.

2.3.2 Epithelial-to-mesenchymal transition (EMT)

The transient or permanent formation of migratory mesenchymal cells from primitive epithelial cells during embryonic development through EMT, is one of the hallmarks of metazoans. In addition to its function in early development, EMT plays a crucial role during the histogenesis of the heart, peripheral nervous system and musculoskeletal system in vertebrates. Moreover, the reverse process of EMT, mesenchymal to epithelial transition (MET), in conjunction with EMT is involved in the formation of the heart, kidney, and somites.

The manipulation of this evolutionarily conserved process is one of the characteristic properties of cancer cells, where the epithelial cells transform into mesenchymal stem cells, cancer stem cells, and exhibit loss of cell-cell adhesion/ cell-cell junctions, as well as apico-basal polarity (Thiery, 2002), (Fig 8).

The underlying mechanisms modulating EMT are somewhat convoluted. Its induction can be attributed to various factors, such as signalling pathways, among which are transforming growth factor beta (TGF-β), Wnt and Notch (Thiery & Sleeman, 2006), as well as mechanical changes in the stress and the density of the extracellular matrix (Gomez *et al.* 2010, Kumar *et al.* 2014). Tumor protein p53 (p53) and microRNA 200 and 34, as well as select transcription factors act as EMT repressors (Chang *et al.* 2011, Li and Yang, 2014, Zaravinos and Zaravinos, 2015). The master regulation of EMT is attained by interconnected double negative feedback loops comprising the Zinc Finger E-Box Binding Homeobox 1/2 (ZEB-1 and -2) and the microRNA 200 family on one side, and the miR-34 family and zinc finger proteins SNAI1 and SNAI2 (SNAIL1/2) on the other (Siemens *et al.* 2011, Brabletz and Brabletz, 2010, Jia *et al.* 2017).

2.3.3 EMT-mediated actin cytoskeletal rearrangement

The organization of the actin cytoskeleton in the cell is crucial for various cellular processes, among which are cell signalling, and the development and maintenance of cellular junctions and cell polarity (Shankar *et al.* 2015; Doherty and McMahon, 2008; Dominguez and Holmes, 2011). The rearrangement of the actin cytoskeleton is one of the characteristic properties of EMT (Fig. 8). The presence of cortical actin networks is associated with the epithelial phenotype, whereas mesenchymal cells exhibit the formation of actin stress fibers. This EMT fundamental reorganization is orchestrated by the Rho GTPases, Ras homolog gene family member A (RhoA), Ras-related C3 botulinum toxin substrate 1 (Rac-1), and cell division control protein 42 homolog (Cdc42) (Bhowmick *et al.* 2001; Yoon *et al.* 2017; Kristy Stengel and Yi Zheng, 2011).

The Rho GTPases RhoA, Rac-1, and Cdc42 are the most studied members of the Ras superfamily of small GTPases. They share a characteristic Rho-type GTPase-like domain and range in size from 190 to 250 residues. In addition to their cytoskeletal organizational roles, they also promote growth and hinder apoptosis (Hall, 1998). Moreover, Rac-1 and Cdc42 are required for the formation of the cellular motility associated cytoskeletal projections, as well as the polymerization of actin (Wennerberg and J. Der, 2004). While RhoA mediates actin-myosin contractility and hence modulates cell shape through promoting the formation of focal adhesions and stress fibers (Amano *et al.* 1996). The assembly of stress fibers, which are made up of bundles of F-actin, actin binding proteins, and non-muscle myosin II is dependent

on the phosphorylation-mediated activity of the latter, a major motor protein involved in actin cytoskeleton organization (Chang and Kumar, 2015). Myosin II is activated by the phosphorylation of its regulatory light chains (MRLC) (Somlyo and Somlyo, 2003). Mono-phosphorylation at serine 19 (S19) increases the stability of formed myosin II filaments, and actin-activated Mg^{2+}-ATPase activity. Di-phosphorylation at threonine 18 and S19, enhances myosin II activity and increases the stability of its filaments to a much higher degree compared to the mono-phosphorylated counterpart (Ikebe and Hartshorne, 1985; Ikebe *et al.* 1988; Watanabe *et al.* 2007). Rho-associated protein kinase (ROCK), the main effector of RhoA, has been previously implicated directly in both mono, and di-phosphorylation of MRLC (Amano *et al.* 1996 ; Ueda *et al.* 2002), and indirectly through the inhibition of myosin light chain phosphatase (MCLP), an enzyme that dephosphorylates the MRLC of myosin II (Kawano *et al.* 1999).

EMT is also associated with disruption in the levels of many actin regulatory proteins (Lamouille *et al.* 2014), such as the actin severing protein cofilin-1, one of the most crucial and conserved proteins that promote actin depolymerization in the cell (Wang *et al.* 2006).

2.4 ADF/Cofilin

The actin-depolymerizing factor (ADF)/cofilin (CFL) family members were identified in the 1980s as small (around 18 kDa) actin binding proteins that modulate the cellular actin dynamics by inducing the disassembly of actin filaments. This family is present in all eukaryotes. In mammals it comprises three members, ADF, also termed destrin, non-muscle cofilin, commonly referred to as n-cofilin/cofilin-1 (CFL1), and muscle cofilin, known as m-cofilin/cofilin-2 (CFL2). The three are encoded by separate genes and ADF shares around 70% amino acid homology with CFL 1 and 2. (Bamburg *et al.* 1980, Maciver and Hussey, 2002; Kanellos and Frame, 2016).
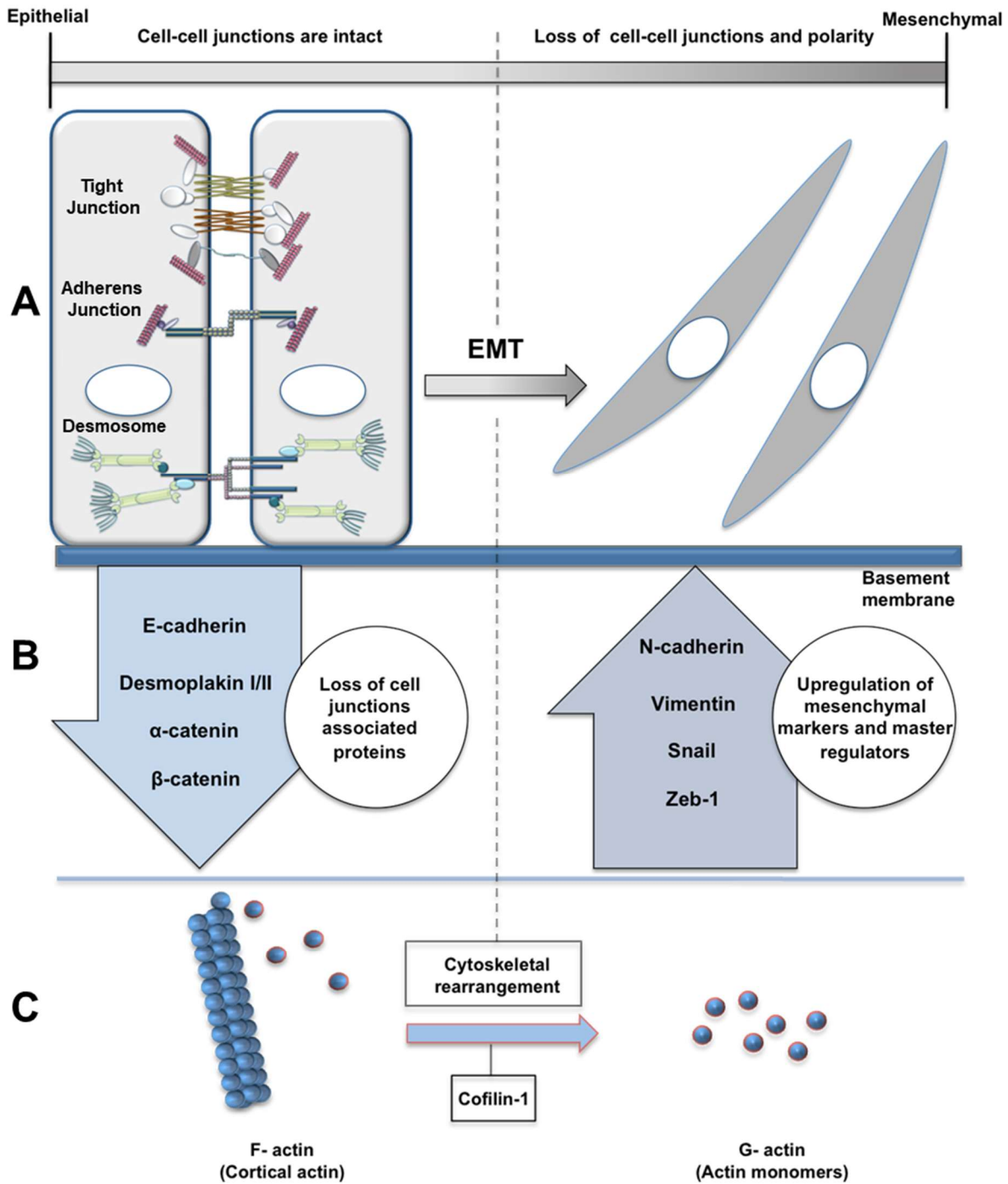
Figure 8. Changes in the molecular markers and actin cytoskeleton reorganization during EMT. A: EMT is characterized by the disassembly of the epithelial junctions and the loss of polarity. B: Cell junctions/cell-cell contact proteins, such as E-cadherin, DSP I/II, α- and β- catenin are characteristic to the epithelial cells and are downregulated upon the transition from the epithelial to the mesenchymal state. Whereas N-cadherin, vimentin, SNAIL, and ZEB1 are associated with the mesenchymal phenotype and are elevated following EMT transition. C: The transition of the cortical actin rich epithelial cells to the actin stress fiber forming mesenchymal counterpart through EMT is also marked by the remodelling of the actin cytoskeleton, mediated by the actin severing protein CFL-1. Based on (Serrano-Gomez *et al.* 2016).

The affinity of ADF and CFL towards actin is influenced by their localization. Where those expressed in tissues, where high degree of actin turnover is required, demonstrated higher affinity towards actin. Hence, the neuronal and epithelial cells located ADF and the ubiquitously expressed CFL1 show much higher actin affinity than the muscle centric CFL2 (Vartiainen *et al.* 2002).

CFL1 is the most studied member of the (A/C), owing to its expression pattern, crucial developmental roles and unique ability to depolymerize, disassemble, sever, and assemble actin filaments (Bamburg and Bernstein, 2010). CFL1 can bind the monomeric globular actin (G-actin), as well as its polymerized filamentous counterpart (F-actin) (Fig. 9). The binding of myosin sub-fragment (S1) to F-actin filaments confers polarity upon the filament, characterized by the presence of a positive barbed end (ATP-bound) and a negative pointed one (ADP-bound; Moore *et al.* 1970). Utilizing its very high affinity for ADP-actin, CFL1 acts by inducing depolymerization at the pointed end of the actin filaments and inhibiting their reassembly, as well as triggering the severing of the filaments through the generation of more barbed ends and the release of actin monomers from the pointed ends (Ono, 2007). The key determinant of CFL1 action on actin filaments assembly or disassembly is the ratio between CFL and actin, as well as other actin binding proteins (Andrianantoandro and Pollard, 2006). At high CFL1 levels, stabilization of actin filaments is attained along with initiation of the G-actin monomers nucleation, leading to filaments branching and elongation through recruiting other actin-binding proteins (Bamburg and Bernstein, 2008, Tsai and Lee, 2012).
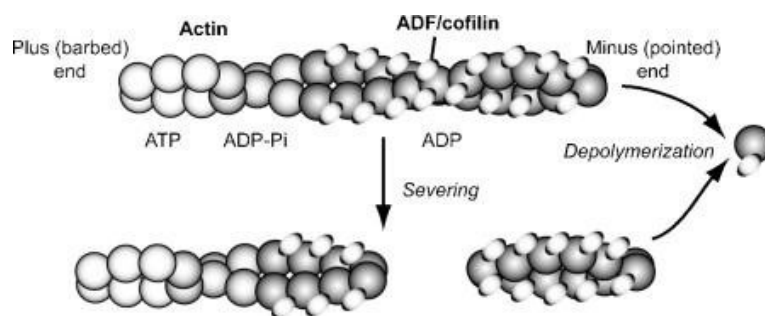
Figure 9. The actin severing and depolymerizing activity of CFL. Adapted from (Ono, 2007).

The non-phosphorylated form of CFL1 is the active form. Hence its activity is decreased through its inhibitory phosphorylation on serine 3 (S3), as well as the consequent dephosphorylation (Agnew *et al.* 1995; Moriyama *et al.* 1996). The change in CFL1 activity and the consequent modulation of the actin filaments is brought about by extracellular stimuli, which trigger the activation of the Rho GTPases, RhoA/Rac-1/Cdc42 leading to the activation of their downstream effectors, ROCK and p21-activated kinase (PAK) respectively. The activated Rho GTPases downstream kinases, ROCK and PAK then proceed to phosphorylate

and activate LIM kinases (LIMKs), the main kinases behind the inhibitory phosphorylation of CFL1 at S3 (Denhardt, 1996, Zigmond, 1996).

LIM kinases are serine/threonine kinases which are crucial modulators of the actin filament dynamics (Khurana *et al.* 2002). The LIM kinase family comprises two isoforms, LIMK-1 and LIMK-2. Structurally, LIM kinases have two N-terminally situated LIM domain repeats, succeeded by the protein targeting and protein complex assembly regulator PDZ domain and finally a kinase domain located near the C-terminus (Okano *et al.* 1995, Hung and Sheng, 2002). Furthermore, the PDZ domain contains two nuclear export signals, whereas the kinase domain includes a nuclear localization sequence, hence conferring the ability on the kinases to shuttle between the nucleus and the cytoplasm (Goyal *et al.* 2005, 2006). Both LIMK isoforms share the highest structural homology among their kinase domains (around 70%), followed by the LIM (around 50%) and PDZ domains (around 46%) (Manetti, 2012).

The negative regulation of the activity of LIMK-1 is mediated by the LIM domains. They directly interact with the C-terminal kinase domains, resulting in the blocking of the kinase substrate binding site, or the locking of the kinase domain in an inactive confirmation (Nagata *et al.* 1999). On the other hand, phosphorylation on specific serine and threonine residues, activates LIM kinases. ROCK phosphorylates LIMK-1 and LIMK-2 on threonine residues 508 and 505 (Thr 508 and 505) respectively within the activation loop (Ohashi *et al.* 2000; Sumi *et al.* 2001) (Fig 10).
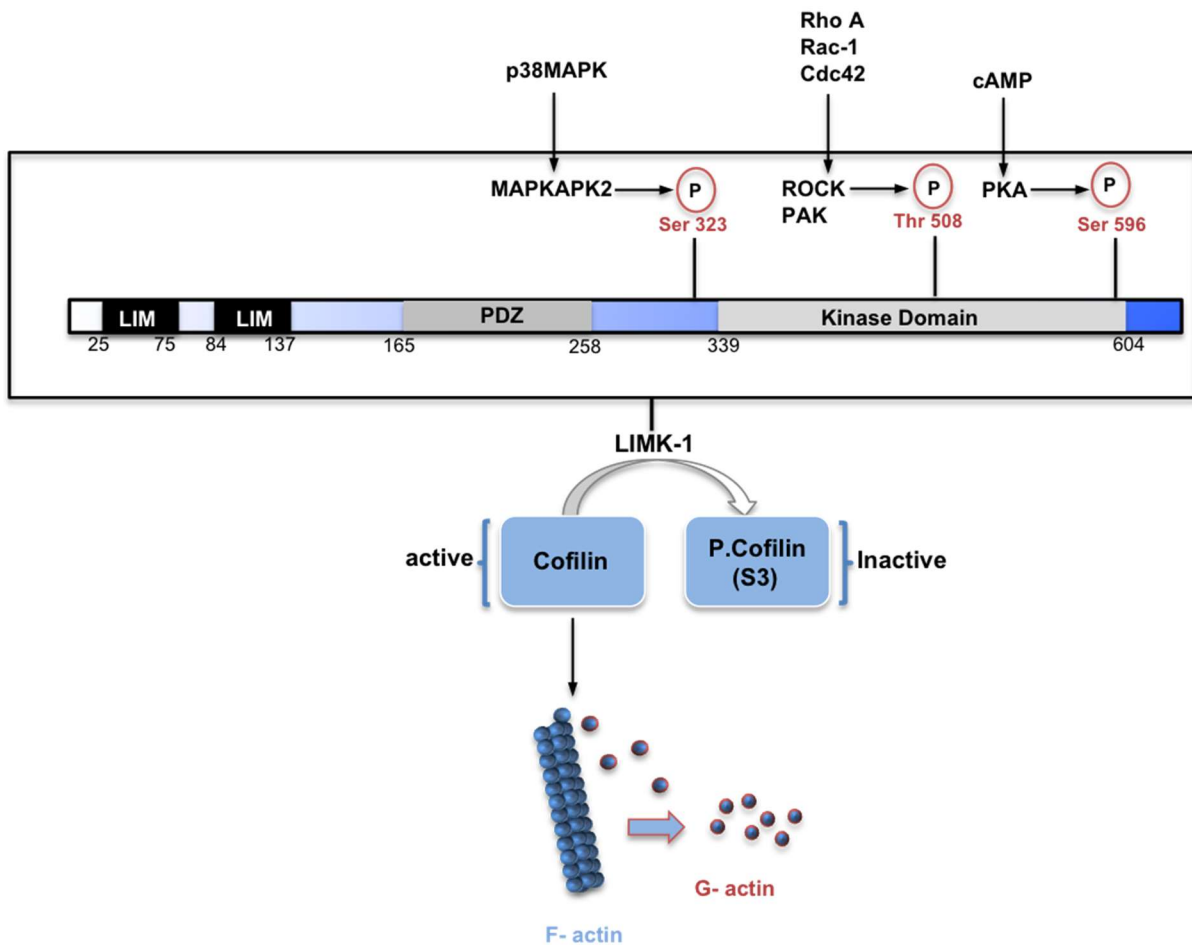
Figure 10. The structure and regulation of LIMK-1. Based on (Nadella *et al.* 2009)

The Rac-1 and Cdc42 downstream effector PAK-1, as well the as the Cdc42 effector PAK-4 also mediate threonine 508 phosphorylation and activation of LIMK-1 (Edwards *et al.* 1999; Dan *et al.* 2001) (Fig. 11). Kobayashi *et al.* uncovered a novel role for MAP kinase-activated protein kinase-2 (MAPKAPK-2; MK2), a downstream kinase of p38 mitogen-activated protein kinase (p38 MAPK) in the activation of LIMK-1, by phosphorylating serine residue 323 (S323), which is located in the region between the PDZ and kinase domains (Kobayashi *et al.* 2006). Moreover, another LIMK-1 activating phosphorylation site was identified by Nadella *et al.*; PKA phosphorylates serine residue 596 (S596) in the kinase domain. Hence the enhanced phosphorylation of CFL1 at S3, and its inactivation can be attributed to the increased activity of LIMK-1, following its phosphorylation at Thr508, and/or S323, and/or S596 (Nadella *et al.* 2009).

Acting in tandem with LIMK to regulate the phosphorylation-dependent activity of CFL1 are the downstream phosphatases. The first phosphatase family acting on phosphorylated CFL1 (P-CFL1; S3) to be identified was the dual specificity Slingshot (SSH) phosphatase family. Initially, it was discovered in *Drosophila melanogaster* as a single gene essential for normal epidermal cells morphogenesis. In humans, three genes encoding for three isoforms,

SSH1, SSH2, and SSH3, were identified (Niwa *et al.* 2002, Ohta *et al.* 2003). The phosphatases activities, tissue distribution, and subcellular localization were found to differ. SSH1 and SSH2 showed high affinity towards F-actin and structures in which F-actin is incorporated, such as stress fibers and cortical actin networks. SSH3 is localized to the nucleus and cytoplasm with diminished F-actin binding affinity (Mizuno, 2013, Ohashi, 2015). SSH1 was also found to inactivate LIMK-1 by directly interacting with its kinase domain and inducing its dephosphorylation at Thr508, hence contributing to the activation of CFL1 directly through its dephosphorylation and indirectly through LIMK-1 activity manipulation (Soosairajah *et al*. 2005).

The contrast in the ubiquitous expression of CFL1 and the majorly epithelial expression pattern of SSH, coupled with the inessentiality of SHH for the biological process associated with CFL1-mediated actin turnover, such as cellular adhesion and proliferation, pointed towards the existence of another CFL1 regulatory phosphatase. Gohla *et al.* isolated and characterized chronophin, a mammalian evolutionary conserved member of the haloacid dehalogenase (HAD) hydrolases superfamily, which functions as a CFL1 phosphatase (Gohla *et al.* 2005). Unlike SHH, chronophin exhibits broad expression, shows much higher specificity towards P-CFL1; S3 and demonstrated very little activity towards LIMK (Huang *et al.* 2005, Kestler *et al.* 2014). Moreover, the disruption of chronophin activity caused cell division defects similar to the ones encountered upon the manipulation of CFL activity (Gohla *et al.* 2005, Huang *et al.* 2005) .
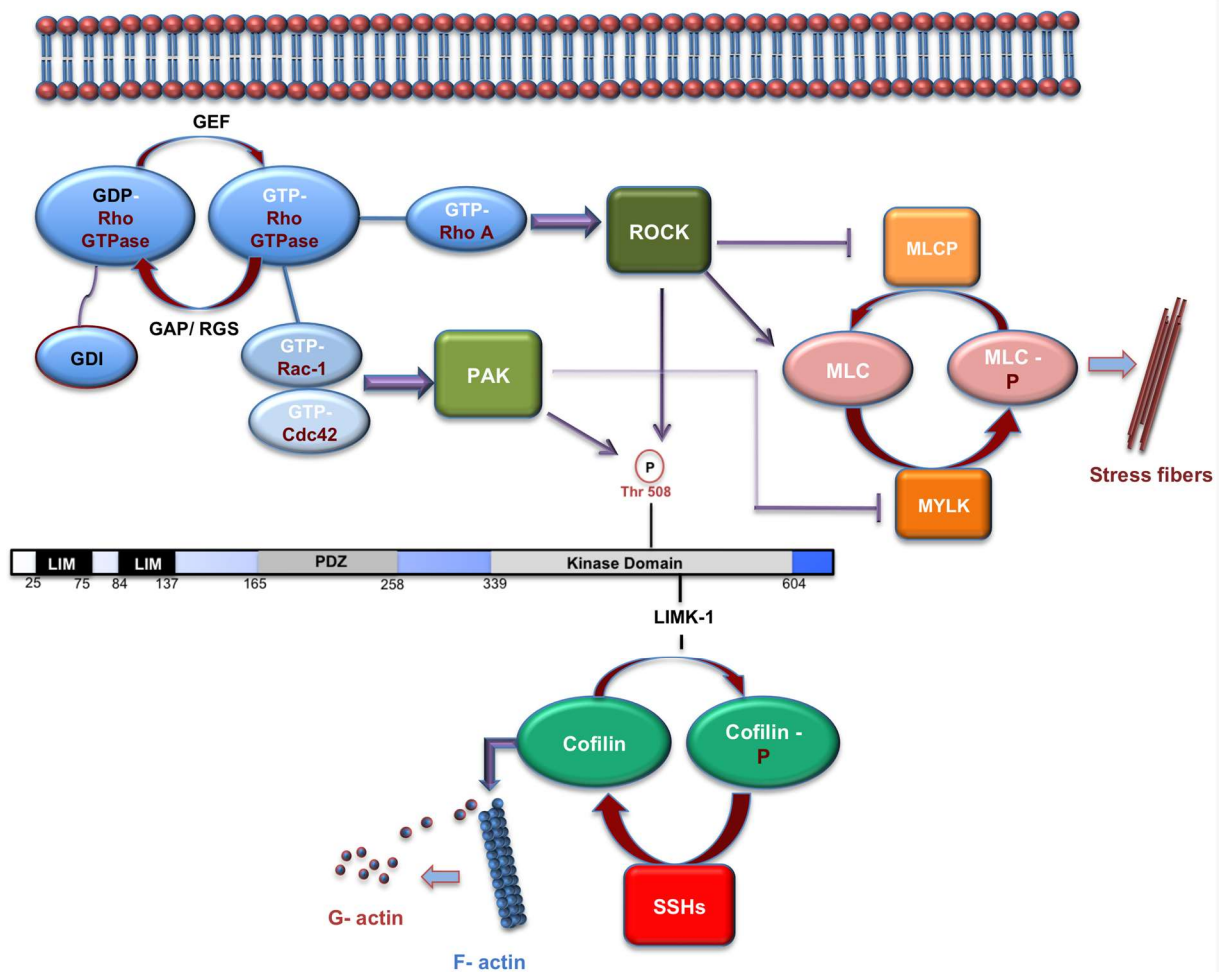
Figure 11. The CFL pathway and the regulation of CFL phosphorylation and activity. The Rho GTPases upon activation by guanine nucleotide exchange factors (GEFs), proceed to activate their downstream targets, ROCK and PAK, both of which phosphorylate LIMK-1 on Thr508, resulting in its activation and the consequent phosphorylation and inactivation of CFL at S3. SSHs dephosphorylate CFL resulting in its activation. ROCK, in addition to modulating the phosphorylation of LIMK-1, also mediates the phosphorylation of myosin light chain (MLC) and promotes stress fiber assembly. PAK phosphorylates myosin light chain kinase (MYLK), another kinase phosphorylating MLC, resulting in its inactivation.

2.4.1 CFL-1 induces EMT

The ubiquitously expressed CFL1 exhibits increased expression levels and activity in cancer cells, correlating with the tumours' EMT (Turhani *et al*. 2006, Maimaiti *et al*. 2017). CFL1's role in defining the direction of cells motility by inducing the formation of cytoskeletal protrusions has been established (Ghosh *et al*. 2004). The small interfering RNA (siRNA)-mediated knockdown (KD) of CFL1, or the promotion of its phosphorylation at S3, owing to the overexpression of a constitutively active LIMK domain, resulted in the disruption of the cellular motility. (Hotulainen *et al*. 2004, Zebda *et al*. 2000, Wang *et al*. 2006). Wang *et al*. confirmed the role of CFL1 in the cytoskeletal reorganization-mediated promotion of EMT. In gastric

cancer, as well as in BGC-823 gastric adenocarcinoma cells, elevated CFL1 levels correlated with the EMT markers. Moreover, treatment of BGC-823 cells with the EMT inducer, TGF-β1 successfully established the EMT phenotype in the un-transfected cells, while cells where CFL1 was knocked down, did not demonstrate the phenotype. The inhibition of cytoskeletal rearrangement mediated by the abolished F-actin depolymerization upon CFL1 KD in the cells was confirmed by TEM. These results were also found *in vivo*, hence highlighting the important role of CFL1 as an EMT inducer (Wang *et al*. 2017).

2.5 PKA signalling enforces the epithelial phenotype

Nadella *et al.* suggested a potential role for PKA in MET. The activation of PKA results in the downregulation of the mesenchymal markers Vimentin and N-cadherin, as well as the upregulation of the epithelial marker E-cadherin. Multiple systems were employed (Mouse Embryonic Fibroblasts; MEFs, HeLa, and HEK293 cells) to confirm the generality of the phenomenon. Interestingly, even though the phenotype was identified and the associated changes in the levels of markers were extensively studied and validated, the protein levels of the master regulator transcription factors SNAIL and twist showed no change upon the manipulation of PKA activity (Nadella *et al.* 2008).

Pattabiraman *et al*. showed that in mesenchymal human mammary epithelial cells, PKA signalling activation induced by cholera toxin (choleragen) and forskolin stimulation, resulted in MET. This was marked by a decrease in the protein levels of mesenchymal markers, vimentin and fibronectin, as well as increased abundance of the epithelial marker, E-cadherin. The epigenetic PKA-mediated alteration in the phenotype of the cells was found to be induced by the histone demethylase PHF2, a PKA substrate and tumour suppressor (Baba *et al.* 2011, Lee *et al.* 2015). PHF2 promoted MET by inducing the demethylation and de-repression of epithelial genes, hence implicating PKA as an enforcer of the epithelial phenotype (Pattabiraman *et al*. 2016).

2.6 Aims of the thesis

AKAPs tether PKA and various other signalling proteins to defined subcellular compartments to create local signalling hubs and bring about spatial and temporal regulation of PKA signalling. This thesis aims to shed light on the biological function of the AKAP GSKIP. GSKIP directly binds PKA and GSK3β and facilitates the PKA inhibitory phosphorylation of GSK3β. The anchoring of PKA to GSKIP also modulates the PKA-mediated phosphorylation of various other substrates, such as that of β-catenin at S675 and of Drp1 at S637. In addition, the scaffolding of GSK3β to GSKIP was found to modulate the phosphorylation of GSK3β substrates, among which is β-catenin. This implicates GSKIP as a modulator of the activity of both GSK3β and PKA.

Previous work in the lab has revealed GSKIP to be a potential regulator of actin dynamics in A549 non-small lung cancer cells. The GSKIP-mediated regulation of the phosphorylation dependent activity of CFL, a unique actin binding protein possessing the ability to sever and depolymerize actin filaments, is the focus of the first part of the thesis. The second part aims to characterize the role of GSKIP in modulating the integrity of cellular junctions and their associated components and examines whether EMT is involved in such modulation.

3. Material and Methods

3.1 Materials

3.1.1 Equipment and software

Table 1a : General equipment

Equipment	Description	Supplier
Beckmann Coulter Centrifuge	Large scale centrifuge	Beckmann Coulter GmbH (Krefeld, DE)
Centrifuge 5415 D	Benchtop centrifuge	Eppendorf (Hamburg, DE)
Centrifuge Universal 320 R	Centrifuge	Hettich (Tuttlingen, DE)
Duomax 1030	Rocking shaker	Heidolph Instruments (Schwabach, DE)
Enspire® 2300	Microplate reader	PerkinElmer (Rodgau, DE)
GFL 3017	Orbital shaker	Gesellschaft für Labortechnik mbH (Burgwedel, DE
IKA® MS 3 basic	Small shaker	IKA (Wilmington, US)
IKA® RCT Standard	Heating plate	IKA (Wilmington, US)
Keyence BZ-8100E	Digital microscope	Keyence (Osaka, Japan)
MicroCentrifuge 2	Micro-scale centrifuge	NeoLab (Heidelberg, DE)
Mini Star Galaxy	Mini-scale centrifuge	VWR (Randor, US)
MiniProtean®	Polyacrylamide gel electrophoresis cell	Bio-Rad Laboratories GmbH (München, DE)
NanoDrop ND-1000	Spectrophotometer	PeqLab Biotechnologie GmbH (Erlangen, DE)
Odyssey Imager	Western blot detection system	LI-COR Biosciences (Bad Homburg, DE)
PipetBoy acu IBS	Pipettor	Integra Biosciences/ Ibs (Fernwald, DE)
Pipettes 2,5/ 10/ 20/ 200/ 1000/ 5000 µL	Pipetting	Eppendorf (Hamburg, DE)

Equipment	Description	Supplier
Power Pac 1000/ 3000	Power supply	Bio-Rad Laboratories GmbH (München, DE)
Sonopuls HD 207	Ultrasond homogenizer	Bandelin electronic GmbH and Co (Berlin, DE)
Thermomixer Compact	Shaking heater	Eppendorf (Hamburg, DE)
Titramax 100	Plate shaking device	Heidolph Instruments (Schwabach, DE)
Trans-Blot	Western blot Transfer System	Bio-Rad Laboratories GmbH (München, DE)
Zeiss Axioskop HBO 50	Fluorescence microscope	Carl Zeiss MicroImaging GmbH (Jena, DE)
Zeiss LSM 780	Confocal microscope	Carl Zeiss MicroImaging GmbH (Jena, DE)

Table 1b : Cell culture equipment

Equipment	Description	Supplier
Cryo-container 5100-0001	Freezing container	Thermo Fisher Scientific/NALGENE (Bonn, D)
GFL 1072	Waterbath	Gesellschaft für Labortechnik mbH (Burgwedel, DE)
Incubator CB210	Cell culture incubator	Binder (Tuttlingen, DE)
Safe 2020	Biological safety cabinet	Thermo Electron LED GmbH (Langenselbold, DE)
ScepterTM 2.0	Cell counter	Merck Millipore (Schwalbach, DE)
Tempcontrol 37-2 digital	Temperature regulator plate	PeCon GmbH (Erbach, DE)
Zeiss Axiovert 25	Inverted microscope	Carl Zeiss MicroImaging GmbH (Jena, DE)

Table 1c : Disposable equipment

Material	Description/Purpose	Supplier
4–20% Mini-PROTEAN® TGX™ Precast Protein Gels	Commercial gradient gels for SDS-PAGE	Bio-Rad Laboratories GmbH (München, DE)
6- and 96-Well Plates	Cell culture plates	TPP (Trasadingen, CH)
96-Well Microplate	96-Well clear microplate	Greiner Bio-One GmbH (Frickenhausen, DE)
Cell Culture Dish (60 and 100 mm)	Cell culture dish	TPP (Trasadingen, CH)
Cell Scraper	Scraping of cells	TPP (Trasadingen, CH)
Centrifuge Tubes (15 and 50 mLs)	Polypropylene centrifuge tubes	Greiner Bio-One GmbH (Frickenhausen, DE)
Cryo-vials	Cryoconservation of cells	Carl Roth GmbH & Co KG (Karlsruhe, DE)
FAST READ 102®	Disposable cell counting slides	Biosigma (Venezia, Italy)
Filter Tips	Sterile pipette tips for cell culture	StarLab (Hamburg, DE)
Hypodermic Needles	Sterile hypodermic needles	B. Braun Melsungen AG (Hessen, DE)
Pipette Tips	Laboratory essential	StarLab (Hamburg, DE)
PVDF Membranes	Western blotting membranes	Carl Roth GmbH & Co KG (Karlsruhe, DE)
Reaction Tubes	Tubes tailored for scientific research	Sarstedt (Nümbrecht, DE)
ScepterTM Sensors 60 µM	Cell counting	Merck Millipore (Schwalbach, DE)
Syringes	Sterile 1 mL syringes	B. Braun Melsungen AG (Hessen, DE)
T75 Cell Culture Flask	Cell culture flask	TPP (Trasadingen, CH)

Table 2 : Software

Software	Description and Purpose	Supplier/URL
Adobe Illustrator CS4	Graphics editor	Adobe Systems, Inc. (San Jose, US)
Adobe Photoshop CS4	Image processing	Adobe Systems, Inc. (San Jose, US)
EndNote X7	Reference management	Thomson Reuters (Toronto, CA)
Image J 1.48v	Image Processing	https://imagej.nih.gov/ij/
Image Studio Lite	Western blot analysis	LI-COR Biosciences (Bad Homburg, DE)
Microsoft Excel 2008	Spreadsheet	Microsoft (Redmond, US)
Micorsoft Power Point 2008	Presentation	Microsoft (Redmond, US)
Microsoft Word 2008	Word processing	Microsoft (Redmond, US)
Prism 5.0c	Biostatistics and graphing	GraphPad Software (CA, US)
ZEN 2011	Confocal microscopy, image processing	Carl Zeiss MicroImaging GmbH (Jena, DE)

3.1.2 Antibodies

Table 3a : Primary antibodies used for Western blot (WB) or Immunofluorescence (IF)

Primary Antibody	Origin	Supplier/Catalogue number
Actin	Mouse	Calbiochem (Nottingham, UK) #CP01
Cofilin	Rabbit	Cell Signalling Technology (Danvers, US); #5175
E-Cadherin	Rabbit	Cell Signalling Technology (Danvers, US); #3195
N-Cadherin	Rabbit	Cell Signalling Technology (Danvers, US); #13116
β-Catenin	Rabbit	Cell Signalling Technology (Danvers, US); #9582
β-Catenin	Rabbit	Santa Cruz Biotechnology (Dallas, US); sc-7199
Chronophin/PDXP	Rabbit	Cell Signalling Technology (Danvers, US); #4686
Desmoplakin I/II	Rabbit	Santa Cruz Biotechnology (Dallas, US); sc-33555
Drp1	Rabbit	Cell Signalling Technology (Danvers, US); #8570
GAPDH	Mouse	Genetex (Irvine, US); GT239
GAPDH	Rabbit	Cell Signalling Technology (Danvers, US); #2118

Primary Antibody	Origin	Supplier/Catalogue number
GSK3β	Rabbit	Cell Signalling Technology (Danvers, US); #9315
GSKIP	Rabbit	Custom-made as described in (Hundsrucker *et al.* 2010) by Biogenes.
HSP90	Mouse	Stressgen (Victoria, CAN); SPA-830
Lamin A/C	Goat	Santa Cruz Biotechnology (Dallas, US); sc-6215
LIMK-1	Mouse	Santa Cruz Biotechnology (Dallas, US); sc-135973
LIMK-1	Mouse	Santa Cruz Biotechnology (Dallas, US); sc-515585
LIMK-1	Rabbit	Santa Cruz Biotechnology (Dallas, US); sc-5576
p38 MAPK α	Rabbit	Cell Signalling Technology (Danvers, US); #2371
OPA-1	Mouse	Abcam (Cambridge, UK); #ab55772
Phospho-cofilin (S3)	Rabbit	Cell Signalling Technology (Danvers, US); #3313
Phospho-Drp1 (S637)	Rabbit	Cell Signalling Technology (Danvers, US); #6319
Phospho-GSK3β (S9)	Rabbit	Cell Signalling Technology (Danvers, US); #9323
Phospho-LIMK-1/2 (Thr 508/505)-R	Rabbit	Santa Cruz Biotechnology (Dallas, US); sc-28409-R
Phospho-p38 MAPK	Rabbit	Cell Signalling Technology (Danvers, US); #4511
Phospho-PKA substrate (RRXS*/T*)	Rabbit	Cell Signalling Technology (Danvers, US); #9624
PP1	Mouse	Santa Cruz Biotechnology (Dallas, US); sc-7482
Phospho-RhoA (S188)	Rabbit	Abcam (Cambridge, UK); #ab41435
Protein Kinase Cα (PKCα)	Mouse	BD Biosciences (Heidelberg, DE); #610107
Rac-1	Mouse	BD Biosciences (Heidelberg, DE); #610650
RhoA	Mouse	Santa Cruz Biotechnology (Dallas, US); sc-418
Rock-1	Rabbit	Santa Cruz Biotechnology (Dallas, US); sc-5560
SNAIL	Rabbit	Cell Signalling Technology (Danvers, US); #9582
α-Tubulin	Mouse	Calbiochem (Nottingham, UK) #CP06
ZEB1/TCF8	Rabbit	Cell Signalling Technology (Danvers, US); #3879

Table 3b : Secondary antibodies used for WB or IF

Secondary Antibody	Origin	Supplier/Catalogue number
Cy3-anti-Rabbit IgG	Mouse	Jackson ImmunoResearch Laboratories; #211-165-109
Cy5-anti-Rabbit IgG	Donkey	Jackson ImmunoResearch Laboratories; #711-175-152
Peroxidase (POD)-anti-Mouse IgG	Donkey	Jackson ImmunoResearch Laboratories; #705-035-151
Peroxidase (POD)-anti-Rabbit IgG	Donkey	Jackson ImmunoResearch Laboratories; #711-036-152
Peroxidase (POD)-anti-Goat IgG	Donkey	Jackson ImmunoResearch Laboratories; ##705-035-147
Protein A-HRP Conjugate	-	Bio-Rad Laboratories GmbH (München, DE); #170-6522

3.1.3 Chemicals and buffers

Table 4a : Chemicals and dyes

Substance	Supplier/Catalog #
30% Acrylamide / Bis Solution	Bio-Rad Laboratories GmbH (München, DE); #1610156
4', 6-Diamidine-2'-phenylindole dihydrochloride (DAPI)	Roche Diagnostics GmbH (Mannheim, DE); #10236276001
Alexa Fluor 647 Phalloidin	Invitrogen (Darmstadt, DE); #A22287
Bovine Serum Albumin (BSA)	SERVA Electrophoresis GmbH (Heidelberg, DE); #11926.04
Coomassie PlusTM Protein Assay Reagent	Thermo Fisher Scientific (Bonn, DE); #1856210
Complete mini EDTA-free	Roche Diagnostics (Mannheim, DE); #REF0693159001
DMEM, GlutaMAX™	Life Technologies GmbH (Darmstadt, DE); #21885108
DMEM/F-12, GlutaMAX™	Life Technologies GmbH (Darmstadt, DE); #31331028
DPBS (1x)	Life Technologies GmbH (Darmstadt, DE); #A1285601
DPBS (10x)	Life Technologies GmbH (Darmstadt, DE); #14200067
Fetal calf serum (FCS) Superior	Biochrom/ Merck Millipore (Schwalbach, DE); #S0615
Forskolin (FSK)	Biaffin GmbH & Co KG Life Sciences Institute (Kassel, DE); #PKE-FORS-050
Glutathione Sepharose® 4 Fast Flow GST-tagged protein purification resin kit	GE Healthcare Europe GmbH (Freiburg, DE); #17-5132-01
ImmobilonTM Western Chemiluminescent HRP substrate	Merck Millipore (Schwalbach, DE); #WBKLS0500

Substance	Supplier/Catalog #
Lumi-Light Western Blotting Substrate	Roche Diagnostics (Mannheim, DE); #12015200001
Immu-MountTM	Thermo Fisher Scientific (Bonn, DE); #99-904-12
Penicillin/Streptomycin	Biochrom/ Merck Millipore (Schwalbach, DE); #A2213
PhosSTOP EASY pack	Roche Diagnostics (Mannheim, DE); #REF04906837001
Precision Plus Protein Standard Dual Color	Bio-Rad Laboratories GmbH (München, DE); #1610374
Skim milk powder	Fluka Analytical/ Sigma (Taufkirchen, DE); #70166
Streptavidin agarose beads	Invitrogen (Darmstadt, DE); #15942-050
Trypsin-EDTA (0.25%)	Life Technologies GmbH (Darmstadt, DE); #25200056
Trypsin-EDTA (0.5%)	Biochrom/ Merck Millipore (Schwalbach, DE); #L2153
Trans blot transfer buffer (5X)	Bio-Rad Laboratories GmbH (München, DE); #1610156

Table 4b : Buffers and solutions

Buffer	Composition
Actin stabilization buffer	0.1 M PIPES; pH 6.9, 30% glycerol; 5% DMSO; 1 mM $MgSO_4$; 1 mM EGTA; 1% TX-100; 1 mM ATP; protease and phosphatase inhibitors
Actin solubilization buffer	1.5% SDS, 25mM Tris HCL pH 6.8
Blocking buffer A (Immunofluorescence; IF)	0.27% fish skin gelatin in 1x DPBS
Blocking buffer B (IF)	5% BSA in 1x DPBS
Blocking buffer A (Western blot)	1% bovine serum albumin (BSA) in 1x TBS-T

Buffer	Composition
Blocking buffer B (Western blot)	5% non-fat milk in 1x TBS-T
Mild lysis buffer (MLB; Immunoprecipitation)	0.2% Triton X-100; 2 mM EDTA; 2 mM EGTA in 1x DPBS; supplemented with protease and phosphatase inhibitors
Phosphate-buffered saline (PBS)	137 mM NaCl 2.7 mM KCl; 1.5 mM KH_2PO_4; 8.1 mM Na_2HPO_4; pH 7.4
Ponceau Red	0.25% Ponceau-S in 3% (v/v) acetic acid
Rhotekin lysis buffer	50 mM Tris; pH 7.2; 1% (w/v) Triton X-100 ; 0.5% sodium deoxycholate; 500 mM NaCl; 10 mm MgCl2 ; PhosSTOP EASY (1 tablet for 10 mL), Complete mini EDTA-free (1 tablet for 10 mL)
RIPA lysis buffer 1 x	50 mM Tris HCl pH 7.4; 150 mM NaCl; 1 mM EDTA; 0.5% Na- Desoxycholate; PhosSTOP EASY (1 tablet for 10 mL), Complete mini EDTA-free (1 tablet for 10 mL)
Sample buffer 4 x	40% glycerine; 8% SDS; 0.4% bromophenol blue; 312.5 mM Tris-HCl; 200 mM DTT; pH 6.8
SDS-polyacrylamide gel electrophoresis (PAGE) running buffer	25 mM Tris; 192 mM glycine; 0.1% SDS
Semi-dry transfer buffer (Western blot)	48 mM Tris; 39 mM glycine; 1.3 mM SDS; 20% (v/v) methanol
Separating gel buffer (SDS-PAGE)	0.625 M Tris-HCl; pH 6.8
Stacking gel buffer (SDS-PAGE)	0.75 M Tris-HCl; pH 8.8
Standard lysis buffer (SLB)	10 mM K$_2$HPO4; 150 mM NaCl; 5 mM EDTA; 5 mM EGTA; 0.5% Triton X- 100; pH 7.4; PhosSTOP EASY (1 tablet for 10 mL), Complete mini EDTA- free (1 tablet for 10 mL)
Tank-blot transfer buffer	20 mM Tris; 150 mM glycine; 0.052 mM SDS; 20% (v/v) methanol
Tris-buffered saline (TBS)	10 mM Tris-HCl; 150 mM NaCl; pH 7.4

Buffer	Composition
Tris-buffered saline + Tween (TBS-T)	0.05% Tween-20 in 1x TBS
Trans blot transfer buffer (1x)	20% (v/v) Trans blot transfer buffer (5x); 20% (v/v) 100% ethanol

3.1.4 Cells

Table 5 : Mammalian cells used, their growth conditions and supplier.

Cell line	Description	Culture medium	Supplier
A549	Human lung adenocarcinoma	DMEM, low glucose, GlutaMAXTM Supplement, pyruvate, 10% fetal bovine serum (FBS); 1% penicillin/streptomycin (100 U/ml)	American Type Culture Collection (ATCC) (Virginia, US) ATCC® CCL-185
HeLa-S3	Human cervical adenocarcinoma	DDMEM, low glucose, GlutaMAXTM Supplement, pyruvate, 10% fetal bovine serum (FBS); 1% penicillin/streptomycin (100 U/ml)	DSMZ (Braunschweig DE)
MCF7	Human breast adenocarcinoma	DMEM, low glucose, GlutaMAXTM Supplement, pyruvate, 10% fetal bovine serum (FBS); 1% penicillin/streptomycin (100 U/ml)	DSMZ (Braunschweig DE)
SHSY5Y	Human bone marrow neuroblastoma	DMEM/F-12, GlutaMAXTM supplement,10% fetal bovine serum (FBS); 1% penicillin/streptomycin (100 U/ml)	DSMZ (Braunschweig DE)

Cell line	Description	Culture medium	Supplier
SW480	Human colon adenocarcinoma	DMEM, low glucose, GlutaMAXTM Supplement, pyruvate, 10% fetal bovine serum (FBS); 1% penicillin/streptomycin (100 U/ml)	DSMZ (Braunschweig DE)
U2-OS	Human bone osteosarcoma cells	DMEM, low glucose, GlutaMAXTM Supplement, pyruvate, 10% fetal bovine serum (FBS); 1% penicillin/streptomycin (100 U/ml)	DSMZ (Braunschweig DE)

3.1.5 siRNAs and recombinant plasmids

Table 6a : siRNAs employed in this thesis

Name	Target/sequence (5'-3')	Supplier/Catalog #
GSKIP (siGENOME-SMART pool)	CCAGGUAGAUGAUCAUUUA, CAACAUGUUUGUCUCGAAA, CGGAUGAUGUGGCCUAUAU, GCUCAAGGUGGUAGGCUAU	Thermo Fisher Scientific (Darmstadt, DE) and GE Healthcare, Chalfont St (Giles, UK)
NT#2 (siGENOME Non-targeting siRNA Pool #2)	(Firefly luciferase) : UAAGGCUAUGAAGAGAUAC, AUGUAUUGGCCUGUAUUAG, AUGAACGUGAAUUGCUCAA, UGGUUUACAUGUCGACUAA	Thermo Fisher Scientific (Darmstadt, DE)

The recombinant plasmids used in this work were generated by Alessandro Dema (Dema *et al.* 2016) and Maike Schulz (AG Klußmann). The GSKIP manipulated sequences were cloned into FLAG tag containing pCMV vector and transformed into TOP10 chemically competent E.Coli cells (Fig. 12) .
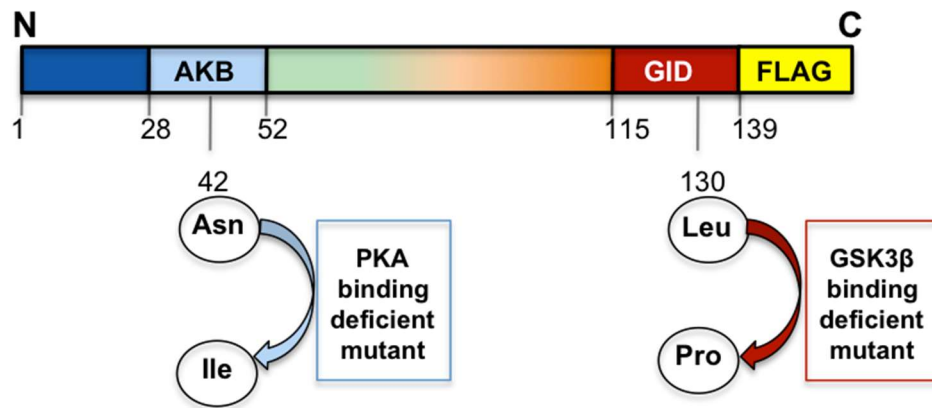
Figure 12. GSKIP-binding deficient mutants, where the interaction between GSKIP and the RII subunits of PKA was abolished by replacing asparagine (Asn) 42 with isoleucine (Ile), while leucine (Leu) 130 was substituted with proline (Pro) to generate the GSK3β binding deficient mutant (Dema *et al.* 2016).

Table 6b : Recombinant plasmids employed in this thesis

Plasmid Name	Target Region/Region	Description
pEGFP_RIIα_WT	WT PKA-RIIα	Full length wild-type PKA-RII
pCMV6_Gskip_Hs_WT_Flag _Non resistant	WT GSKIP	Full length wild-type GSKIP
pCMV6_Gskip_Hs_L130P_F lag_Non resistant	GSK3β-interacting domain (GID) of GSKIP	GSK3β-binding deficient mutant
pCMV6_Gskip_Hs_N42I_Fla g_Non resistant	RII subunits-binding domain (RII BD) of GSKIP	PKA-binding deficient mutant

3.2 Methods

3.2.1.Cell culture techniques

3.2.1.1 *Culturing of cancer cells*

A549, HeLa-S3, SW480, MCF7, and U2-OS cancer cells were grown in DMEM low glucose, GlutaMAXTM and pyruvate supplemented media. SHSY5Y cells were cultured in DMEM/F-12 media containing GlutaMAXTM supplement. 10% fetal bovine serum (FBS) and 1% penicillin/streptomycin (P/S) (100 U/ml) were added to all cell culture media. Confluent cells were washed with ice-cold 1x PBS and treated with 0.25% trypsin-EDTA for 3-5 minutes (mins) at 37°C. The trypsin was inactivated and the cells were resuspended in 5 times the trypsin volume of FBS containing media. A volume of the cell suspension was then transferred into a T75 cell culture flask containing fresh medium and the flask was placed at 37°C and 5% CO_2. The cells were sub-cultured two times per week.

3.2.1.2 *Cryopreservation of cells*

At around 90% confluency, adherent cells were trypsinized and centrifuged (150 g for 5 mins at 4°C) following the conduction of a cell count. The cell pellet was then resuspended in antibiotics free medium containing 10% FBS and 10% dimethyl sulfoxide (DMSO), and around 1 mL of cell suspension ($2x10^6$ cells) was transferred to each 2 mL cryovial. The cryovials were then transferred to an isopropanol filled freezing container and placed at -80°C overnight, to cool the cells down by 1°C/min. The following day, the cryovials were moved to a liquid nitrogen tank for long-term storage.

3.2.1.3 *Thawing frozen cells*

To subculture frozen cells, 10 mL of the cell culture medium were added to a T75 cell culture flask, as well as to a 15 mL conical tube. The cryovial containing ≈ 1 mL of frozen cell suspension was then removed from liquid nitrogen and quickly thawed in a 37°C water bath. The thawed cells mixture was transferred to the conical tube and centrifuged at 1250 rpm for 5 mins. The toxic DMSO containing supernatant was discarded and the cells pellet was resuspended in 5 mL of fresh medium and transferred to the culture medium containing T75 flask for overnight incubation. Upon reaching confluency, the cells were sub-cultured for at least two passages before being employed for experimental procedures.

3.2.1.4 *Cell counting*

Following trypsinization and trypsin quenching, 100 µL of cell suspension were diluted with 1x PBS for a 1:10 final dilution and the cells of 9-21 µM size were counted using either the Scepter™ 2.0 handheld automated cell counter or the Fast-Read 102 disposable slides from Biosigma.

3.2.1.5 *Reverse siRNA transfection*

Lyophilized human GSKIP siRNA SMARTpool and Non-targeting siRNA #2 (NT#2) were reconstituted using RNAse free water and the concentration of the prepared aliquots was measured using NanoDrop ND-1000 (20µM). All transfections were conducted in a 6-well plate format employing siRNA, Opti-MEM® and Lipofectamine® 2000 mixture. For each well of the 6-well plate, two mixtures were prepared, each comprising 250 µL of Opti-MEM and either 5 µL of siRNA (20µM) or 2.5 µL of Lipofectamine 2000. Both were left to stand at room temperature for 5 mins, following which the two mixtures were added together and gently mixed, then incubated for further 15 minutes at room temperature. During the incubation, the confluent cells to be transfected were trypsinized and 350,000 cells in 1.5 mL of antibiotic free culture media were seeded per well. Finally, the siRNA mixture was added to the cells for a final volume of 2 mL per well and the plate was manually and gently shaken to ensure even distribution of the cells, as well as proper mixing of the cells and the transfection mixture. The plate was then placed at 37°C for 24 hours (hrs), after which the culture media was replaced with a fresh one containing antibiotics and the cells were harvested 48 hrs post the introduction of the transfection media.

3.2.1.6 *Rescue experiments: forward DNA transfection*

The rescue of GSKIP KD following reverse siRNA transfection was attained by using plasmid DNA comprising a coding sequence denoting the unmutated wild-type protein, or its kinase-binding deficient mutants. The basis of the rescue experiments was the lipid-mediated (ViaFect™) delivery of the FLAG-tagged vectors to the siRNA-transfected cancer cells. Transfection of the cells with siRNA to knock down GSKIP or with a non-targeting sequence was conducted per protocol (3.2.1.5) and 24 hrs following the introduction of the siRNA transfection mixture, the media was changed to a fresh antibiotics free one, and forward DNA transfection was conducted in a 6-well plate format. Two 6-well plates were employed per each forward transfection experiment, one initially transfected to KD GSKIP and the other transfected with a non-targeting siRNA to serve as a control. For each well 1 µg of DNA was dissolved in 99 µL Opti-MEM® and gently mixed by flicking the tube, then 3 µL of ViaFect were

added and the mixture was incubated for 10 mins at room temperature. 103 µL of forward transfection mixture were added to 2 mL of fresh media in each well and the cells were incubated at 37°C. The media was then replaced with a fresh one after 24 hrs and finally the cells were harvested 48 hrs after the introduction of the forward transfection media.

3.2.1.7 *Transwell migration assay*

The cells were transfected using siRNA to KD GSKIP according to the protocol previously described, such that the cells were around 30%-40% confluent on the subsequent day. P/S free media was changed to media containing 1%P/S and on the following day, cultures were ensured to be below 80% confluency, so that the cells are properly starved without becoming confluent during the 24 hrs starvation period. Serum-containing medium was removed and the cells were gently rinsed with 1x PBS. Culture medium containing 0.1% FBS was added to the cells and they were returned to the incubator for 18-24 hrs at 37°C. On the following day, the cells were harvested using Trypsin/EDTA solution and 0.1% FBS containing media was used to quench the Trypsin. The cells were spun down to remove trypsin/media mixture and the pellet was resuspended in serum-free medium. The cell count was determined and the cell suspension was diluted with serum free media to the necessary seeding concentration.

The trans-wells were set up, such that that 0.1-0.2 mL of the cells in serum free media were seeded to the upper compartment, whereas 0.65 mL of 10% FBS containing media were added to the lower compartment/reservoir and the cultures were incubated for 18 hrs at 37°C. Some receiver wells with serum-free medium (no chemo-attractant) in the lower compartment/reservoir were set up as a control. The day after, the media from inside the upper compartment of the trans-well inserts was aspirated and they were rinsed very well twice in 1x PBS. In 6-well plates, 0.2 ml trypsin/EDTA were added to clean wells and the inserts were transferred to the wells, such that the microporous membrane was fully immersed. The wells were shaken gently and the plate was incubated at 37°C, to ensure complete detachment of the migrated cells from the microporous membrane.

Following incubation, some of the trypsin from each well was transferred to the lower part of the microporous membrane to dislodge any residual cells. The trypsin/EDTA solution was quenched with 10% FBS containing media. The cells were spun down to remove trypsin/media mixture and around 0.1 mL of each mixture was left behind. 0.1 mL of 10% FBS containing media was added to each remaining cells mixture and each mixture was transferred to a 96-well plate, then incubated for around 3 hrs at 37°C. The media was removed, the cells were fixed with 100% ice-cold methanol, and then stained with 0.5% crystal violet for 10 mins at room temperature. The cells were washed twice in a gentle stream of tap water and the plate was left to air dry. 1% SDS was added to each well containing stained cells and the plate was

placed on a bench rocker with a frequency of 120 oscillations per min for around 30 mins. The absorbance was measured at 570 nm and the cellular migration was analysed.

3.2.2.Biochemical methods

3.2.2.1 *Lysis of cells*

The confluent cells were washed with ice cold 1x PBS thrice and scraped into ice cold lysis buffer, where SLB was used for western blot analysis (a), whereas MLB was used for immunoprecipitation experiments (b).

(a) The scraped cells were then passed through a syringe fitted with a 20 G x 1.5" hypodermic needle for 5 times, centrifuged at 14000 RPM for 15 mins at 4°C, and the protein concentration of the collected supernatant was determined using Bradford assay.

(b) The scraped cells were mixed with the lysis buffer by rotation (25 RPMs) for 15 mins at 4°C, then centrifuged at 14000 RPM for another 15 mins and the supernatant was collected and the protein concentration was determined.

3.2.2.2 *Bradford assay*

The protein concentration of the lysates was determined using Coomassie Plus^{TM} Protein assay (Thermo Scientific). The aforementioned assay is based on the acidic environment-mediated binding of proteins to the Coomassie dye, where this binding elicits a spectral shift of the reddish/brown form of the dye (absorbance maximum at 465 nm) to the blue form (absorbance maximum at 610 nm), with the highest difference between the two dye forms being recorded at 595 nm. A standard curve was blotted after measuring the absorbance (Enspire® 2300 microplate reader; 595 nm) of various known concentrations of BSA (0.125-2 mg/ml BSA in deionized water) upon mixing with Coomassie Plus reagent and was used to determine the unknown protein concentrations of the freshly prepared lysates. Following cell lysis, a 1:5 dilution of both the lysate and lysis buffer (control) was prepared and mixed with 250 µL of Commasie Plus reagent per well of the 96-well plate in a triplicate format and the absorbance was measured at 595 nm. Using the linearly fitted standard curve slope as a reference, the concentrations of the lysates were determined and lysis buffer was added to adjust the concentration when required.

3.2.2.3 *SDS-polyacrylamide gel electrophoresis (PAGE)*

SDS-PAGE is an electrophoretic technique employed to separate proteins according to their molecular weights. The rate by which the proteins move through the gel matrix is dependent on their size, with the smaller proteins exhibiting less resistance during migration and hence moving at a faster rate. Total proteins (8-50 µgs) were separated at 25 mA per gel, with 12% SDS-PAGE gels generally used for separation, whereas 15% gels were used for separation of low molecular weight proteins and 8% gels were used for separating their high molecular weight counterparts. 4–20% Mini-PROTEAN® TGX™ precast protein gels were employed for the separation of pulled down complexes comprising proteins of sizes spanning $\simeq$15 kDa through 300 kDa. All gels were run in SDS-PAGE running buffer (Table 4b), using MiniProtean® electrophoresis chambers, and Precision Plus Protein Standard Dual Color (Biorad) marker to indicate the molecular weight of the proteins during separation.

3.2.2.4 *Western blotting*

Proteins separated by electrophoresis were transferred to polyvinylidene fluoride (PVDF) membranes for quantitative analysis. For the transfer of low molecular weight proteins either the Trans-Blot® SD Semi-Dry Electrophoretic Transfer Cell system from Biorad (20 v for 1.5 hrs at RT), or the Trans-Blot® Turbo™ Transfer System from Biorad (1.3 A per gel for 10 minutes at RT) were employed and the corresponding transfer buffer was used for each system. The transfer of the high molecular weight proteins was attained with a wet transfer system/tank-blot (110 V for 150 mins at 4°C), and tank-blot transfer buffer. Following the transfer, the PVDF membranes were washed with deionized water and blocked in 1% BSA in TBS-T for 1 hr at room temperature, then incubated with the blocking buffer diluted primary antibodies for 24-48 hrs at 4°C. The membranes were washed three times, 10 mins each in TBS-T to wash off the non-specific binding and then incubated with the blocking buffer diluted horseradish peroxidase-conjugated secondary antibodies for 1 hr at room temperature, followed by another three washing steps in TBS-T. A peroxidase substrate containing ECL substrate (Millipore/Roche) was added to the membrane and the protein bands were detected using an Odyssey Imaging System. The quantification of the protein bands was conducted using ImageJ 1.48V, where a housekeeping gene was always employed as a loading control.

3.2.2.5 *Immunoprecipation*

Cells were lysed as priorly described in (3.2.2.1) and the protein concentration of the lysates was determined by Bradford assay. A sample of the total protein (input) was collected and boiled with Laemmli buffer at 95°C for 10 mins. The beads to be employed for immunoprecipitation were then equilibrated with the lysis buffer in three rotation cycles (25 RPMs) for 2 mins each at room temperature. Aliquots of samples, each containing 500 μg of protein content in around 500 μL were prepared and 25 μL of the equilibrated beads were added to each sample. 5 μg of the antibody against the protein to be immunoprecipitated were added to the beads-lysate mixture and 5 μg of the corresponding IgG were added to another mixture as a control, then the samples were incubated for 90 mins on a rotator (25 RPMs) at 4°C. Following incubation, the samples were spun down at 700g for 2 mins at 4°C, and the supernatant was collected and boiled with Laemmli buffer at 95°C for 10 mins. The beads were then exposed to 4-5 lysis buffer wash cycles, where after each cycle, the samples were spun down to remove the buffer, fresh lysis buffer was added and the samples were placed on rotation for 2 mins to ensure efficient washing of the beads. Finally the immunoprecipitated protein and its potential interaction partners were eluted from the beads by boiling with Laemmli buffer, in conjunction with vigorous vortexing and analysed by western blotting.

3.2.2.6 *Rhotekin-pulldown assay*

After the siRNA-mediated KD of GSKIP, the cells were incubated for 10 mins with Rhotekin lysis buffer at 4°C, then the cells were scraped and placed on rotation for 15 mins at 4°C with the lysis buffer. Cell debris was removed by centrifugation for 5 mins at 15,000g and 4°C and the supernatant was collected, and its protein content was determined by Bradford assay. Lysates containing 400 μg of protein each were incubated with 100 μL of Rho binding domain (RBD) beads (prepared by Dr. K. Zuehlke), on a rotator (25 RPM) for 90 mins at 4°C. A negative (purified RhoA with GDP; inactive) and a positive control (purified RhoA with GTP; active) were also employed to reaffirm the specificity and efficiency of the used beads. Following incubation, the beads were gently washed three times with Rhotekin lysis buffer, then the bound RhoA was eluted from the beads by boiling with Laemmli buffer and the activity of RhoA was determined through relating the bound fraction to the loading control normalised total protein.

3.2.2.7 *Immunofluorescence*

A549 and HeLa-S3 cells were grown/transfected on 12 mm round coverslips. The media was aspirated and the cells were washed twice with 1x PBS, then fixed with either 10% trichloroacetic acid for 10 mins at room temperature, or ice cold 100% methanol for 15 mins at -20°C. The cells were washed three times with 1x PBS and permeabilised with 0.1% Triton-X for 5 mins at room temperature. The cell coverslips were incubated with blocking buffer (fish skin gelatin (0.27%), or 5% BSA in 1x PBS) for 45 mins at 37°C. The cells were then treated with the blocking buffer diluted primary antibody for 1 hr at room temperature or 45 mins at 37°C, depending on the antibody employed and washed for three times, 10 mins each, with 1x PBS following the incubation. The cells were later incubated with the secondary antibody mixture (fluorophore-attached antibody, the nuclear stain DAPI, and Phalloidin-TRITC or Alexa Fluor 647-Phalloidin) for 45 mins at 37°C and washed thrice with 1x PBS for 10 mins each. Finally the cell coverslips were mounted on microscopic slides employing Immu-MountTM and stored overnight at 4°C. In the case of transfected cells, those cells grown around the glass coverslips were lysed and analysed by western blotting to confirm the success of the siRNA mediated GSKIP KD.

3.2.2.8 *Confocal microscopy (Laser scanning microscope; LSM 780)*

The mounted cover slips were visualized using Zeiss LSM780 confocal microscope at 10x, 40x, and 63x magnifications. Three channels were used for capturing images, DAPI, using a 405 nm laser/415-195 nm filter, CY3, using a 561 nm laser/566-631 nm filter, and CY5, using a 633 nm laser/638-740 nm filter. Digital gain was fixed at 1 and master gain for all channels was set at around 650, while the pinholes were adjusted to 40-70 µm.

3.2.2.9 *Actin fractionation assay*

Following reverse siRNA transfection in a 6-well plate format, confluent A549 cells were washed with ice-cold 1x PBS. 100 µL actin stabilization buffer (Table 4b) were added per well and the plate was placed on a shaker for 10 mins at 115 rpm/min and 4°C. Cells were then dislodged by scraping and the whole lysate was centrifuged at 4°C for 10 mins at 14000 rpm. The globular monomeric G-actin containing supernatant was collected and the filamentous polymerized F-actin containing pellet was solubilised with boiling actin depolymerization buffer (Table 4b). Complete solubilisation of the pellet was ensured through multiple vortexing and heating at 95°C cycles. G- and F- actin samples were separated on 12% SDS-PAGE gels, and then western blotted with actin, CFL, and phospho-CFL antibodies, following blocking in 1% BSA in TBS-T. (Protocol adapted from Rasmussen *et al.* 2010).

4. Results

Previous work in our lab suggested GSKIP acts as a potential regulator of the actin cytoskeletal dynamics in non-small lung cancer A549 cells. In addition, GSKIP was found to interact with SMYD2, an important oncoprotein in various cancers (PhD thesis of Ekaterina Perets). Hence, several cancer cell lines were studied to elaborate on GSKIP's potential role in tumorigenesis.

4.1 GSKIP is expressed in cancer cells of various origins

Different cancer cell lines of varying origins were studied for their endogenous GSKIP abundance (Fig. 13). The cells tested were adenocarcinoma, osteosarcoma, and neuroblastoma cells. Adenocarcinomas are malignant epithelial tumours. They originate from glandular or secretory epithelium, most commonly from lungs, colon, breast, and to a lesser extent from the cervix (Gazdar and Maitra, 2001). Osteosarcoma, the most prevalent bone tumour in children and adolescents, exhibit the formation of malignant spindle cells of mesenchymal origin, which are implicated in osteoid matrix anomalies (Durfee *et al*. 2016). Neuroblastoma is a malignancy that originates in the sympathetic nervous system in infants and young children, with the adrenal medulla and paraspinal ganglia being the major sites of tumour development (Cole and Maris, 2012). GSKIP is ubiquitously expressed in cancer cells, while adenocarcinoma cells express variable levels of GSKIP.
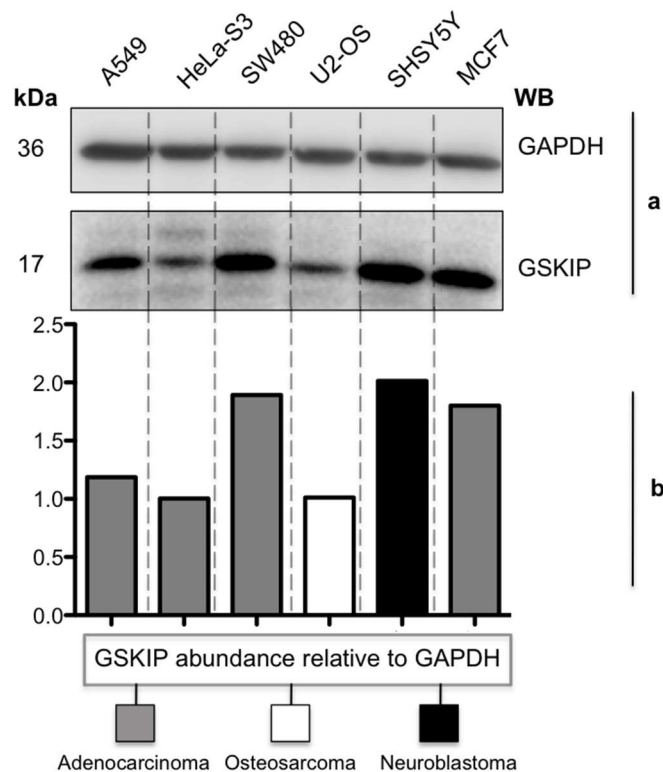
Figure 13. The endogenous GSKIP abundance in cancer cells of varying origins and types. Fig 14a : Western blot signals of GSKIP and of the loading control, GAPDH. Fig 14b : Semi-quantitative analysis of GSKIP protein abundance was conducted by densitometry and normalized to the loading control. A549 : a human non-small lung adenocarcinoma cell line. HeLa-S3, a subclone of the HeLa cell line : a human cervical adenocarcinoma cell line. SW480 : human colorectal adenocarcinoma cell line. U2-OS : human osteosarcoma cell line. SHSY5Y : a human bone marrow neuroblastoma cell line. MCF7 : a human breast adenocarcinoma cell line.

4.2 GSKIP modulates the actin cytoskeleton in A549 cells

4.2.1 GSKIP regulates the activity of CFL, a cytoskeleton modulator

In order to study the potential role of GSKIP in cytoskeletal dynamics, transient KD of GSKIP expression was accomplished by using SMARTpool siGENOME siRNA, where two SMARTpools were employed throughout the practical work to confirm the findings. The KD was found to be stable for 72 hrs post transfection and resulted in around 70% downregulation of the GSKIP protein compared to the non-targeting (siRNA NT) control (Fig. 14).
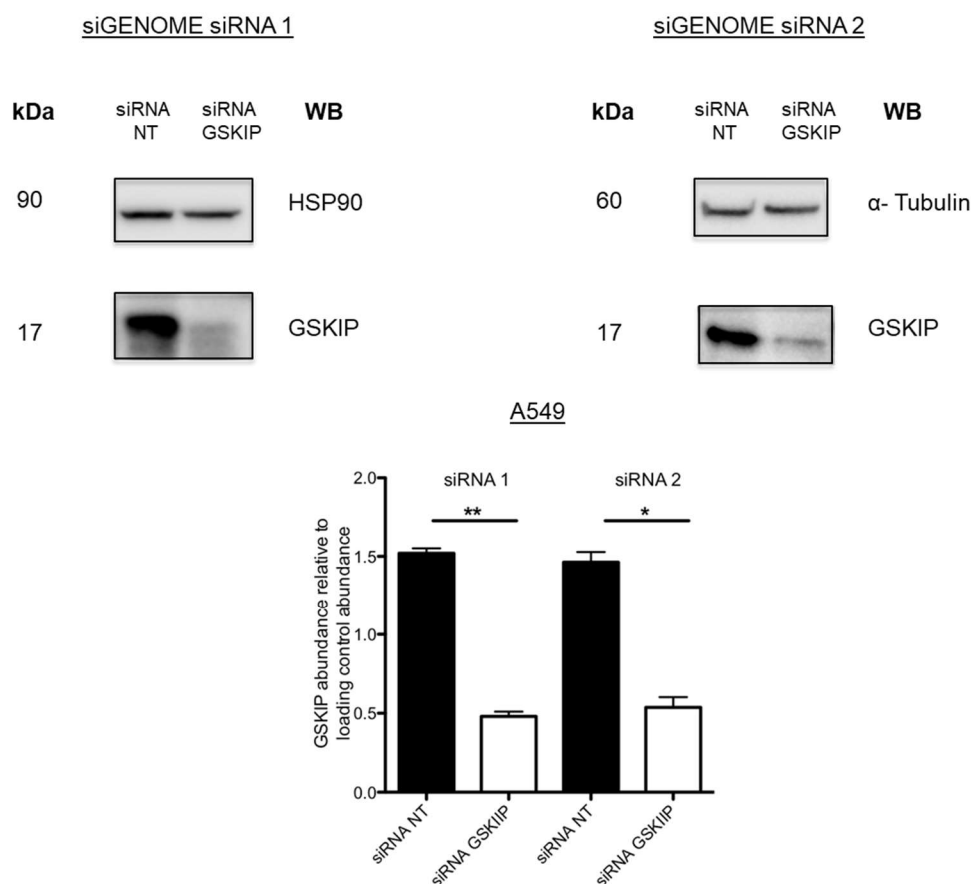
Figure 14. GSKIP KD in A549 cells. A549 cells were treated with two different siRNAs to knock down the expression of GSKIP or with siRNA NT. GSKIP, HSP90, and α-tubulin were detected by Western blotting. Signals

were semi-quantitatively analysed by densitometry and the ratio of GSKIP to loading control was calculated; n = 3, mean ± standard error of the mean (SEM), Paired T-test, *p < 0.05

CFL modulates the actin cytoskeleton through its action on actin filaments, with its activity being tightly regulated by its inhibitory phosphorylation at S3 (section 2.4). Hence the total protein expression levels and the phosphorylation of CFL were studied upon the KD of GSKIP in A549 cells. GSKIP KD significantly reduced the phosphorylation of CFL at S3, relative to the total protein abundance (Fig. 15), which in turn translates to increased activity.
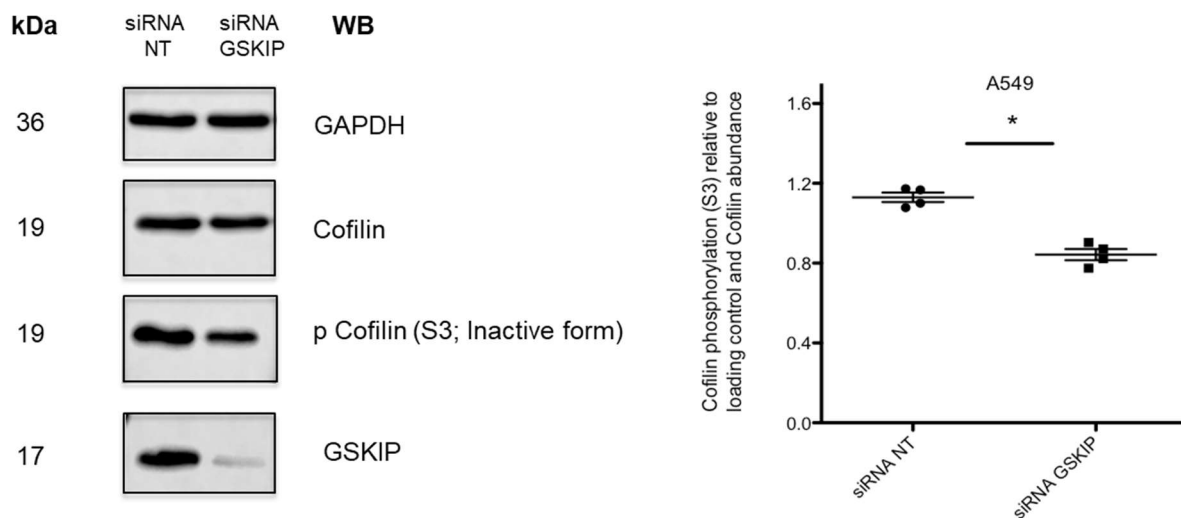
Figure 15. GSKIP KD in A549 cells decreases CFL S3 phosphorylation. A549 cells were treated with siRNA to knock down the expression of GSKIP or with siRNA NT. CFL and phospho-CFL (S3) were detected by Western blotting. Signals were semi-quantitatively analysed by densitometry and the ratio of phosphorylated CFL to normalised CFL (total CFL to GAPDH) was calculated; n = 4, mean ± SEM, Paired T-test, *p < 0.05

4.2.2 Actin fractionation reveals altered CFL abundance and distribution upon GSKIP KD

Actin exists in two states within the cell, the monomeric globular (G) and the polymerized filamentous (F)-actin forms. Each actin monomer maintains strong interactions with two other monomers through its tight binding sites, eventually forming polymerized actin filaments (Cooper, 2000). Actin fractionation was employed to separate the two actin fractions and study the CFL levels in each fraction. Whereas the majority of the CFL pool appears to be associated with G-actin (Fig. 16), a marked decrease in the abundance of CFL under the F-actin fraction was observed when GSKIP was knocked down (Fig. 16), indicating changes in the actin dynamics. The KD-mediated decrease in the CFL pool under both actin fractions is on par with the decrease in its total abundance (Fig. 17). Despite the pronounced decrease in CFL levels under the polymerized F-actin fraction, most of CFL is associated with the monomeric G

fraction, which explains why the decrease concerning the total CFL pool and the G actin associated one mimic each other.
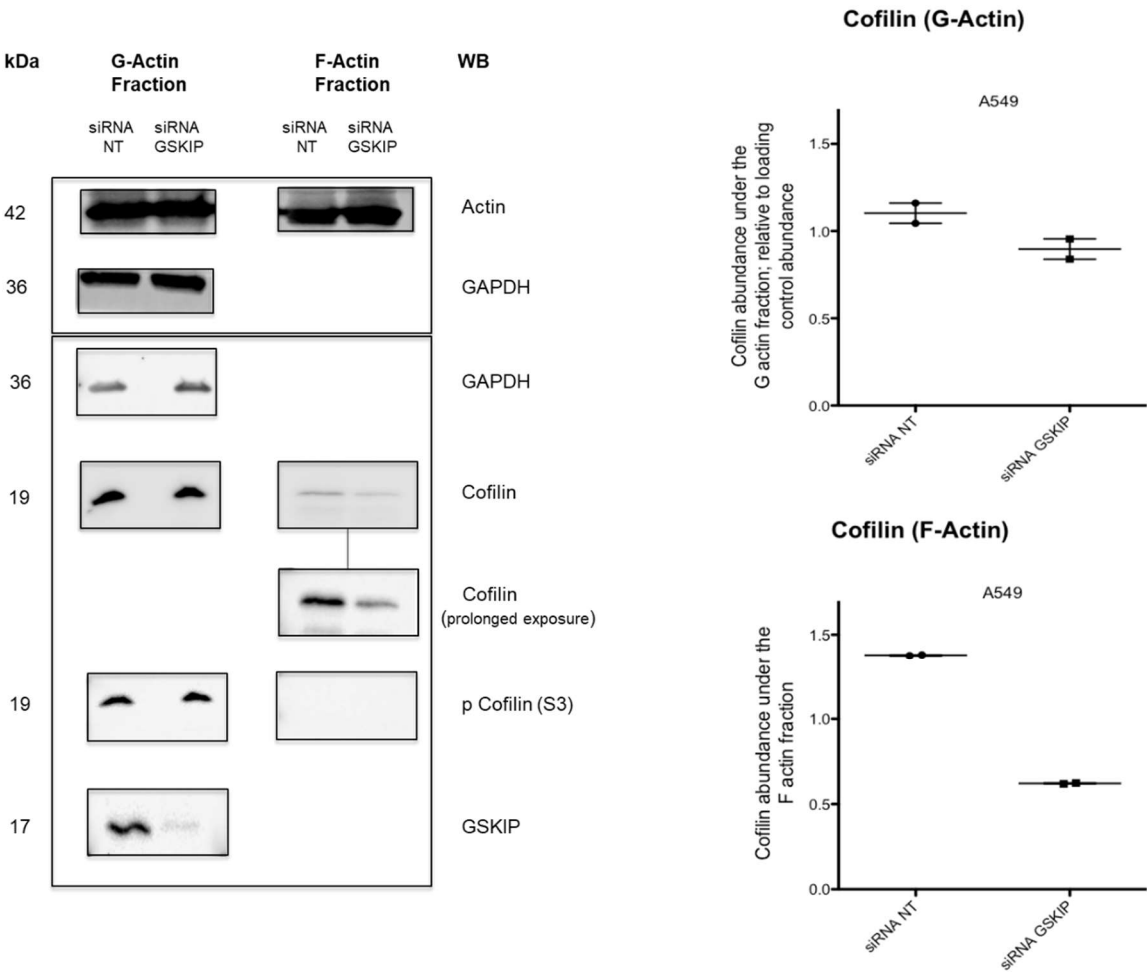
Figure 16. GSKIP KD in A549 cells decreases CFL abundance in the F-actin fraction. A549 cells were treated with siRNA GSKIP to knock down the expression of GSKIP or with siRNA NT. The G-actin and the F-actin fractions were separated and the fraction relating to each siRNA treatment was studied for CFL and phospho-CFL (S3) by Western blotting. Signals were semi-quantitatively analysed by densitometry and the ratio of CFL to GAPDH and phosphorylated CFL to GAPDH calculated; n = 2, mean ± SEM.
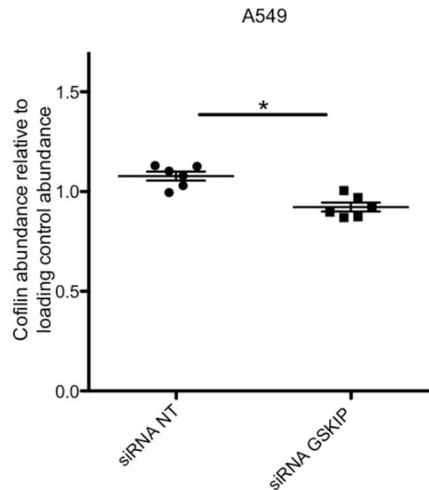
Figure 17. GSKIP KD in A549 cells decreases the total CFL abundance. A549 cells were treated with siRNA to knock down the expression of GSKIP or with siRNA NT. CFL was detected by Western blotting. Signals were semi-quantitatively analysed by densitometry and the ratio of total CFL to GAPDH was calculated; n = 6, mean ± SEM, Paired T-test, *p < 0.05

4.2.3 Junctional actin anomalies upon GSKIP KD in A549 cells

The KD-induced decrease in the phosphorylation of CFL relative to its total abundance and its decreased distribution under the polymerized actin fraction indicates modified CFL activity. Therefore fluorescence microscopy experiments were conducted in order to study the F-actin cytoskeleton in A549 cells. The KD of GSKIP resulted in increased depolymerization at the cellular junctions, reaffirming the increase in CFL activity (Fig. 18).
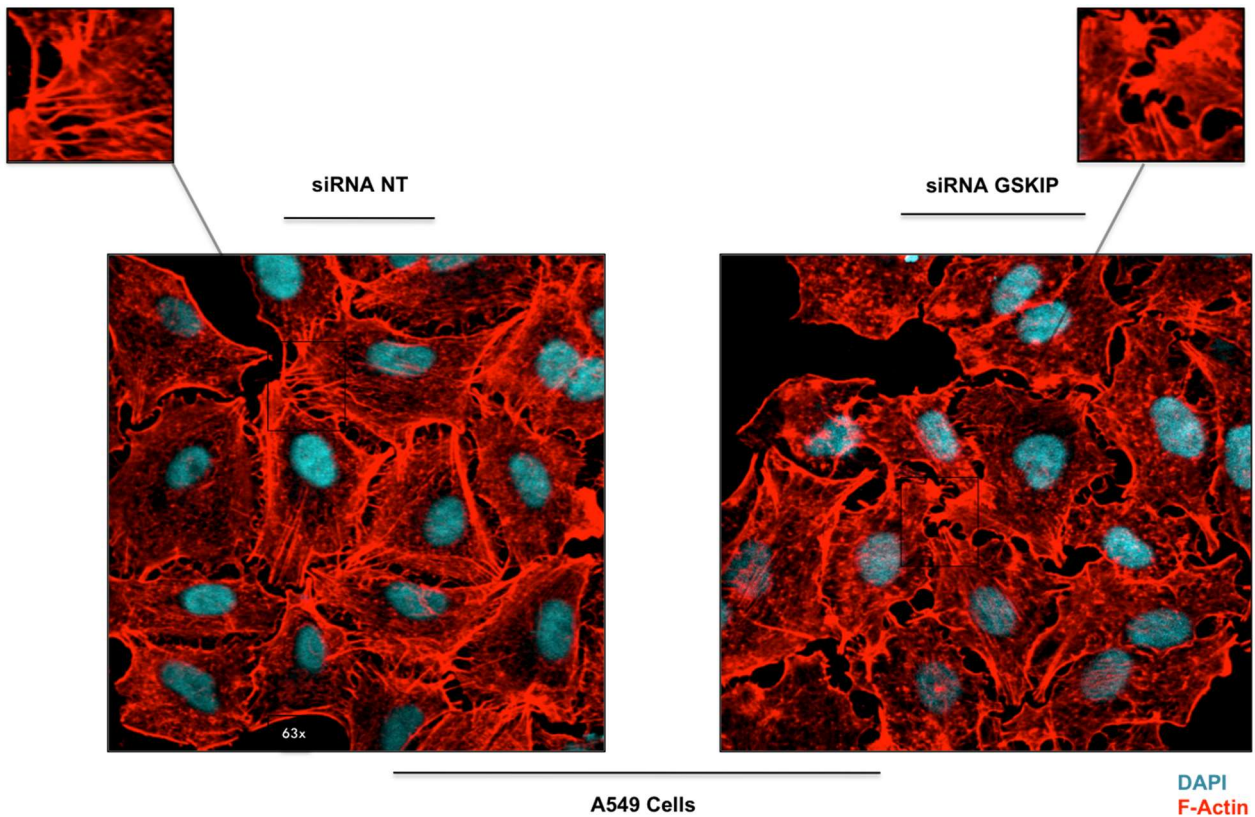
Figure 18. GSKIP KD in A549 cells causes increased actin depolymerization at cellular junctions. Representative fluorescence microscopic analysis of A549 cells transfected with siRNA to knock down the expression of GSKIP or with siRNA NT. Cyan: DAPI (nuclear staining), Red: Phalloidin (F-actin staining). Shown is a representative result of three independent experiments

4.3. GSKIP influences actin dynamics in various cancer cells

4.3.1 GSKIP modulates CFL phosphorylation at S3 in various cancer cell models

Actin cytoskeleton dynamics are essential for various processes in cancer cells. In order to better understand the extent of GSKIP's CFL modulatory effect on CFL, various cancer cell models were evaluated for CFL protein expression levels and phosphorylation at S3 upon the KD of GSKIP. The reduction in the inhibitory phosphorylation of CFL was consistent throughout all adenocarcinoma cell lines tested, whereas an elevation was recorded in the osteosarcoma cell line. No marked change was observed in the neuroblastoma cells (Fig. 19).
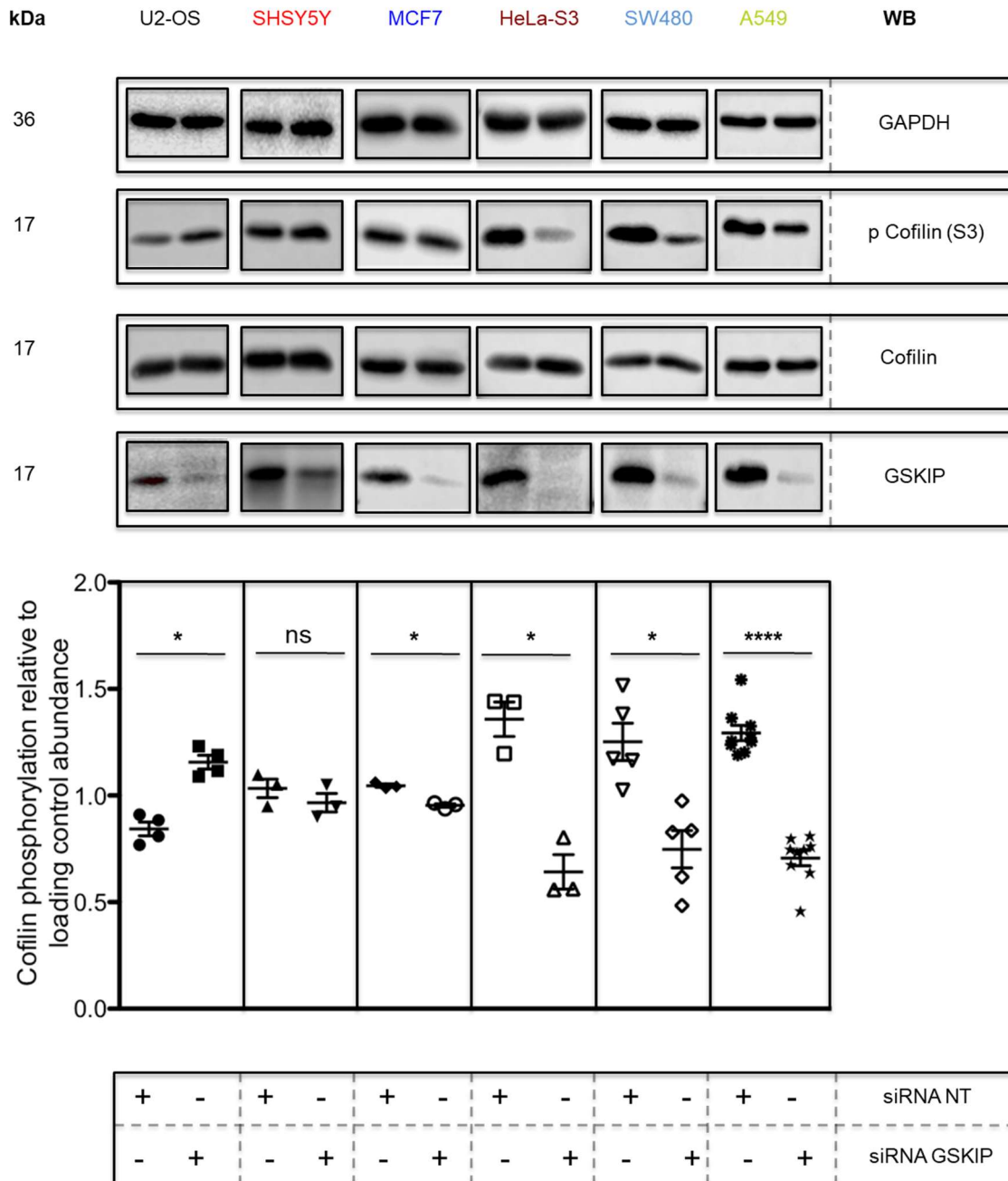
Figure 19. GSKIP KD in U2-OS, MCF7, HeLa-S3, SW480, and A549 cells alters CFL phosphorylation at S3. Cells were treated with siRNA to knock down the expression of GSKIP or with siRNA NT. CFL and phospho-CFL (S3) were detected by Western blotting. Signals were semi-quantitatively analysed by densitometry and the ratio of phosphorylated CFL to GAPDH calculated; n = 4, n = 3, n = 3, n = 3, n = 5, n = 9, mean ± SEM, Paired T-test, *p < 0.05. A549 : a human non-small lung adenocarcinoma cell line. HeLa-S3, a subclone of the HeLa cell line : a human cervical adenocarcinoma cell line. SW480 : human colorectal adenocarcinoma cell line. U2-OS : human osteosarcoma cell line. SHSY5Y : a human bone marrow neuroblastoma cell line. MCF7 : a human breast adenocarcinoma cell line.

4.3.2 GSKIP abundance is unrelated to the changes in CFL phosphorylation status

The KD of GSKIP in various cancer cells yielded varying outcomes, and hence the endogenous GSKIP protein levels were evaluated against the average change in the phosphorylation of CFL at S3 (Fig. 20). The highest endogenous levels were recorded for SHSY5Y and MCF7 cells, both of which exhibited the least change in the KD-induced alteration in CFL phosphorylation. On the contrary, the lowest endogenous GSKIP abundance was detected in HeLa-S3 cells, which demonstrated the highest CFL phosphorylation change.
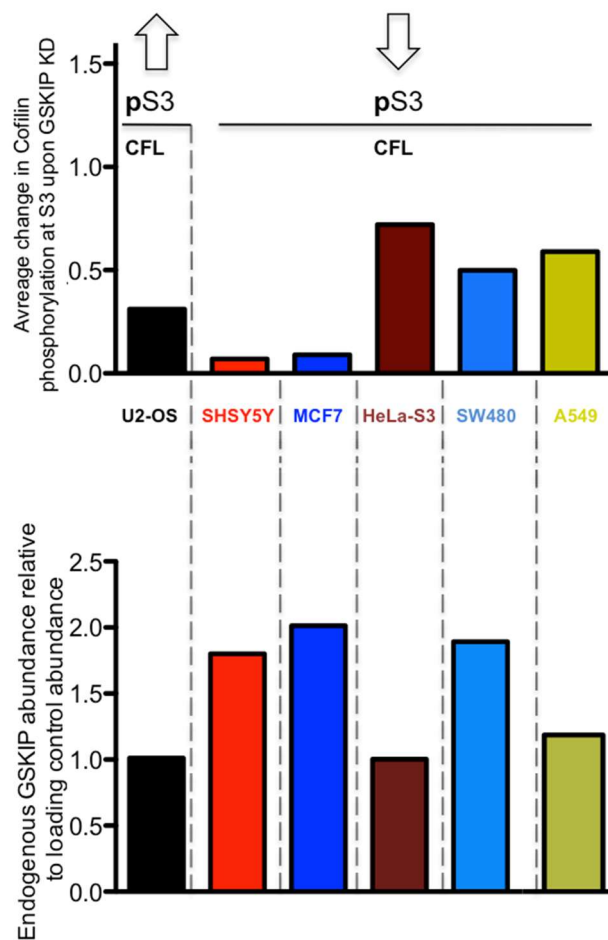
Figure 20. Average change in CFL phosphorylation upon GSKIP KD compared to the endogenous GSKIP abundance in U2-OS, SHSY5Y, MCF7, HeLa-S3, SW480, and A549 cells. The change in the phosphorylation of CFL at S3 (elevation in U2-OS and reduction in other cell models) is unrelated to the endogenous protein levels of GSKIP.

4.3.3 GSKIP KD causes cytoskeletal and junctional anomalies in HeLa-S3 cells

The highest reduction in CFL phosphorylation upon GSKIP KD was encountered in HeLa-S3 cells. To evaluate the potential changes of the cellular cytoskeleton, F-actin was stained with phalloidin. GSKIP KD resulted in decreased F-actin at the junctions, and increased stress fibers in the cells (Fig. 21). Moreover, a phenotypic change that resembled the one seen during EMT was also apparent upon the KD.
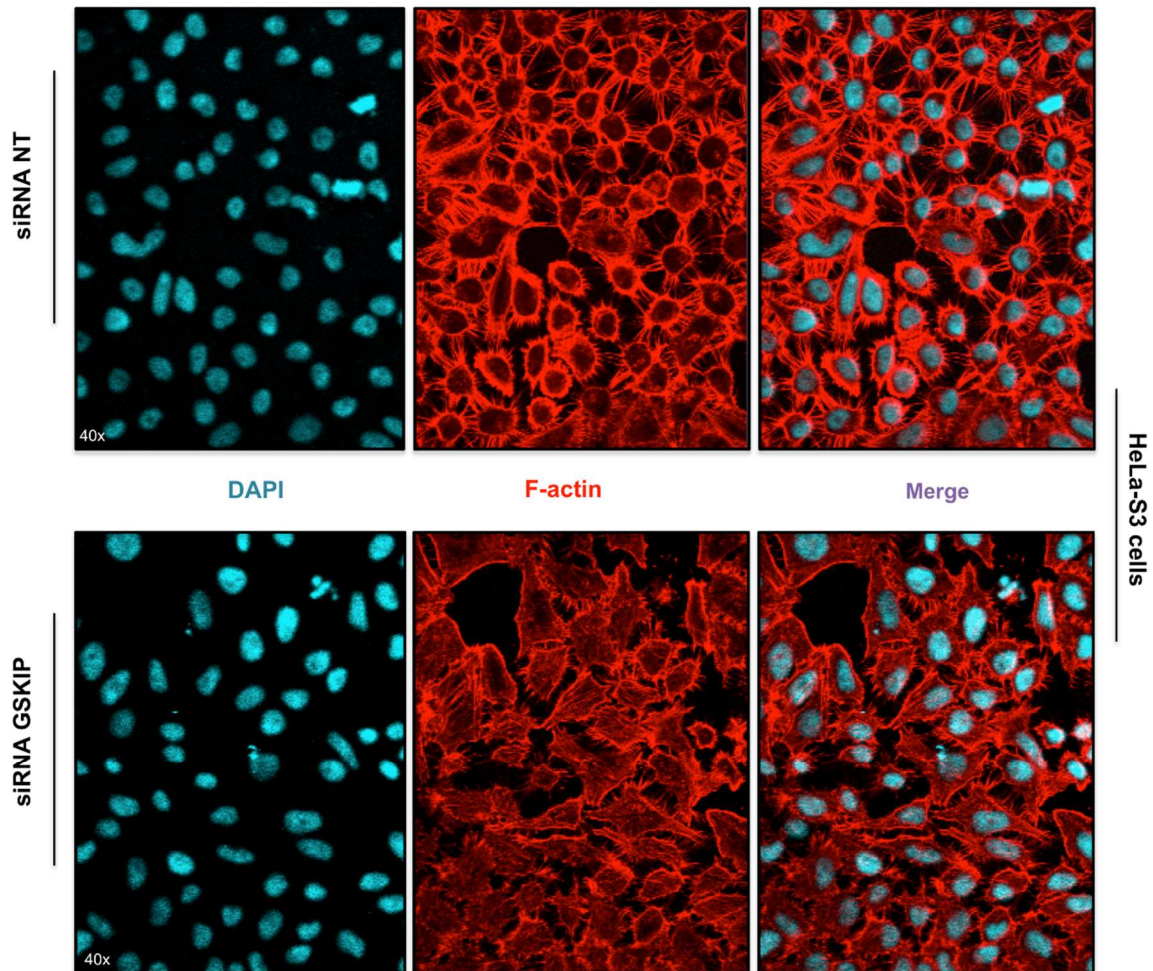
Figure 21. GSKIP KD in HeLa-S3 cells alters the cytoskeleton. Representative fluorescence microscopic analysis of HeLa-S3 cells transfected with siRNA to knock down the expression of GSKIP or with siRNA NT. Images were taken at 40x magnification. Red: Phalloidin (F-actin cytoskeleton staining), Cyan : DAPI (nuclear staining). Shown is a representative result of three independent experiments.

4.4   GSKIP alters CFL phosphorylation independently of Rho GTPases and MAP Kinases

4.4.1 GSKIP KD upregulates Rho GTPases in A549 and HeLa-S3 cells

The activity of CFL is dependent on its negative regulatory phosphorylation by LIMK-1 on S3. Therefore, the expression levels of the LIMK-1 upstream regulators the Rho GTPases, RhoA and Rac-1 were examined. RhoA and Rac-1 control the activity of the kinases ROCK and PAK1 respectively, both of which are modulators of the phosphorylation and activity of LIMK-1. The KD of GSKIP significantly upregulated both Rho GTPases (Fig. 22), indicating a potential role in the decreased CFL phosphorylation.
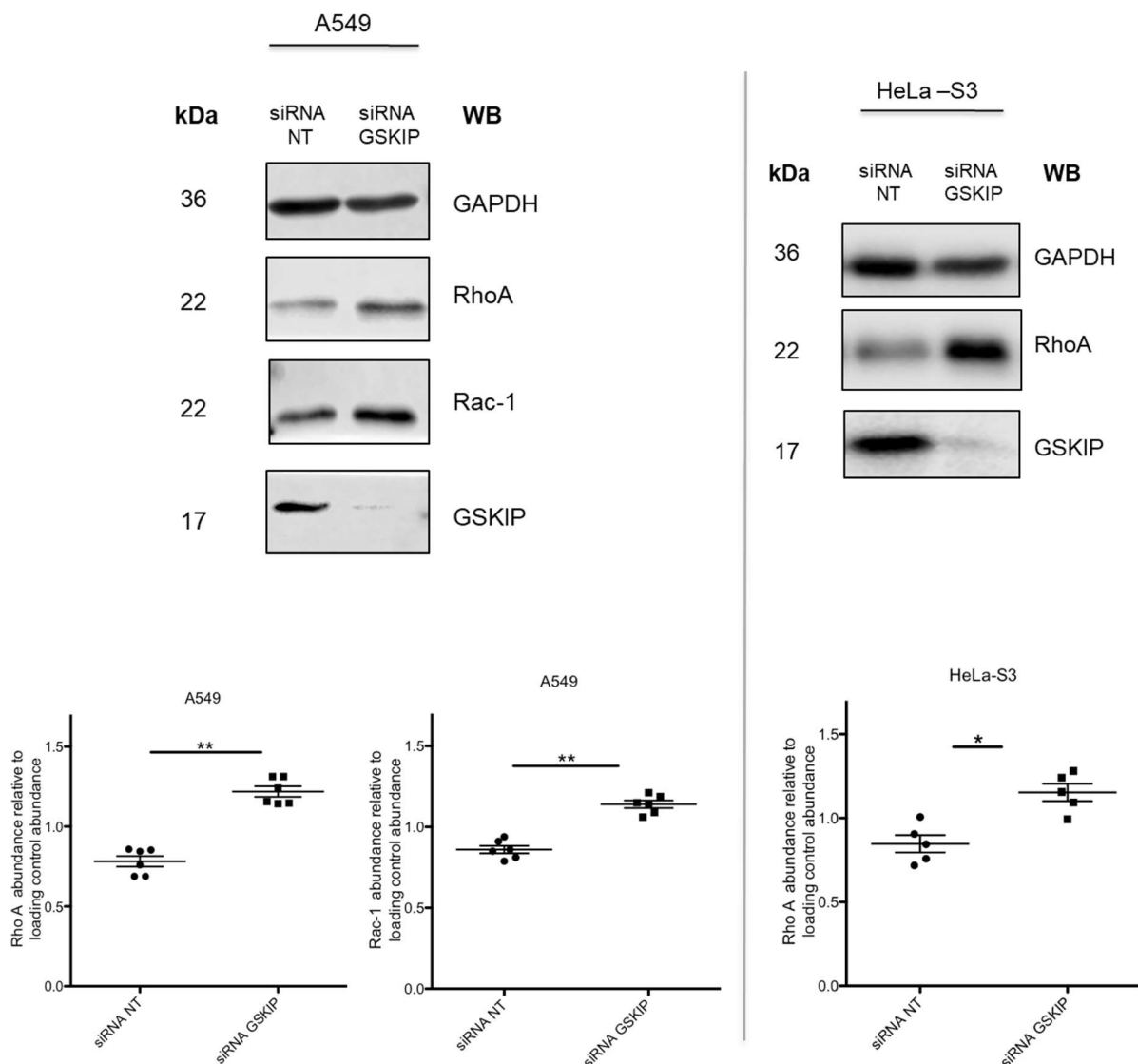
Figure 22. GSKIP KD in A549 and HeLa-S3 cells upregulates Rho GTPases. Cells were treated with siRNA to knock down the expression of GSKIP or siRNA NT. RhoA and Rac-1 were detected by Western blotting. Signals were semi-quantitatively analysed by densitometry and the ratio of Rho GTPases to GAPDH calculated; n = 6, n = 6, n = 5, mean ± SEM, Paired T-test, *p < 0.05.

4.4.2 GSKIP KD has no impact on the activity of RhoA in HeLa-S3 cells

The change in the abundance of the Rho GTPases upon GSKIP KD suggested a potential change in their activity. Thus, employing E-coli competent cells, the Rho binding domain (RBD) of the Rhotekin protein was expressed as a tagged GST fusion protein and purified using affinity chromatography resin. The domain only binds to the GTP-bound active fraction of RhoA and hence was used to precipitate active RhoA from the lysates. GSKIP KD had no significant impact on the activity of RhoA in HeLa-S3 cells (Fig . 23), This, in turn, necessitated studying the Rho GTPases-controlled phosphorylation sites on LIMK-1 to uncover the underlying mechanism behind altered CFL phosphorylation.
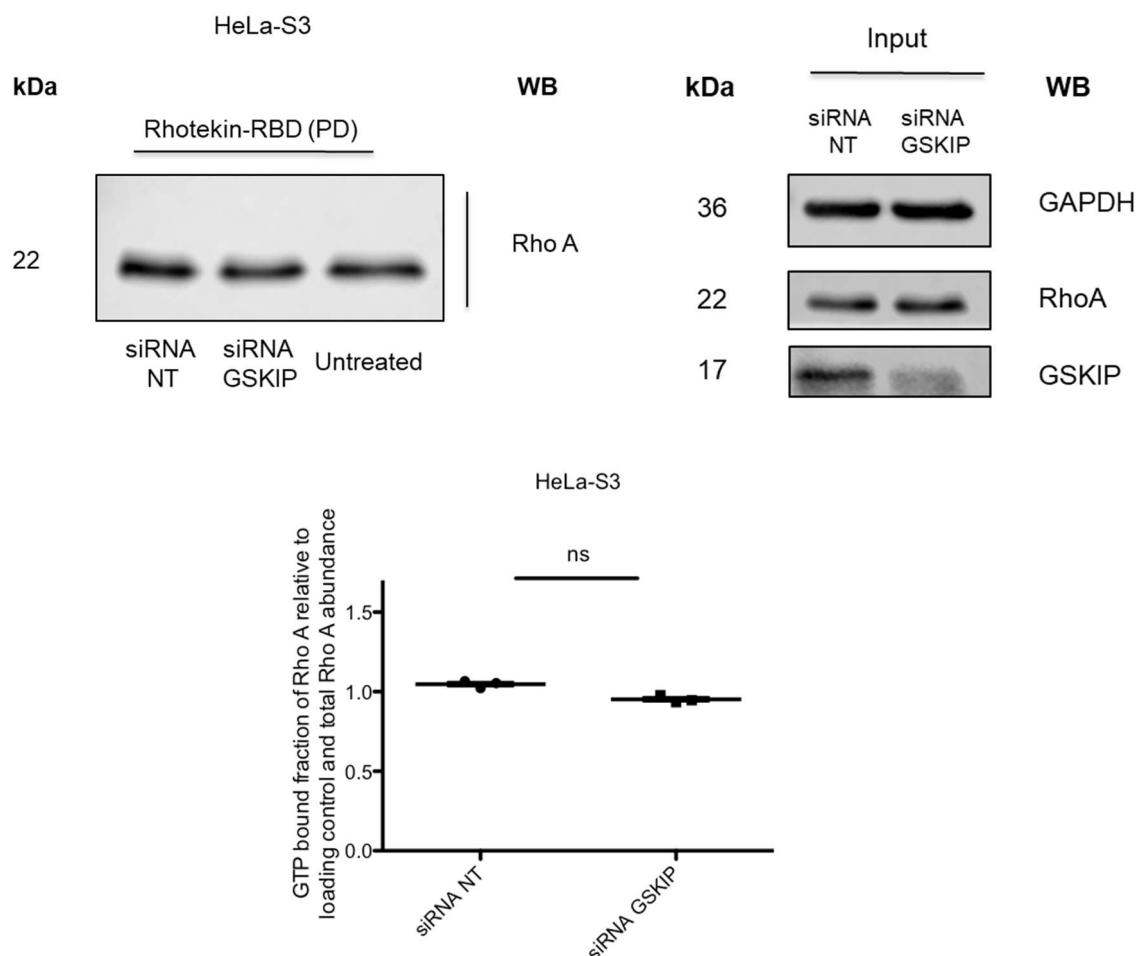
Figure 23. GSKIP KD does not affect RhoA activity in HeLa-S3 cells. Cells were left untreated or treated with siRNA to knock down the expression of GSKIP or with siRNA NT. Active GTP-bound RhoA was precipitated with

(RBD) affinity chromatography resin. RhoA, GAPDH, and GSKIP were detected in the input fraction, and RhoA was detected in the pulldown (PD) one by Western blotting, with GAPDH being employed as a loading control for the input . Signals were semi-quantitatively analysed by densitometry and the ratio of active RhoA to normalized total RhoA (total RhoA to GAPDH) was calculated; n = 3, , mean ± SEM, Paired T-test, *p < 0.05. ns: non-significant.

4.4.3 GSKIP KD does not affect the PKA phosphorylated GDP-bound fraction of RhoA in A549 cells

The PKA-mediated phosphorylation of RhoA at serine 188 (S188), enhances its binding to RhoGDI and hence suppresses its activity. While the GTP-bound fraction of RhoA was unchanged upon GSKIP KD in HeLa-S3 cells and since GSKIP is a direct interaction partner of PKA, the PKA phosphorylated GDP-bound inactive fraction was studied in A549 cells, as the employed antibody did not work with HeLa cell lysates. The KD of GSKIP had no effect on the S188 phosphorylation of RhoA (Fig. 24).
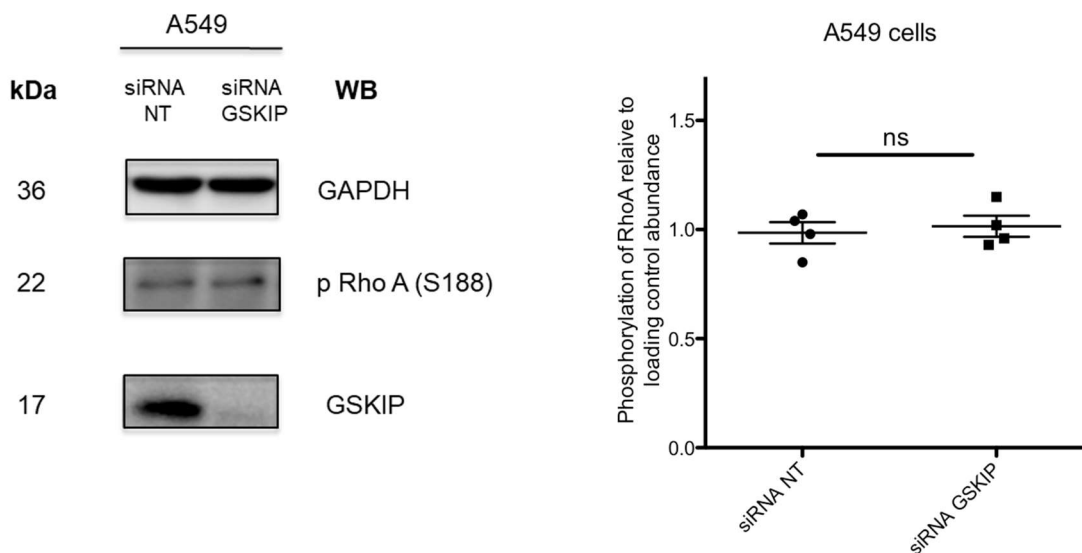
Figure 24. GSKIP KD in A549 does not alter the S188 phosphorylated GDP-RhoA fraction . Cells were treated with siRNA to knock down GSKIP or with siRNA NT. P RhoA (S188) was detected by Western blotting. Signals were semi-quantitatively analysed by densitometry and the ratio of p RhoA (S188) to GAPDH calculated; n = 4, mean ± SEM, Paired T-test, *p < 0.05.

4.4.4 GSKIP does not form a complex with RhoA in A549 and HeLa-S3 cells

Both PKA and GSK3β have been implicated in the regulation of RhoA activity (Lang *et al.* 1996, Jiang *et al.* 2008). Thus, to exclude RhoA from the cytoskeletal reorganizational changes evident upon the KD of GSKIP, the possibility of complex formation between GSKIP and RhoA was examined. In addition, the interactions mediating the potential complex formation between GSKIP and RhoA, whether GSKIP-PKA RIIα-mediated or GSKIP-GSK3β-mediated were also

studied. However, complex formation between GSKIP and PKA RIIα wasn't detectable, neither upon the immunoprecipitation of endogenous GSKIP, nor when overexpressed FLAG-tagged GSKIP was immunoprecipitated. This necessitated the overexpression of both GSKIP and PKA RIIα. The human protein atlas shows that the endogenous RNA levels of GSKIP and PKA RIIα are much lower than those of RhoA in A549 and HeLa cells (at least 12 times lower), pointing towards higher protein levels of RhoA. Therefore, either wild type full-length GSKIP (FLAG-tagged) was expressed or both wild type GSKIP (FLAG-tagged) and wild type PKA RII alpha (GFP-tagged) were co-expressed in A549 and HeLa-S3 cells. Anti-FLAG immunoprecipitation was conducted to isolate the FLAG-tagged GSKIP and the corresponding co-immunoprecipitation (co-IP) with either PKA RIIα or GSK3β was validated. The presence of RhoA was then analysed under each co-IP. The overexpression of PKA RIIα is possibly associated with increased constraint on the catalytic (C) subunits of PKA, since RIIα inhibits the C subunit of PKA and hence forskolin (FSK) stimulation was conducted to elevate cAMP levels, activate PKA, and circumvent the issue in question.
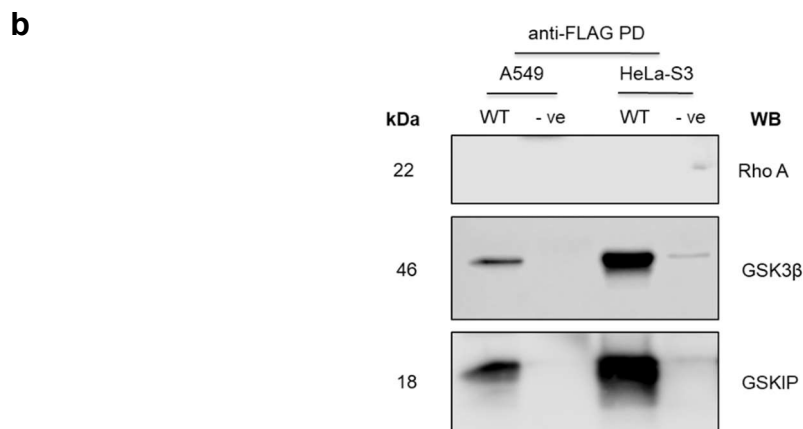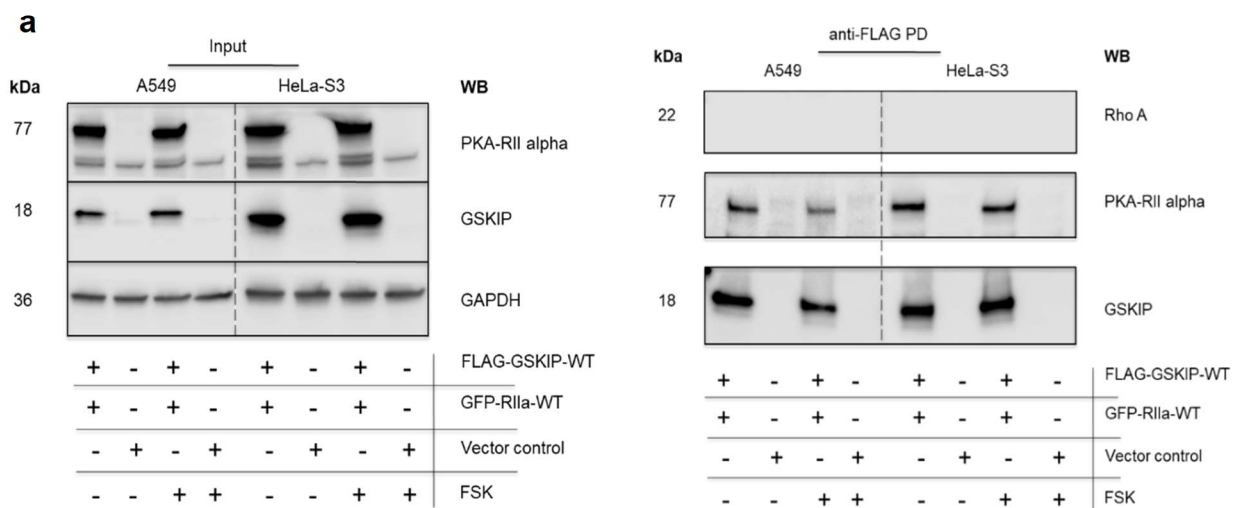
Figure 25. GSKIP is not incorporated into a complex comprising RhoA. A549 and HeLa-S3 cells were transfected with the indicated plasmids and treatments, lysed and anti-FLAG immunoprecipitation was carried out to study the presence of PKA RIIα-mediated complex formation between GSKIP and RhoA (a). A549 and HeLa-S3 cells were transfected with FLAG-GSKIP-WT, lysed, and exposed to an anti-FLAG immunoprecipitation to evaluate the presence of GSK3β-mediated complex formation between GSKIP and RhoA (b). GSKIP, GSK3β, PKA-RII alpha, and GAPDH were detected by Western blotting. n = 2.

4.4.5 GSKIP KD does not influence the Rho GTPase-mediated phosphorylation of LIMK-1 in HeLa-S3 cells

The activity of LIMK-1 is regulated by its phosphorylation at various sites, Thr508, which is mediated by ROCK and PAK1, S323, which is controlled by MK2, a downstream kinase of p38 MAPK, and S596 by PKA. For the phosphorylation of CFL to be altered, the upstream phosphorylation of LIMK-1 would have to be modified. In order to elucidate the GSKIP KD-mediated change in CFL activity, the Rho GTPases-dependent phosphorylation of LIMK-1 was studied in HeLa-S3 cells. The KD of GSKIP had no effect on the phosphorylation of Thr508 (Fig. 26), which in turn implicates either PKA or MK2 as the kinases behind the observed change in CFL phosphorylation at S3.
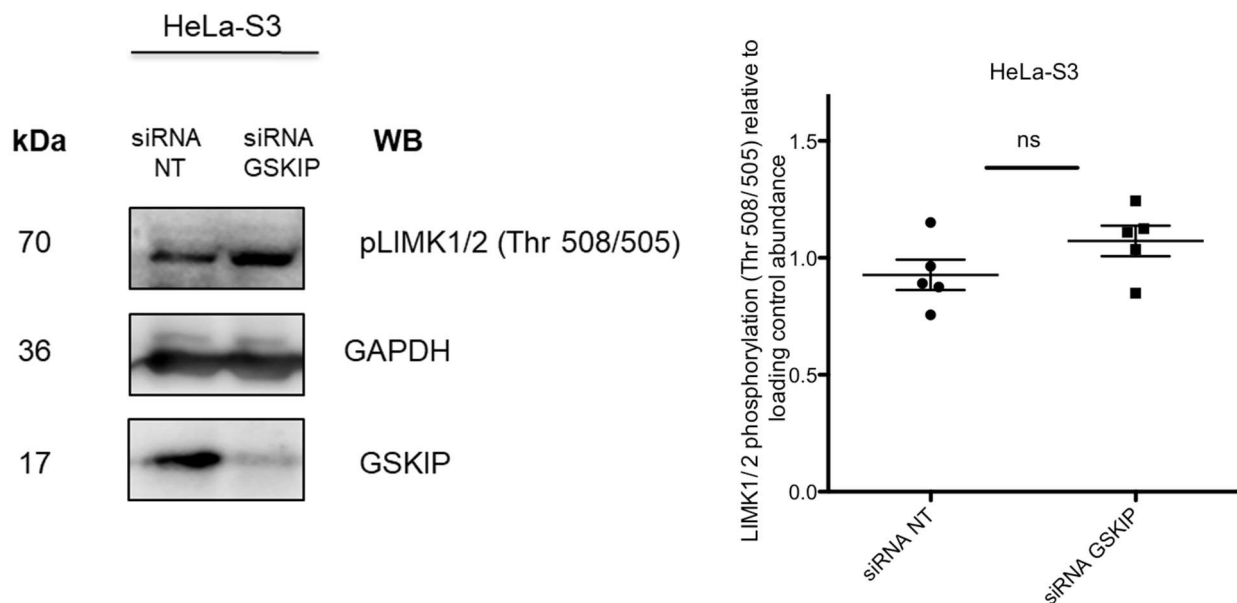
Figure 26. GSKIP KD in HeLa-S3 cells has no effect on active LIMK-1. HeLa-S3 cells were treated with siRNA to knock down the expression of GSKIP or with siRNA NT. pLIMK (Thr 508/505) was detected by Western blotting. Signals were semi-quantitatively analysed by densitometry and the ratio of pLIMK to GAPDH was calculated; n = 5, mean ± SEM, Paired T-test, *p < 0.05

4.4.6 GSKIP does not form a complex with various cytoskeletal regulators in A549 cells

To better understand the underlying mechanisms behind the change in CFL activity upon the KD of GSKIP, the possibility of GSKIP forming a complex with some of the major regulators of actin dynamics was evaluated in co-IP studies in A549 cells.. LIMK-1 appears to form complexes with ROCK1 and p38 MAPKα, but not GSKIP (Fig. 27). However, since the complex comprising both endogenous GSKIP and PKA RIIα has proven to be problematic to immunoprecipitate, as the co-IP between GSKIP and the RIIα subunits was only evident upon the overexpression of both proteins (Fig. 25), there is the possibility that LIMK-1 and GSKIP are involved in a PKA mediated transient complex.
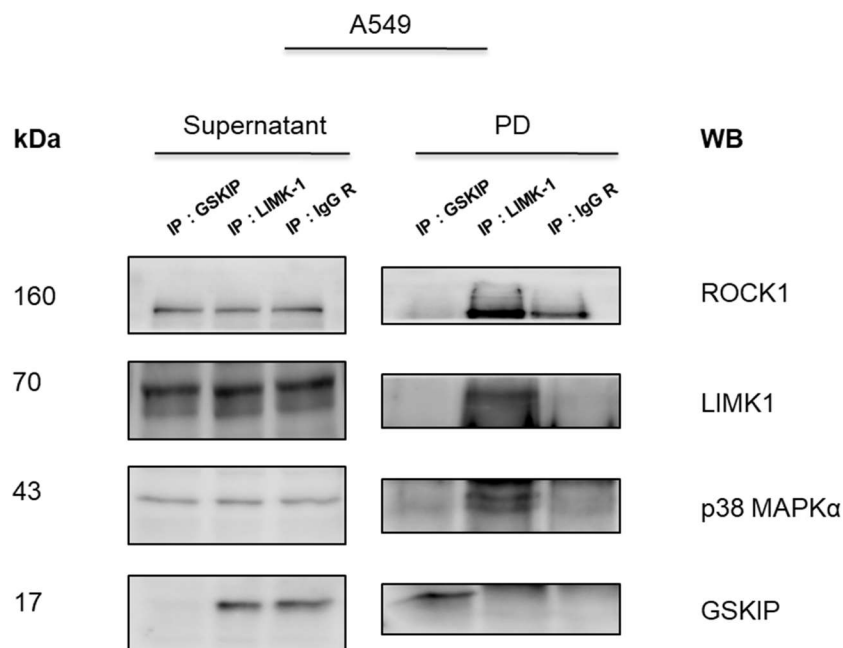
Figure 27. GSKIP is not in a complex with LIMK-1, ROCK1, and p38 MAPKα in A549 cells. Cells were lysed and the lysates were subjected to immunoprecipitation of endogenous GSKIP and LIMK-1, anti-rabbit immunoglobulin (IgG R) was used a negative control. GSKIP, LIMK-1, ROCK1, and p38 MAPKα were detected by Western blotting. n =2. PD: Pull-down.

4.4.7 GSKIP KD does not modulate p38 MAPK phosphorylation in A549 cells

p38 MAPK kinase has been implicated in the regulation of LIMK-1 phosphorylation both, through the direct phosphorylation of LIMK-1 at serine 310 (S310) and indirectly, by phosphorylating and activating MK2, which consequently phosphorylates LIMK-1 at S323. While the direct phosphorylation at S310 does not activate LIMK-1, the MK2-mediated phosphorylation activates LIMK-1 (Kobayashi *et al.* 2006) and hence contributes to the phosphorylation of CFL. The activity of p38 MAPK is regulated by its activating phosphorylation

at threonine 180 (Thr180) and tyrosine 182 (Tyr182). GSKIP KD did not alter the activating phosphorylation of p38 MAPK (Fig. 28).
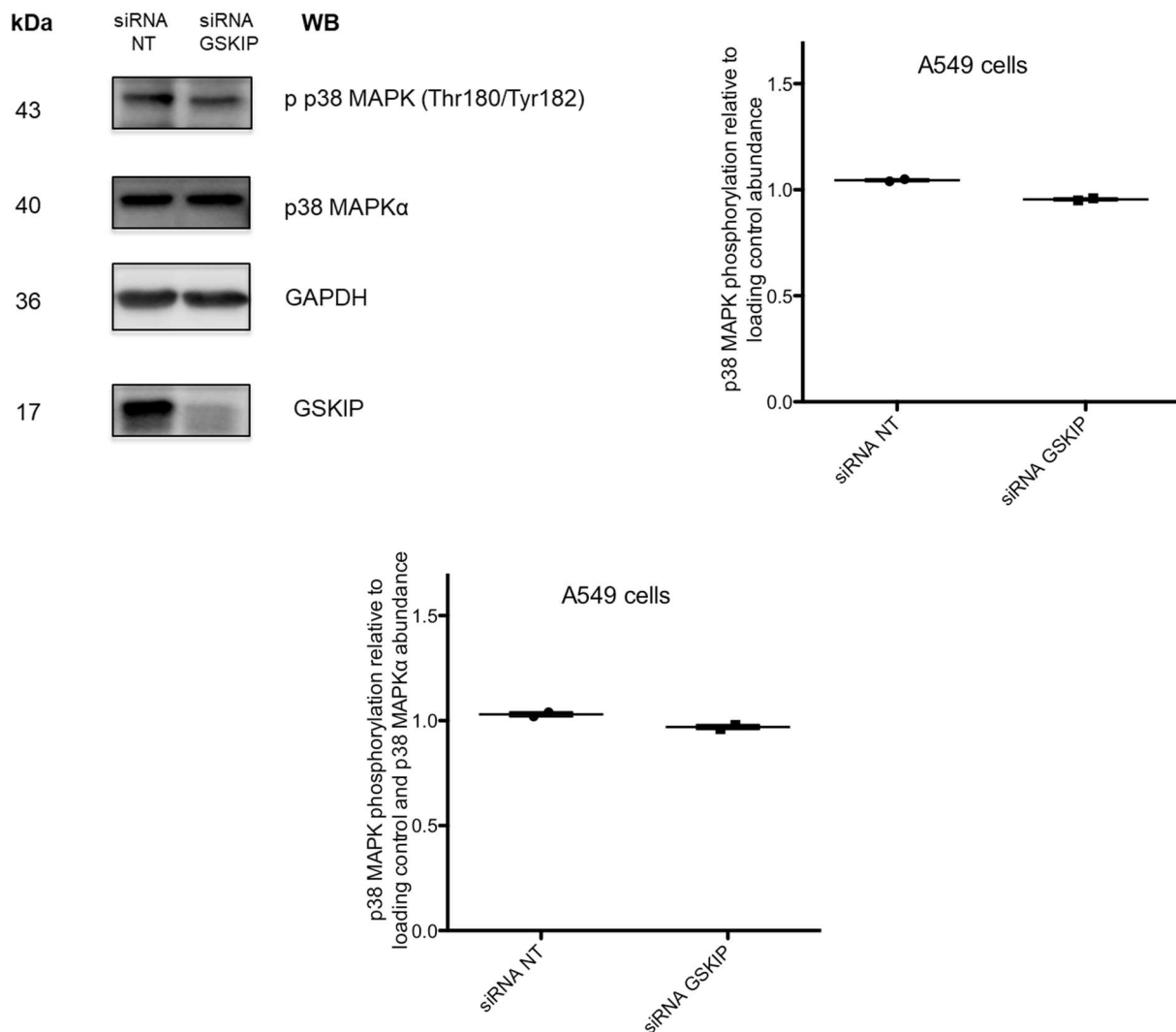
Figure 28. GSKIP KD in A549 cells does not modulate p38 MAPK phosphorylation. Cells were treated with siRNA to knock down the expression of GSKIP or with siRNA NT. p38 MAPKα and p-p38 MAPK (Thr180/Tyr182) were detected by Western blotting. Signals were semi-quantitatively analysed by densitometry and the ratio of p-p38 MAPK to normalized p38 MAPK α (p38 MAPK α/GAPDH) calculated; n =2, mean ± SEM.

4.4.8 GSKIP does not control the levels of the CFL phosphatase chronophin in A549 and HeLa-S3 cells

The GSKIP KD did not significantly change the active fraction of LIMK-1, which depends on the Rho GTPases and p38 MAPK. This points towards a potential implication of PKA in modulating LIMK-1 activity. However in order to confirm this possibility, insight into the abundance of downstream phosphatases that can dephosphorylate and activate CFL had to be gained. The phosphatases known to dephosphorylate CFL at S3, are the SSH family of phosphatases and chronophin. Chronophin was found to be more essential than SSH

phosphatases for processes associated with CFL-mediated actin turnover. Hence, owing to the ubiquitous expression of both CFL and GSKIP, coupled with the broad expression of chronophin against the more limited expression pattern of the SSH phosphatase proteins (Gohla *et al.* 2005), chronophin was chosen to be studied. In both A549 and HeLa-S3 cells, the KD of GSKIP elicited no changes in chronophin abundance, reaffirming the GSKIP-mediated potential involvement of PKA in modulating CFL phosphorylation (Fig. 29).
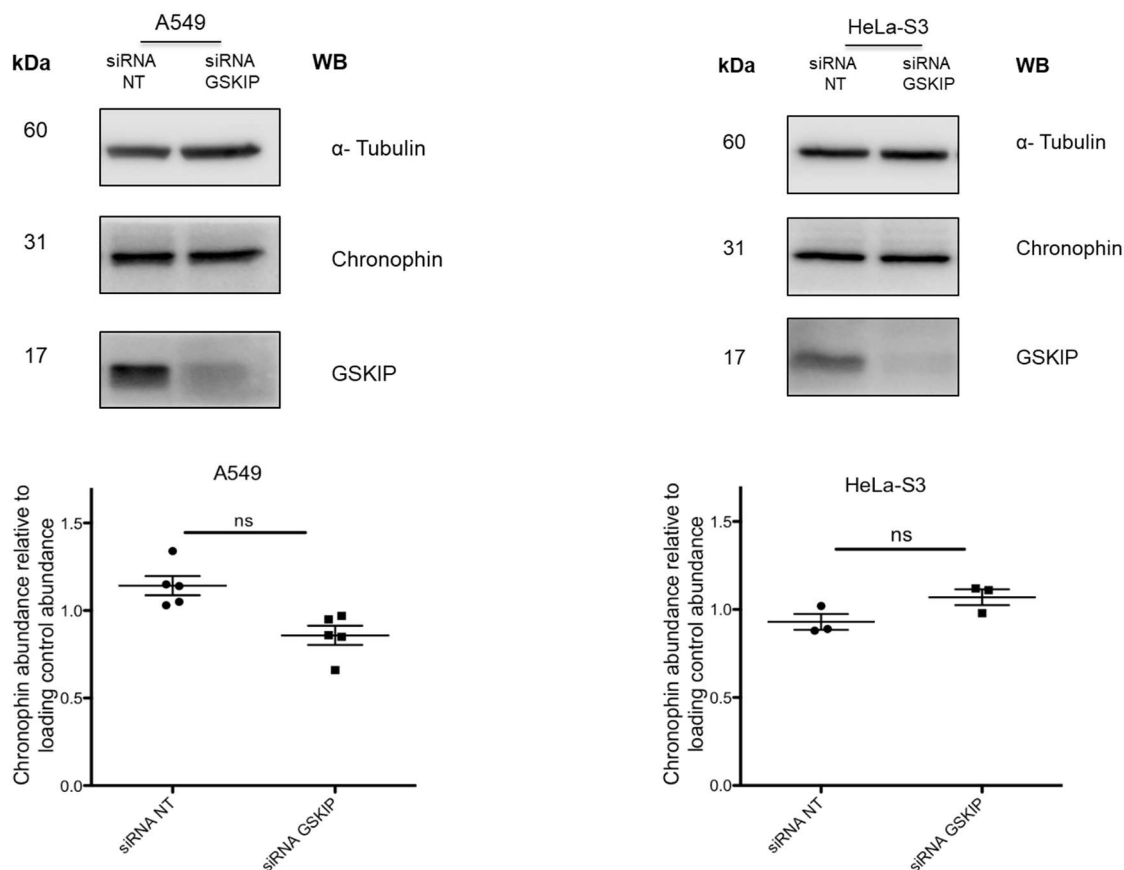
Figure 29. GSKIP KD in A549 and HeLa-S3 cells does not alter total chronophin abundance. A549 cells were treated with siRNA to knock down the expression of GSKIP or with siRNA NT. Chronophin was detected by Western blotting. Signals were semi-quantitatively analysed by densitometry and the ratio of chronophin to GAPDH was calculated; n = 5 and n = 3 respectively, mean ± SEM, Paired T-test., *p < 0.05.

4.5 GSKIP plays a potential role in EMT mirrored by cell junctional aberrations

4.5.1 GSKIP modulates crucial EMT proteins in A549 and HeLa-S3 cells

The phenotype observed upon the knock down of GSKIP in HeLa-S3 cells was reminiscent of the EMT one, exhibiting increased stress fiber formation and altered actin distribution at the cellular junctions. PKA plays a role in MET, characterised by unchanged abundance of the master regulators SNAIL and twist, despite the other markers of MET demonstrating significant changes in their expression levels (Nadella *et al.* 2008). The protein expression levels of

several EMT markers and master regulators were studied in A549 and HeLa-S3. Upon the KD of GSKIP, changes in the abundance of EMT markers such as E-cadherin and β-catenin were encountered, despite the master regulator SNAIL showing no significant difference at a protein level in both cell lines (Figs. 30 and 31). The EMT master regulator and transcription factor, ZEB1 was significantly upregulated in both cell lines. This was surprising, however, Takeyama *et al.* demonstrated that among all EMT master regulators, only ZEB1 expression was significantly correlated with EMT markers expression in non-small lung cancer cell lines such as A549 cells, hence implicating ZEB1 as an integral factor in lung cancer pathogenesis (Takeyama *et al.* 2010). Larsen *et al.* further confirmed the relevance of ZEB1 as a major EMT inducer and driver, thus highlighting the importance of its targeted inhibition, as well as the characterization of its modulators (Larsen *et al.* 2016).
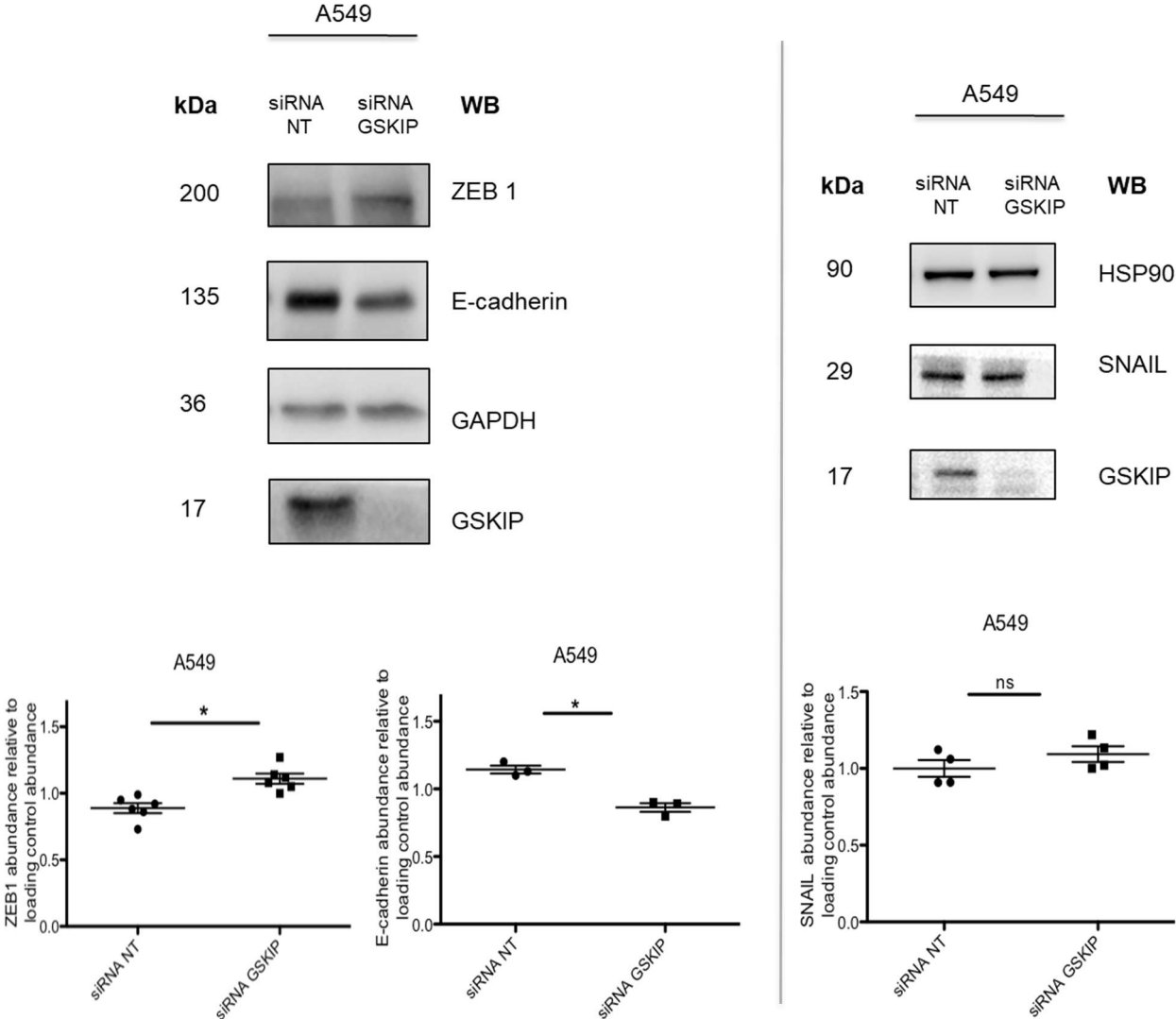
Figure 30. GSKIP controls the abundance of the master regulator ZEB1 in A549 cells and its KD is associated with decreased abundance of the epithelial marker E-cadherin. A549 cells were treated with siRNA to knock down the expression of GSKIP or with siRNA NT. ZEB1, E-cadherin, and SNAIL were detected by Western

blotting. Signals were semi-quantitatively analysed by densitometry and the ratio of each protein to the loading control was calculated; n = 6 , n = 3, and n = 4, mean ± SEM, Paired T-test, *p < 0.05
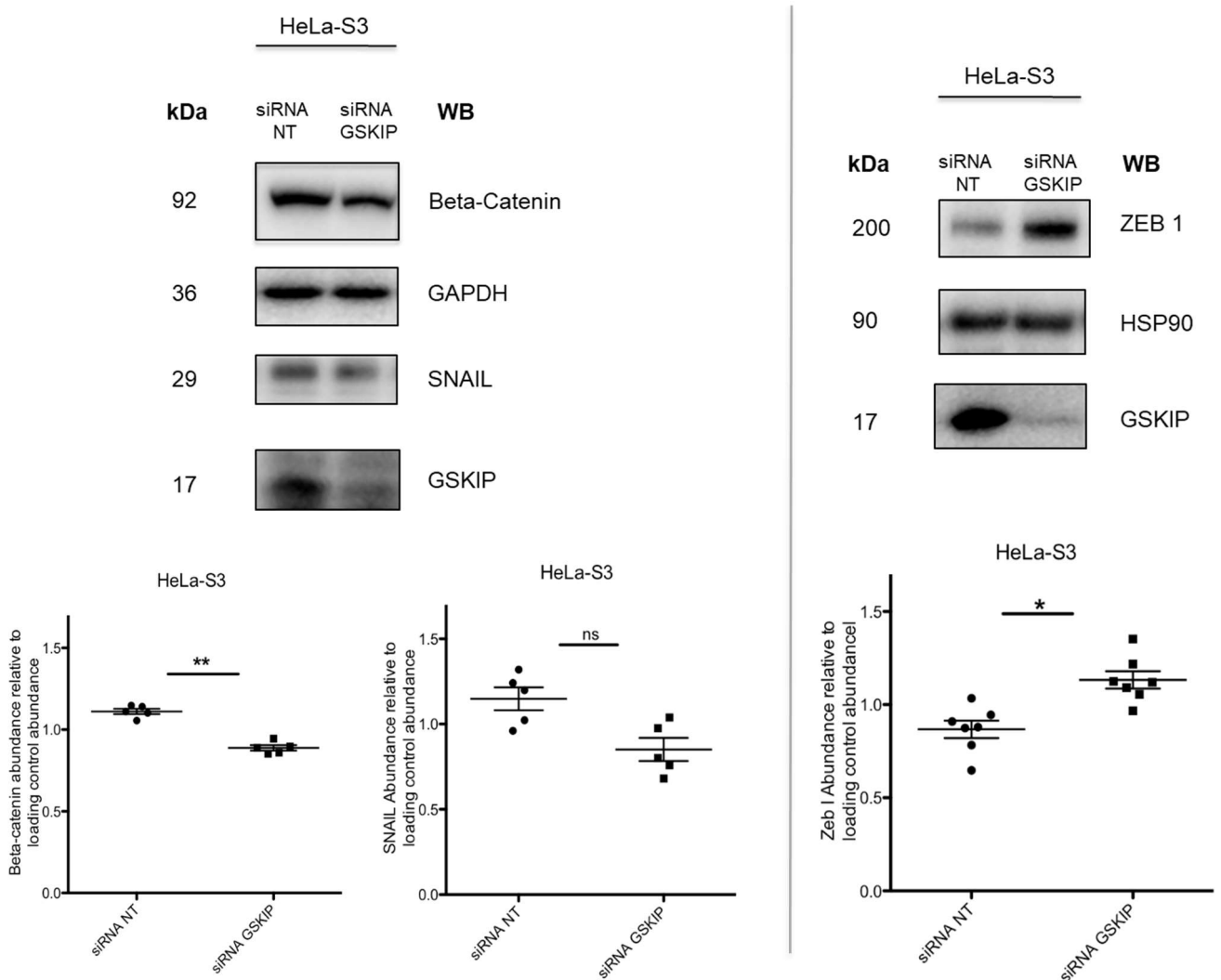
Figure 31. GSKIP upregulates the master regulator ZEB1 in HeLa-S3 cells, and its KD is associated with decreased abundance of the epithelial marker β-catenin. HeLa-S3 cells were treated with siRNA to knock down the expression of GSKIP or with siRNA NT. β-catenin, SNAIL, and ZEB1 were detected by Western blotting. Signals were semi-quantitatively analysed by densitometry and the ratio of each protein to the loading control was calculated; n = 5 , n = 5, and n = 7, mean ± SEM, Paired T-test, *p < 0.05.

4.5.2   GSKIP modulates adherens junction integrity

The shift of the cells from the epithelial to the mesenchymal phenotype is associated with the loss of cell-cell contacts and the disassembly of the cellular junctions, such as AJs and the desmosomal junctions. The KD of GSKIP in HeLa-S3 cells was associated with increased stress fiber formation, a hallmark of mesenchymal cells, as well as altered F-actin at the junctions. Actin is an integral component of the AJ, as is E-cadherin, and both have exhibited marked alterations upon GSKIP KD. Another AJ protein, β-catenin was studied in order to shed light on the junctional integrity following the KD. Decreased localization of β-catenin at the junction was evident after the KD (Fig. 32), hence implicating GSKIP as a modulator of the stability of the AJ.
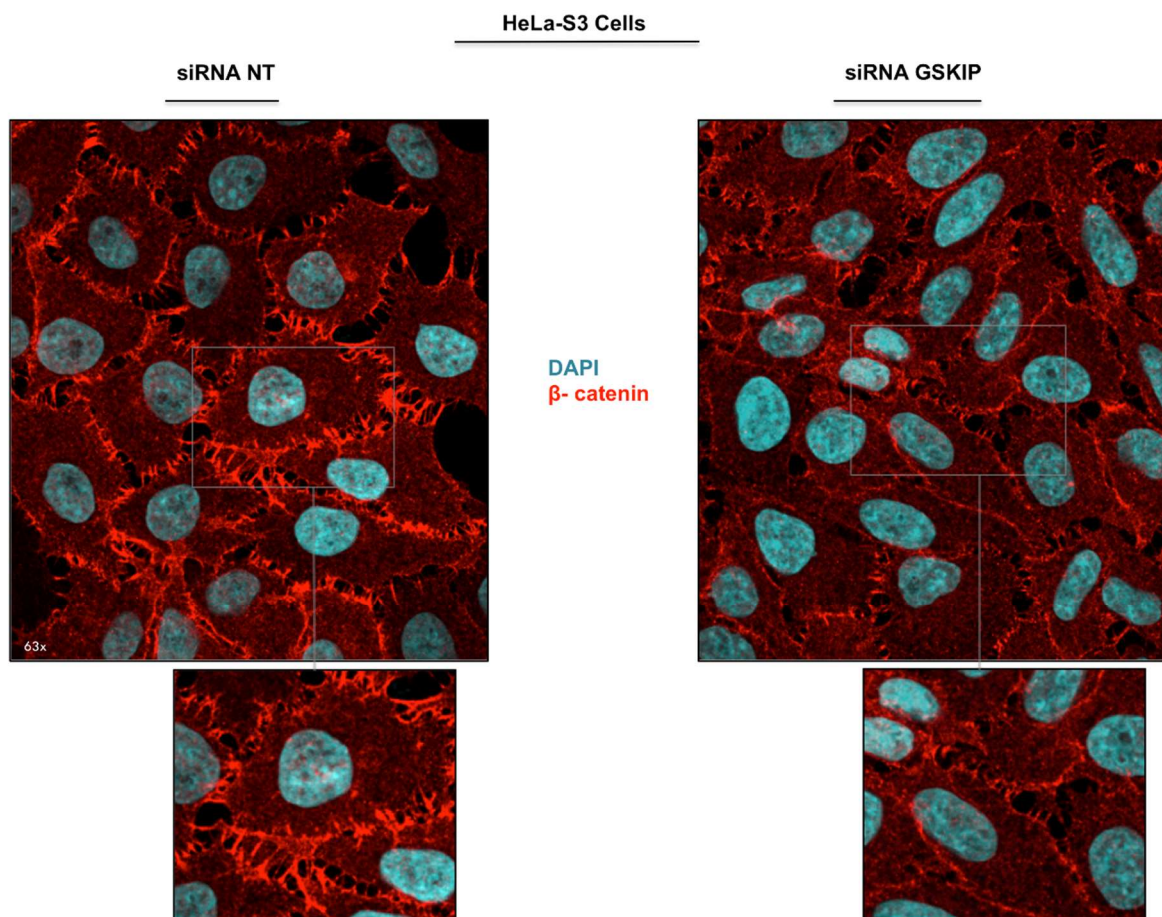
Figure 32. GSKIP modulates junctional β-catenin in HeLa-S3 cells. Representative fluorescence microscopic analysis of HeLa-S3 cells transfected with siRNA to knock down the expression of GSKIP or with siRNA NT. Cyan: DAPI nuclear staining, Red: Beta-catenin. Shown is a representative result of two independent experiments.

4.5.3 GSKIP regulates GSK3β activity in HeLa-S3 cells

GSK3β modulates the stability of AJs and β-catenin levels through its ability to regulate the activity of atypical protein kinase C (Colosimo *et al.* 2010). The activity of GSK3β is inhibited by its PKA mediated phosphorylation at S9. GSKIP facilitates this inhibitory phosphorylation in HEK293 cells (Hundsrucker *et al*. 2010). As expected, GSKIP KD experiments conducted in HeLa-S3 cells also showed decreased phosphorylation of GSK3β at S9 and hence this may explain the potential decrease in the β-catenin-mediated AJ stability (Fig. 33).
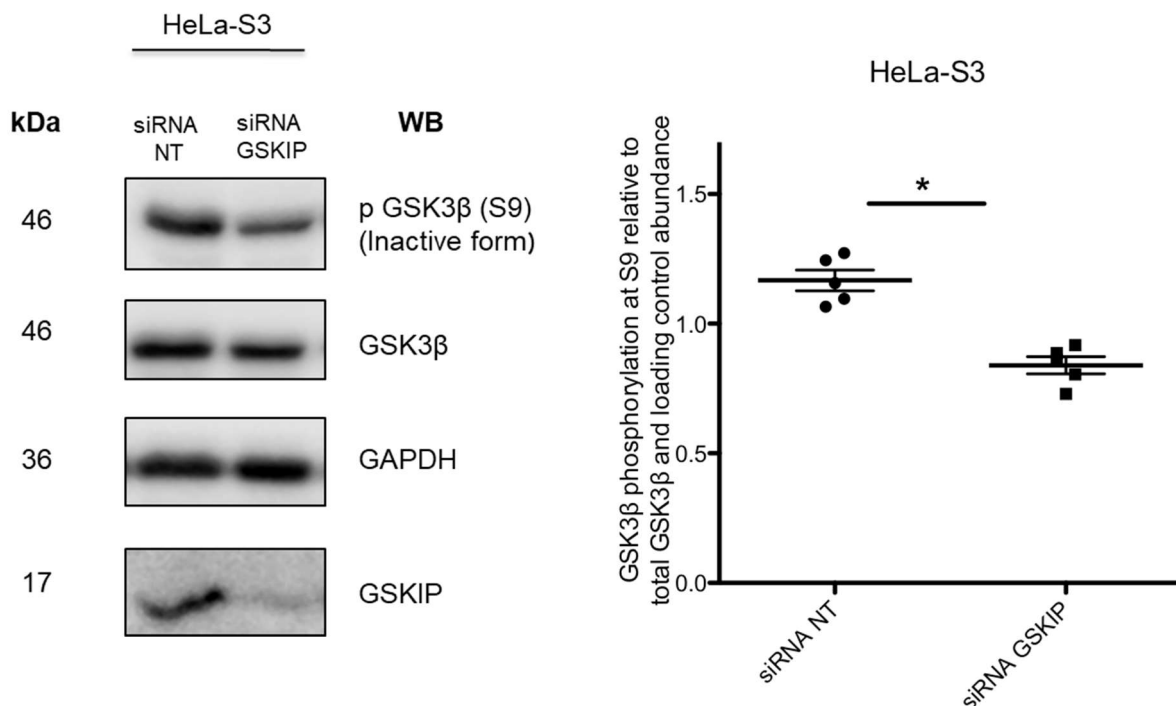
Figure 33. GSKIP modulates GSK3β activity in HeLa-S3 cells. HeLa-S3 cells were treated with siRNA to knock down the expression of GSKIP or with siRNA NT. GSK3β and p-GSK3β (S9) were detected by Western blotting. Signals were semi-quantitatively analysed by densitometry and the ratio of phosphorylated GSK3β to normalised GSK3β (GSK3β/GAPDH) calculated; n = 5, mean ± SEM, Paired T-test, *$p < 0.05$.

4.5.4 GSKIP modulates the desmosomal intermediate filament binding proteins DSP I and II in A549, HeLa-S3, and SW480 cells

Proteomics revealed the muscle-specific intermediate filament Desmin to be at least 50% downregulated in GSKIP-depleted lungs at E18.5. The downregulation was validated by Western blotting (PhD thesis Veronika Deak). Since the phenotype concerning the cell junctions was suspected in different cell lines, it was more likely that the GSKIP KD-mediated disruption involved an integral member of the desmosomes, as opposed to the intermediate filaments, whose composition differs from one cancer cell type to another. Following GSKIP

KD the abundance of the desmosomal cadherins binding protein, plakoglobin was unchanged, while that of the intermediate filament (IF) binding proteins DSP I/II was significantly downregulated in all tested adenocarcinoma cell lines, indicating a potential disruption in the interaction between the intermediate filaments and the desmosomal cadherins. (Fig. 34).
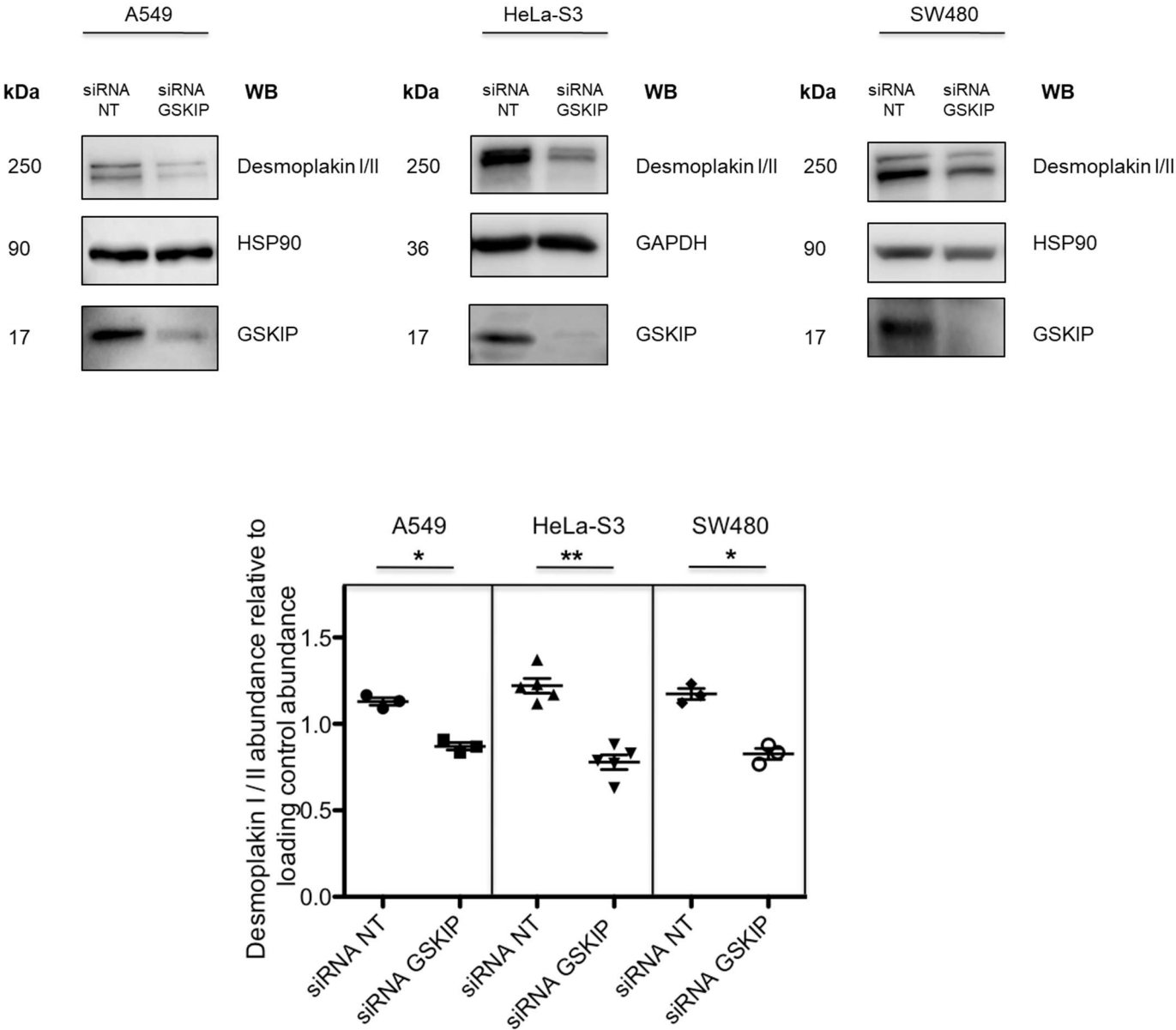
Figure 34. GSKIP KD in A549, HeLa-S3, and SW480 cells decreases the abundance of IF binding proteins DSP I/II. Cells were treated with siRNA to knock down the expression of GSKIP or with siRNA NT. DSP I and II were detected by Western blotting. Signals were semi-quantitatively analysed by densitometry and the ratio of DSP I/II to the loading control calculated; n = 3, n = 5, n = 3, mean ± SEM, Paired T-test, *p < 0.05.

4.5.5 GSKIP KD elicits a prominent downregulation of DSP I/II abundance in HeLa-S3 cells

The consistent reduction at the protein level of the intermediate filament binding proteins DSP I/II suggested a potential destabilization of the desmosomal junctions. To validate the GSKIP mediated desmosomal aberrations, the siRNA-induced GSKIP KD was rescued by expressing FLAG-tagged full length GSKIP (FLAG-GSKIP WT) and the levels of DSP I/II were examined. Moreover, given GSKIP's intrinsic ability to directly interact with PKA and GSK3β, the interactions with both kinases were studied to evaluate their necessity for the desmosomal junctions integrity. The overexpression of WT GSKIP following the KD did not appear to rescue the KD-induced reduction in DSP I/II abundance (Fig. 35) and unsurprisingly the GSK3β and PKA binding deficient mutants (L130P and N42I respectively) exhibited the same changes, an indication that the KD of GSKIP might be irreversibly altering DSP I/II abundance.
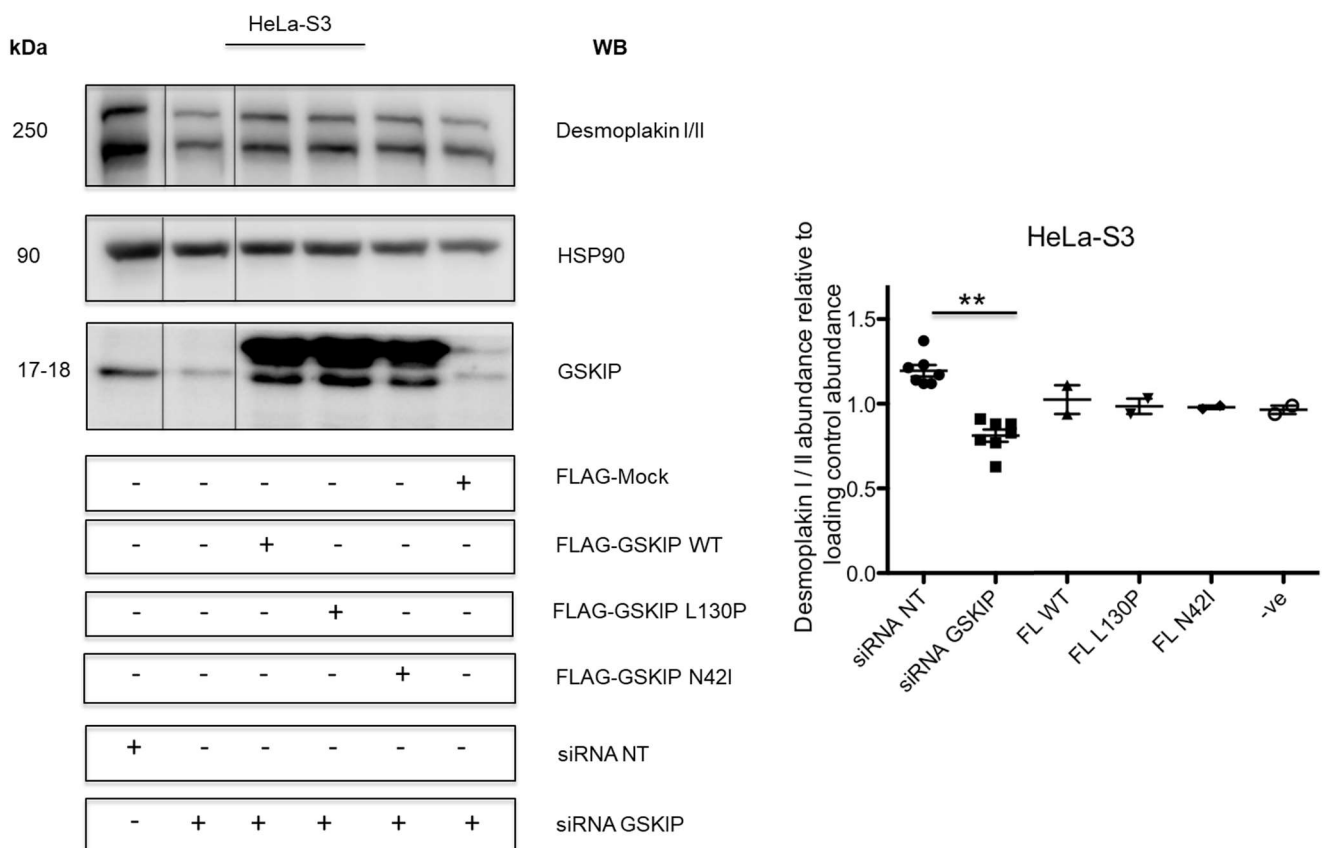
Figure 35. Rescue of GSKIP KD in HeLa-S3 cells does not rescue the altered DSP I/II abundance. HeLa-S3 cells were treated with either siRNA GSKIP or siRNA NT and transfected 24 hrs later with the indicated plasmids, lysed and Western blot analysis was conducted to detect GSKIP, DSP I/II, and HSP90. Signals were semi-quantitatively analysed by densitometry and the ratio of DSP I/II to the loading control calculated; n =7 for siRNA treatment (KD + control), mean ± SEM, Paired T-test, *p < 0.05. n = 2 for plasmid treatment (overexpression + control), mean ± SEM.

The phosphorylation of DSP at a site neighbouring its keratin binding domain, by PKCα has been implicated in the disruption of desmosomal junctions and their consequent reorganization. The signalling events preceding the activation of PKCα, however, are not fully understood (Kröger *et al.* 2013) and the mechanisms concerning the consequent phosphorylation of DSP are still unknown (Hobbs and Green. 2012) . The phosphorylation of DSP was found to be influenced by keratins and was found to regulate the desmosomal stability, where the increased DSP phosphorylation was associated with desmosomal compromises. The decrease in the phosphorylation was marked by increased desmosomal stability. Hence the protein levels of PKCα were studied upon the KD of GSKIP in HeLa-S3 cells to evaluate the possibility of GSKIP modulating the junctional integrity through PKCα and keratins. The KD of GSKIP in HeLa-S3 cells was found to cause an elevation in the protein levels of PKCα (Fig. 36) which could point towards increased DSP phosphorylation and consequently a demise in the desmosomal integrity. However, this hypothesis would require further validation.
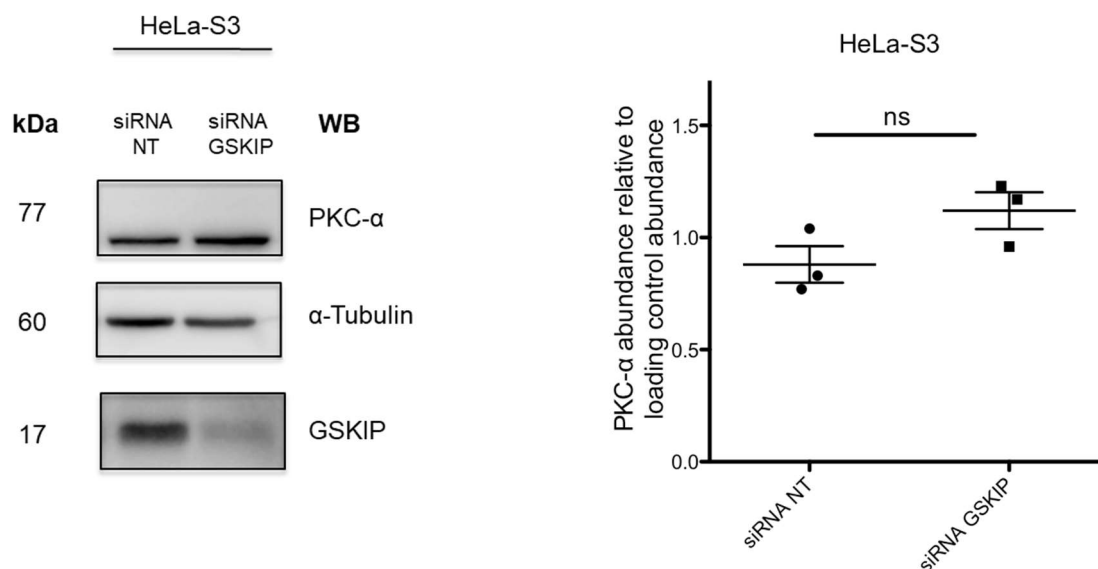
Figure 36. GSKIP KD non-significantly upregulates PKC-α in HeLa-S3 cells. HeLa-S3 cells were treated with siRNA to knock down the expression of GSKIP or with siRNA NT. PKCα, GSKIP, and α-tubulin were detected by Western blotting. Signals were semi-quantitatively analysed by densitometry and the ratio of each protein to the loading control was calculated n = 3, mean ± SEM, Paired T-test, *p < 0.05.

4.5.6   Mitochondrial fission/fusion appear unaltered upon GSKIP KD

Loh *et al.* suggested that GSKIP can act as an anchoring protein in the cAMP/PKA/dynamin related protein 1 (Drp1) signalling axis and that it plays a role in the phosphorylation of the mitochondrial fission regulator Drp1 (Loh *et al.* 2015). Moreover, Kim *et al.* revealed that changes in the levels of Drp1 are associated with human lung and colon

cancers (Kim *et al.* 2018). Furthermore, actin polymerization was previously found to encourage Drp1 mediated mitochondrial fission, while EMT in A549 cells was demonstrated to be associated with elevation of the overall mitochondrial content (WK *et al.* 2015, Xu *et al.* 2015, Gugnoni *et al.* 2016). Hence, the inhibitory PKA-mediated phosphorylation of Drp1 at S637 was studied following the KD of GSKIP in A549 cells. The KD was found to elicit a minor but significant decline in the phosphorylation of Drp1 at S637, whereas the phosphorylation relative to the total abundance appears unchanged (Fig. 37).
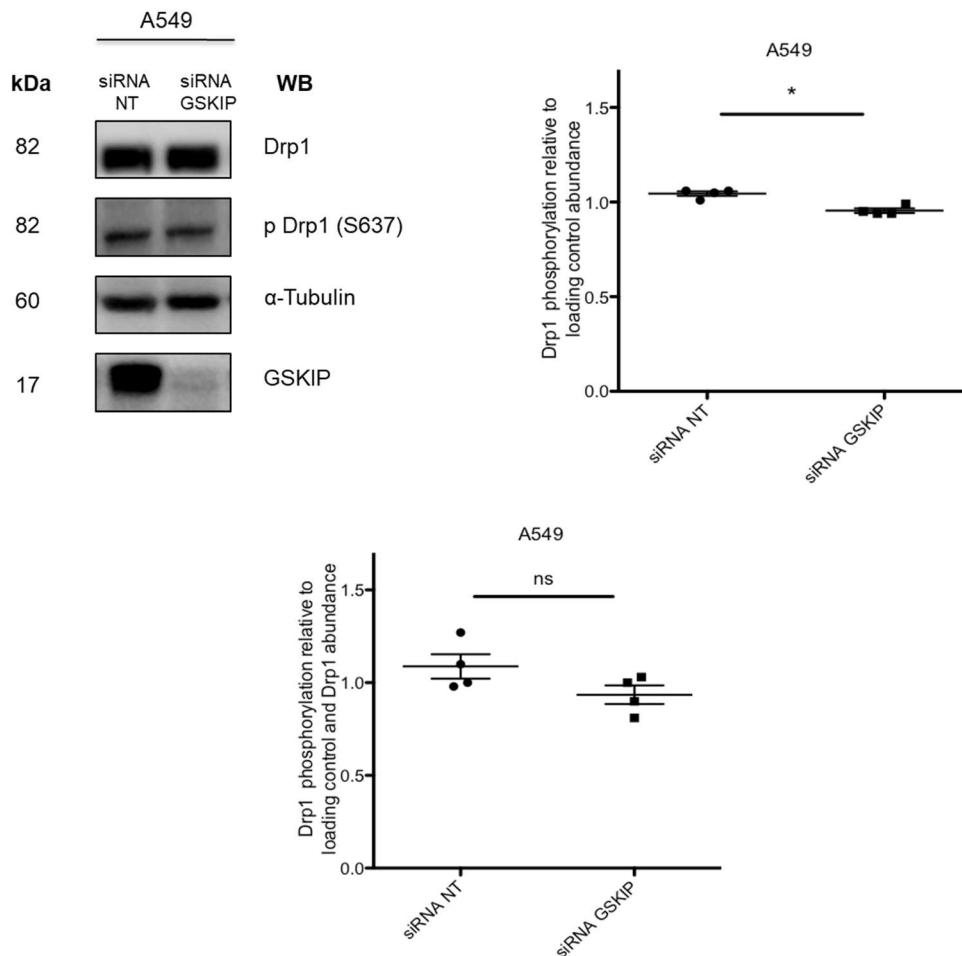
Figure 37. GSKIP KD in A549 cells decreases Drp1 phosphorylation at S637. A549 cells were treated with siRNA to knock down the expression of GSKIP or with siRNA NT. Drp1 and phospho-Drp1 (S637) were detected by Western blotting. Signals were semi-quantitatively analysed by densitometry and the ratio of phosphorylated Drp1 to normalised Drp1 (total Drp1 to α-Tubulin) was calculated; n = 4, mean ± SEM, Paired T-test, *p < 0.05

Studies in our lab conducted on E18.5 mouse lungs, and A549 cells suggested a GSKIP related potential modulation of another mitochondrial fission protein, dynamin-like 120 kDa protein (OPA-1). Similar to Drp1, OPA-1 is a regulator of mammalian mitochondrial fission and fusion (Lee *et al.* 2004) exhibiting high expression in lung, cervical, and colorectal cancers. Thus, A549, HeLa-S3, and SW480 cells were studied for OPA-1 abundance upon the KD of

GSKIP. Data obtained showed little to no change in OPA-1 protein levels when GSKIP is knocked down (Fig. 38). Taken together with the Drp1 data, this indicates that the GSKIP KD induced phenotype does not suffer from mitochondrial fission or fusion aberrations.
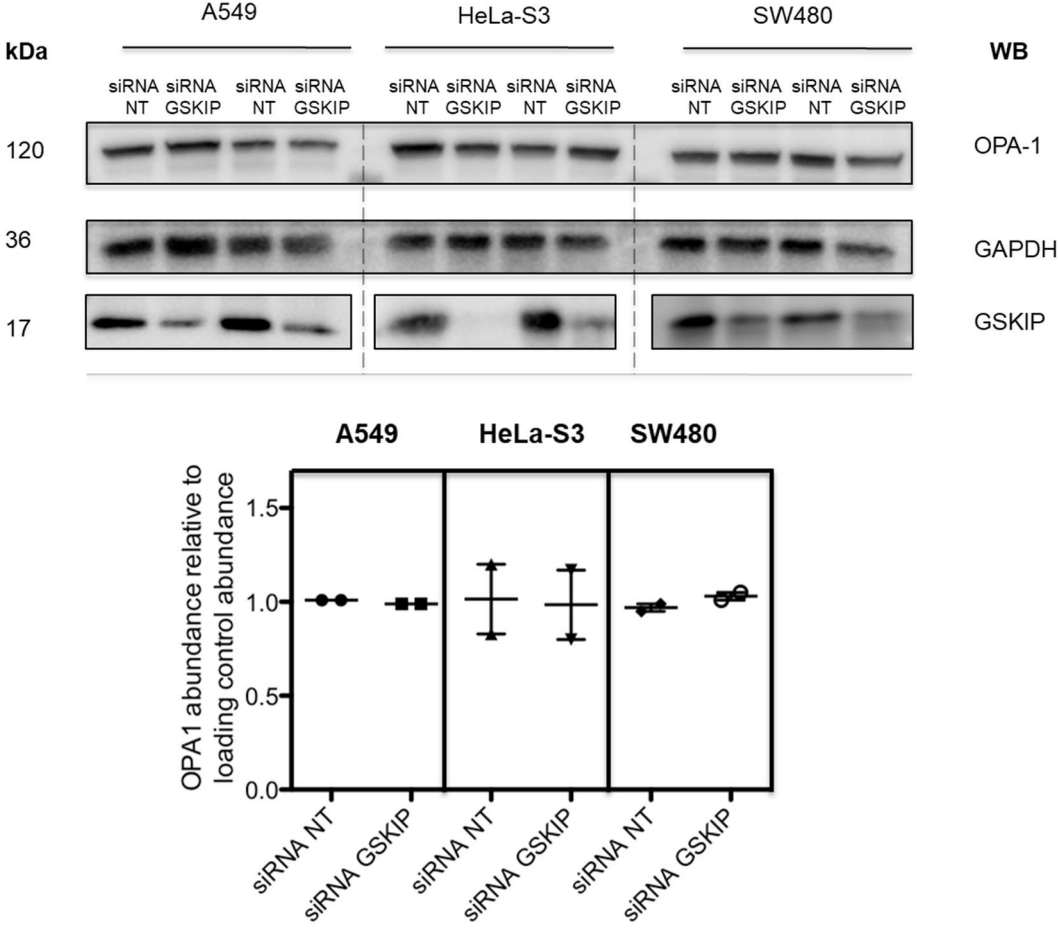
Figure 38. GSKIP KD in A549, HeLa-S3, and SW480 cells does not impact OPA-1 abundance. Cells were treated with siRNA to knock down the expression of GSKIP or with siRNA NT. OPA-1 was detected by Western blotting. Signals were semi-quantitatively analysed by densitometry and the ratio of OPA-1 to the loading control calculated; n = 2, mean ± SEM.

5.   Discussion

5.1 GSKIP modulates actin dynamics in various cell lines

GSKIP, a ubiquitously expressed AKAP, directly binds both PKA and GSK3β, both of which are crucial components of various signalling pathways. The decrease of the inhibitory phosphorylation of the actin severing protein CFL, is a characteristic of GSKIP KD in adenocarcinoma cells originating from epithelia, whereas the cancer cells of mesenchymal origin exhibited the opposite change (Fig. 21). This suggests a role in the maintenance and regulation of the epithelial phenotype. The actin fractionation studies conducted in A549 cells revealed down-regulation of CFL in the F-actin fraction upon GSKIP KD, whereas the abundance of actin appears unchanged (Fig. 17). A decrease in CFL abundance under the F-actin fraction points towards increased actin depolymerization. However, CFL, as an actin severing protein has been implicated as the "steering-wheel" of the cell. Recently it was discovered that CFL possesses the ability to induce both depolymerization of actin filaments through their severing, as well as their assembly and polymerization through the recycling and generation of globular actin monomers, effectively "steering" the actin cytoskeleton of the cell (Andrianantoandro and Pollard, 2006). The change in CFL abundance independent of its actin counterpart in the F-actin fraction, suggests a localized depolymerization of the actin filaments. It may be counteracted by recycling and incorporation of the resulting globular monomers to form actin filaments. This was evident in HeLa-S3 cells, where the KD of GSKIP was associated with increased formation of the F-actin stress fibers (Fig. 22). This serves as an indication that the characteristic epithelial cortical actin filaments are being depolymerized in favor of the mesenchymal F-actin stress fibers.

5.2 GSKIP modulation of CFL phosphorylation is most likely PKA dependent

The activity of CFL is dependent on its phosphorylation by LIMK-1, which is mediated through the LIMK upstream regulators, the Rho GTPases, RhoA, and Rac-1. The KD of GSKIP significantly upregulated both Rho GTPases (Fig. 23), which suggested a potential role in the GSKIP dependent CFL phosphorylation. RhoA and Rac-1 can influence the active LIMK-1 pool by activating their downstream effectors ROCK and PAK1 respectively, whereas the activity of the Rho GTPases is determined according to the proportion of their active GTP bound to the inactive GDP bound forms. In addition, the PKA mediated phosphorylation of RhoA at S188, inhibits RhoA (Van Aelst and D'Souza-Schorey, 1997, Qiao J *et al.* 2003). In HeLa-S3 cells there was no difference in the GTP-bound fraction of the GTPase upon the KD of GSKIP (Fig. 24), and hence no change in its activity. The KD of GSKIP in A549 cells also had no effect on the PKA phosphorylation of GDP-bound fraction of RhoA (Fig. 25), while GSKIP, PKA, and

RhoA did not form a complex in either cell line (Fig. 26). On the other hand, Rac-1 activity assays failed to detect any GTP bound Rac-1. Hence the phosphorylation of LIMK-1 at Thr508, a culmination of the activity of the three Rho GTPases, RhoA, Rac-1, and Cdc42, was studied. The phosphorylation did not increase upon GSKIP KD in HeLa-S3 cells (Fig. 27), effectively eliminating the possibility of Rho GTPases being the modulators controlling the decreased CFL phosphorylation.

Nadella *et al.* proposed a model for the activation of LIMK-1, which necessitates its phosphorylation at different sites by various kinases to achieve full activity (Nadella *et al.* 2009). ROCK and PAK are essential for the activation. Following this phosphorylation, LIMK-1 must be phosphorylated at Thr508 (by ROCK or PAK), at S596 (by PKA), and at S323 (by p38 MAPK downstream effector, MK2) to be fully activated. This activation mode confers a dynamic control over the activity of LIMK-1, thus in addition to Rac/Cdc42 and Rho signalling, Erk/MK and PKA pathways can also influence the CFL-mediated actin reorganization. PKA signalling has been implicated in the reorganization of the actin cytoskeleton, characterized by elevated CFL phosphorylation and increased polymerized actin aggregation. These organizational changes, coupled with the ubiquitous expression patterns of both PKA and LIMK-1 suggest that changes of PKA signalling can be manifested as cytoskeletal alterations. The activity of p38 MAPK, remained unchanged upon GSKIP KD in A549 cells, suggesting the absence of any consequent MK2 mediated phosphorylation changes at S323 and pointing towards PKA signalling as the modulator of the observed cytoskeletal changes. There was also the possibility of increased downstream phosphatases acting on phosphorylated CFL at S3. Given that the Slingshot protein phosphatases are unessential for processes that are associated with CFL-mediated actin reorganization, the abundance of the phosphatase chronophin, a crucial modulator of CFL mediated actin dynamics was studied in A549 and HeLa-S3 cells. The KD of GSKIP did not alter the abundance of chronophin in either of the cell lines tested, hence underlining PKA signalling as the potential mediator of the GSKIP-dependent changes in actin dynamics.

5.3 GSKIP modulates EMT master regulator ZEB1

Both A549 and HeLa-S3 cells following GSKIP KD, showed junctional actin anomalies. Therefore, the integrity of the various cell junctions associated with the epithelial phenotype was investigated. The KD of GSKIP was found to upregulate the EMT inducer ZEB1 in both cell lines, with no changes at the protein level of SNAIL, another EMT master regulator (Fig.31, Fig. 32). This raised the question whether the transition of the cells from the epithelial to the mesenchymal phenotype can be attributed solely to ZEB1.

Takeyama *et al*. studied the four master epithelial-to-mesenchymal transition (EMT) inducing genes ZEB1, SIP1, SNAIL, and Slug, and correlated their expression with the

mesenchymal phenotype in non-small lung cancer cells such as A549 cells (Takeyama *et al.* 2010). ZEB1 expression positively correlated with the degree of the mesenchymal phenotype. On the contrary, the expression levels of the other EMT master regulators showed no correlation with the phenotype degree, thereby implicating ZEB1 as an inducer of EMT in lung cancer.

Nadella *et al.* demonstrated that PKA signalling favours the epithelial phenotype, by promoting MET upon its constitutive activation in primary mouse embryonic fibroblasts (MEFs) (Nadella *et al.* 2008). The MEFs, in which PKA signalling has been constitutively activated, exhibited properties of MET. The epithelial marker E-cadherin was upregulated compared to the control MEFs, whereas the mesenchymal markers Vimentin and N-cadherin were downregulated. Interestingly, upon activation of PKA signalling, the protein levels of the EMT master regulator and transcription factor SNAIL remained unchanged. The universality of the MET phenomenon upon the activation of PKA signalling was later studied by employing heterologous systems, where HeLa and HEK293T cells were transfected to overexpress PKA catalytic subunits and the resulting decline in the abundance of the mesenchymal marker Vimentin was validated. Thus, despite validating the PKA-mediated MET phenotype, changes in the expression of the master regulator SNAIL at the protein level were not detected, even though the associated characteristic markers of MET demonstrated significant changes in their expression levels. Pattabiraman *et al*. later confirmed these findings by employing mesenchymal human mammary epithelial cells, and demonstrating that the elevation in cAMP levels and the consequent activation of PKA signalling is associated with MET (Pattabiraman *et al*. 2016).

5.4 GSKIP is involved in maintaining epithelial cell-cell adhesion

5.4.1 GSKIP is involved in maintaining adherens junction

The increased formation of F-actin stress fibers, a characteristic of mesenchymal cells, coupled with the junctional actin aberrations necessitated the evaluation of the epithelial phenotype upon GSKIP KD. EMT markers were evaluated in both A549 and HeLa-S3 cells following the KD. Complementing ZEB1 upregulation, downregulation of epithelial markers was recorded, namely the exclusively epithelial, E-cadherin and the integral AJ protein, β-catenin (Fig. 31, Fig. 32). β-catenin binding to the cadherins has been revealed to be crucial for the integrity and full adhesive potential of the AJ. Its involvement with various signalling molecules implicates it as a mediator of signalling-induced changes at the AJ (Aberle *et al.* 1996 and Niessen, 2007). Thus the junctional distribution of β-catenin was studied upon the KD of GSKIP in HeLa-S3 cells. Immunofluorescence experiments revealed that GSKIP KD

was associated with decreased β-catenin localization at the junctions, hence pointing towards compromised junctional integrity (Fig. 33).

Colosimo *et al.* uncovered a role for GSK3β in the modulation of the stability of the AJ proteins through its ability to regulate the activity of atypical protein kinase C (aPKC) (Colosimo *et al.* 2009). The loss of GSK3β was found to enhance the activity of aPKC. GSK3β was found to phosphorylate the purified human aPKC protein, consequently marking it for proteasomal degradation. The increase in the levels and activity of aPKC was recorded to stabilize the adheres junction proteins such as β-catenin, by increasing its levels as well. Interestingly, it was noted that the GSK3β-mediated elevation in the levels of β-catenin appears to be restricted to the membrane pool. Taken together this data suggest that GSK3β through its indirect ability to modulate the junctional β-catenin pool can be implicated in regulating the stabilisation of the epithelial cell-cell adhesion and AJ. GSKIP facilitates the PKA-mediated inhibitory phosphorylation of GSK3β at S9 (Hundsrucker *et al.* 2010, Deak *et al.* 2016). Hence the phosphorylation dependent activity of GSK3β was studied. GSKIP KD in HeLa-S3 cells was found to decrease the S9 phosphorylated GSK3β relative to the total abundance (Fig. 34), pointing towards an overall increase in the activity of GSK3β, which in turn would translate to increased destabilization of the AJ.

5.4.2 GSKIP is involved in maintaining desmosomal integrity

The AJs and the desmosomes, another characteristic epithelial junction, have been found to complement the assembly and stability of each other. The loss of desmosomal elements has been associated with AJ actin based anomalies. The presence of an intact actin cytoskeleton was found to be a necessity for the proper assembly and organization of the desmosomes. The formation of a functional desmosomal unit is dictated by the ability of the intermediate filament binding proteins DSP I/II to tightly bind the desmosomal plaque to the intermediate filaments, while the dynamics of DSP during junctional assembly were revealed to depend on actin filaments, as well as the interactions with the intermediate filaments cytoskeleton. (Pasdar and Li, 1993, Vasioukhin *et al.* 2000, Godsel *et al.* 2005, Godsel *et al.* 2010, Kowalczyk and Green, 2013). Various elements of the desmosomal junction were evaluated upon the KD of GSKIP. The intermediate filament binding proteins DSP I and II exhibited downregulation in A549, HeLa-S3 and SW480 cells as a response to the KD (Fig. 35). Rescuing the GSKIP KD by expressing full length WT GSKIP in HeLa-S3 cells did not appear to rescue the KD induced downregulation of DSP I/II (Fig. 36).

Simpson *et al.* demonstrated that the association between the keratin intermediate filaments and the desmosomal components exerts a protective effect on epithelia, serving to resist mechanical stress and hence protecting against the associated injuries, as well as preventing water loss and resisting infections (Simpson *et al.* 2011). Moreover, DSP

aberrations in epidermal tissues during development were associated with compromised keratin cytoskeleton, desmosomal assembly, stabilization, and adhesion anomalies (Gallicano *et al.* 1998). Building on these findings, Kröger *et al.* analysed the DSP/intermediate filaments based maintenance of desmosomes. Mutant keratinocytes lacking type II keratin genes (KtyII$^{-/-}$) were generated and employed against WT control keratinocyte lines expressing the normal keratin set. Keratinocytes are specialized epithelial cells making up the epidermis, a structure which functions as protective barrier to the surrounding environment. Interestingly, the knockout of the intermediate filament Keratin II was associated with a prominent and marked decrease in the endogenous protein levels of DSP I/II compared to the WT control, whereas the PKC-α-mediated phosphorylation of DSP was found to be enhanced upon the manipulation of Keratin expression (Kröger *et al.* 2013). The findings uncovered by this study hint towards the implication of DSP and the intermediate filaments in resisting EMT by favouring and sustaining intercellular adhesion. In addition to mediating DSP phosphorylation and the consequent desmosomal reorganization, PKC-α has also been implicated in the inhibitory phosphorylation of GSK3β at S9 (Moore *et al.* 2013). The possibility that the irreversible down-regulation of DSP upon the KD of GSKIP is due to intermediate filaments aberrations and consequent changes to PKC-α levels was explored. The data obtained, favour this possibility, since the KD of GSKIP in HeLa-S3 revealed a tendency towards the upregulation of PKC-α (Fig. 37). Nevertheless, further repetitions are required to determine whether this elevation is significant or not.
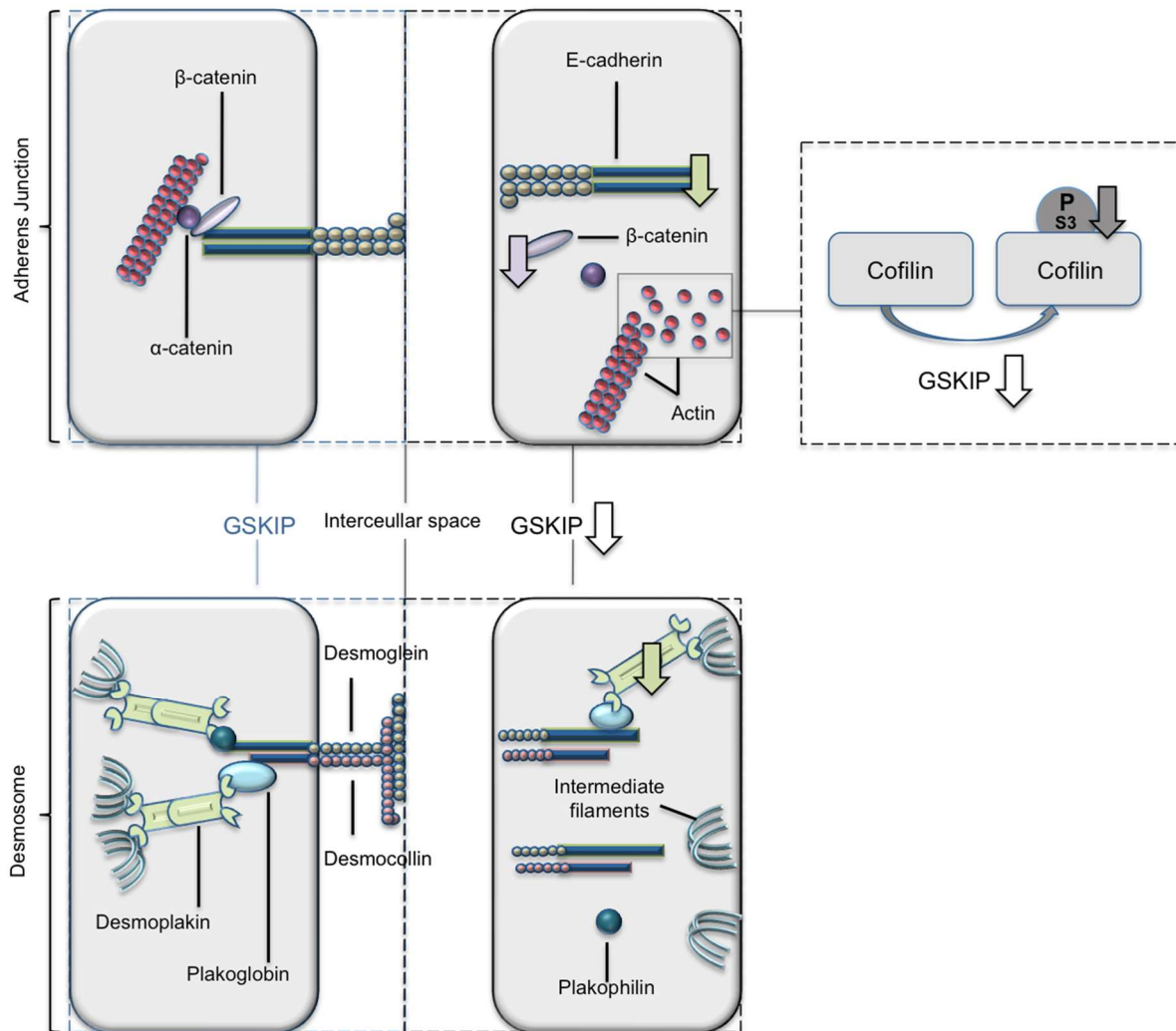
Figure 39. GSKIP is essential for epithelial junctional integrity. Left side : epithelial cells with normal GSKIP expression show intact AJs and desmosomal junctions. Right side : GSKIP KD elicits a disruption in the AJ, manifested as decreased junctional β-catenin, E-cadherin downregulation, and increased CFL mediated actin-depolymerization; GSKIP KD downregulates the intermediate filament binding proteins DSP I/II, attenuating the connection between the desmosomal plaque and the intermediate filaments.

5.5 GSKIP KD does not appear to alter the PKA mediated mitochondrial fission

Drp1, a mitochondrial fission GTPase, was implicated in various signalling events that modulate the morphology, localization, and maintenance of the mammalian mitochondria. The activity of Drp1 is controlled by its phosphorylation at various sites, among which is S637. This diminishes the GTPase activity and suppresses mitochondrial fission (Knott *et al.* 2008). The CFL regulated actin dynamics were also found to modulate the Drp1 mitochondrial fission, whereas the promising natural anti-cancer compound erucin was found to promote mitochondrial fission in human breast cancer cells through inducing the co-translocation and interaction of CFL and Drp1 (Li *et al.* 2015, Rehklau *et al.* 2017). Moreover, Loh *et al.* found GSKIP to be a component of a signalling axis comprising cAMP/PKA/Drp1/GSK3β, serving to modulate the PKA mediated mitochondrial fission inhibitory phosphorylation of Drp1 at S637

(Loh *et al.* 2015). The siRNA-mediated KD of GSKIP in A549 cells was found to elicit a small but statistically significant decline in Drp1 phosphorylation at S637. However, when this phosphorylation was related to the total Drp1 abundance, no changes were recorded (Fig. 38). The decline in the aforementioned phosphorylation upon the KD of GSKIP was smaller than the one encountered by Loh *et al.* However, this could be attributed to the difference in the cell models employed. Loh *et al.* used the embryonic mammalian kidney cells, HEK293 cells, and since cancer cells like A549 usually exhibit altered mitochondrial bioenergetic and biosynthetic properties, the extent of the changes dictated by specific signalling events at a molecular level may differ (Loh *et al.* 2015, Wallace, 2012).

6. Outlook

6.1 The mechanisms behind the GSKIP mediated regulation of CFL activity

PKA directly phosphorylates LIMK-1 and regulates the phosphorylation of CFL at S3, hence it is very plausible that GSKIP could be modulating the activity of CFL through the PKA-mediated phosphorylation of LIMK-1. To confirm this, a system has to be established where the enhanced PKA activity is correlated with increased CFL phosphorylation at S3. Attempts to replicate the data demonstrated in literature using HeLa-S3 and A549 cells proved unsuccessful (Supplementary figures. 2 and 3), despite confirming the forskolin stimulation-mediated elevation of cAMP levels and the consequent increase in PKA activity. It is likely that more substantial activation of PKA signalling has to be attained and hence another approach that could be adopted is transfecting the cells with the active catalytic subunit of PKA and monitoring the phosphorylation of CFL at S3, then coupling the transfection with GSKIP KD and studying the impact on the phosphorylation.

6.2 The impact of GSKIP's depletion on the cytoskeletal dependent processes

The transient, siRNA-mediated KD of GSKIP had no distinct effect on the migration capabilities of A549 cells (Supplementary figure. 1), despite the depletion of GSKIP clearly compromising the stability of various epithelial junctions, as well as upregulating the EMT master regulator, ZEB1. Moreover, GSKIP was found to regulate the activity of CFL, which drives the actin cytoskeletal reorganization and consequently the migration of the cells. Altogether, these GSKIP-dependent organizational changes, characterized by a shift from the stationary epithelial to the highly motile and invasive mesenchymal counterpart, favour increased cellular motility. Hence, to allow for prolonged monitoring of the cytoskeletal dynamics and confirm the underlying signalling changes, a stable KD of GSKIP in the tested cell lines can be conducted. Stable KD of GSKIP can be established by employing lentiviral-based short hairpin RNA (shRNA) depletion of the GSKIP gene in A549 cells, to allow for better characterization of the migratory traits associated with the observed established cytoskeletal changes.

Another possibility worth considering is that the depletion of GSKIP induces a partial transition of the cells from the epithelial to the mesenchymal state, a phenomenon characterized by a hybrid epithelial/mesenchymal (E/M) phenotype. Cells exhibiting this phenotype share properties between the two states, where they show weak cell-cell adhesion, an epithelial attribute, as well as collective cellular migration, a mesenchymal trait. The three phenotypic states, are coordinated through the ratio between EMT inducers such as ZEB1 and EMT inhibitors such as microRNA (miR)-200, where the epithelial phenotype is associated with high levels of miR-200 and low levels of ZEB1, while the mesenchymal state is characterized

by high levels of ZEB1 and low levels of miR-200 and the E/M phenotype exhibits moderate levels of both EMT regulators (Jolly *et al.* 2015).

6.3 The mechanisms underlying the GSKIP KD mediated EMT

PKA and GSK3β have both been implicated in EMT. GSK3β, an inhibitor of tumour cell migration and invasion, is inactivated in epithelial cancers, while the activation of PKA signalling enforces the epithelial state of the cells. GSKIP facilitates the PKA-mediated inhibitory phosphorylation of GSK3β and its KD has been found to decrease this phosphorylation. The depletion of GSKIP is associated with increased activity of GSK3β, which should translate to maintenance of the epithelial phenotype of the cells. The upregulation of ZEB-1 and the disruption of the epithelial junctions upon the KD of GSKIP however, point towards EMT, suggesting a GSK3β-independent, PKA-mediated role. To confirm this and exclude GSK3β inclusion, simultaneous KD of GSKIP and GSK3β could be conducted and the resulting phenotype characterized. In addition, studying the levels of the EMT master regulators upon the overexpression of wild type GSKIP and GSKIP mutants devoid of the PKA or the GSK3β binding sites, can shed some light on the underlying molecular mechanisms associated with the GSKIP KD mediated phenotype.

6.4 Insight into GSKIP's physiological role during development

EMT and MET are essential during vertebrate embryonic development. Both processes alternate and contribute to the formation of the three embryonic germ layers, the ectoderm, the mesoderm, and the endoderm, as well as the delamination of the neural crest. The neural crest delamination is associated with the neural tube closure (NTC), a complex and meticulously coordinated event which represents the earliest stage in the formation of the central nervous system. The neural ectoderm (NE) and the non-neural ectoderm (NNE) have both been implicated in the modulation of NTC. Neural crest cells (NCC) are situated at the border between NE and NNE and undergo delamination mediated migration to various sites to form diverse structures. While the delamination of NCC is coordinated through EMT, both NE and NNE retain their epithelial nature. Very strict coordination between the three participating tissues must be attained for proper NTC to be accomplished (Ray and Niswader, 2016, Kim *et al.* 2017).

The maintenance of the epithelial nature of NE and NNE during NTC has been proven to be essential for the success of the process, as dysregulation in ZEB1 levels was associated with EMT in NNE and consequently resulting in neural tube defects (Cieply *et al.* 2012, Ray and Niswader, 2016). Recent work in our group has identified the failure of NTC as one of the reasons behind the perinatal lethality exhibited by the GSKIP KO mouse embryos. Coupled

with the data obtained from the *in vitro* studies conducted in this project, the coordination of EMT, specifically the ZEB1 mediated regulation of the process, could constitute the molecular mechanisms behind the developmental abnormalities evident in the KO embryos.

7. Summary

Glycogen synthase kinase 3β interaction protein (GSKIP), a ubiquitously expressed protein, was identified as a direct interaction partner of glycogen synthase kinase 3β (GSK3β) and protein kinase A (PKA). It was found to facilitate the PKA-mediated inhibitory phosphorylation of GSK3β, as well as modulate the phosphorylation of GSK3β and PKA substrates. Through this modulation, GSKIP has been implicated in the fine tuning of canonical Wnt signalling and was found to play a role in both mitochondrial fission and cancer cells dynamics. Building upon these findings, this thesis uncovers novel roles for GSKIP in actin cytoskeleton reorganization and maintenance of the epithelial phenotype.

The reorganization of the cellular actin cytoskeleton is essential for various processes, among which are cell signalling, and the development and maintenance of cellular junctions and polarity. The biphasic modulation of actin dynamics is attained by the actin severing protein cofilin (CFL), which can induce either the disassembly or the assembly of the actin filaments through its ability to depolymerize and sever the filaments. The activity of CFL is negatively regulated by the Rho GTPases, p38 mitogen-activated protein kinase (p38 MAPK), and PKA mediated phosphorylation at S3. The knockdown (KD) of GSKIP in various cancer cells was found to modulate this phosphorylation, with the human non-small lung adenocarcinoma cells, A549 and the human cervical adenocarcinoma cells, HeLa-S3 exhibiting the most marked decrease in phosphorylation. The KD of GSKIP in A549 cells was characterized by increased actin depolymerization at the cellular junctions and decreased CFL abundance in the filamentous polymerized actin fraction. Similarly, the KD of GSKIP in HeLa-S3 cells was associated with phenotypic changes and an altered actin cytoskeleton, which was marked by increased actin stress fiber formation. The molecular mechanisms underlying these cytoskeletal changes were found to be most likely PKA-dependent, since the KD of GSKIP in the studied cells did not alter either the Rho GTPases or the p38 MAPK-mediated phosphorylation of CFL. Taken together, these findings implicate GSKIP as a modulator of the PKA-mediated CFL-regulated actin dynamics.

Investigating the GSKIP KD-induced phenotypic changes revealed a shift of the cells from the epithelial to the mesenchymal phenotype. Studying the associated molecular mechanisms showed downregulation of prominent epithelial markers, such as E-cadherin and β-catenin, as well as upregulation of the epithelial to mesenchymal transition (EMT) inducer ZEB1 in A549 and HeLa-S3 cells. The GSKIP KD-mediated loss of the epithelial phenotype was confirmed by investigating the integrity of crucial epithelial junctions, namely the adherens junction and the desmosomes. Both junctions displayed marked anomalies upon the KD of GSKIP, suggesting a decrease in the integrity of both and uncovering the essentiality of GSKIP for the maintenance of epithelial junctions.

8. Zusammenfassung

Das ubiquitär exprimierte Glykogen-Synthase-Kinase-3β-Interaktionsprotein (GSKIP) wurde als direkter Interaktionspartner der Glykogen-Synthase-Kinase-3β (GSK3β) und der Protein-kinase A (PKA) identifiziert. Es erleichtert die PKA-vermittelte inhibitorische Phosphorylierung von GSK3β und moduliert die Phosphorylierung von GSK3β- und PKA-Substraten. Durch diese Modulation ist GSKIP an der Feinregulation des kanonischen Wnt-Signalweges beteiligt und spielt eine Rolle in der mitochondrialen Teilung sowie der Krebszellendynamik. Basierend auf diesen Erkenntnissen deckt diese Thesis neue Rollen von GSKIP in der Reorganisation des Aktinzytoskeletts sowie der Aufrechterhaltung des epithelialen Phänotyps auf.

Die Reorganisation des zellulären Aktinzytoskeletts ist essentiell für eine Vielfalt von Prozessen, darunter die zelluläre Signalvermittlung sowie die Entwicklung und Aufrechterhaltung von Zellverbindungen und der Zellpolarität. Die biphasische Modulation der Aktindynamik wird durch das Aktin-durchtrennende Protein Cofilin gewährleistet. Dieses verfügt über die Fähigkeit, Aktinfilamente zu depolymerisieren und zu durchtrennen und so entweder deren Abbau oder Aufbau zu induzieren. Die Aktivität von Cofilin wird negativ durch eine Phosphorylierung an S3 reguliert, welche durch Rho-GTPasen, die p38 Mitogen-aktivierte Proteinkinase (p38 MAPK) sowie die PKA vermittelt wird. Es konnte gezeigt werden, dass der Knockdown von GSKIP in verschiedenen Krebszelllinien diese Phosphorylierung moduliert. Hierbei konnte in humanen nicht-kleinzelligen Lungenadenokarzinomzellen (A549) und humanen Zervixadenokarzinomzellen (HeLa-S3) die größte Abnahme der Phosphorylierung nachgewiesen werden. Der Knockdown von GSKIP in A549-Zellen wurde durch einen Anstieg der Aktindepolymerisation an den Zellverbindungen und eine Abnahme des Cofilinvorkommens in der filamentösen polymerisierten Aktinfraktion charakterisiert. In ähnlicher Weise war der Knockdown von GSKIP in HeLa-S3-Zellen mit phänotypischen Veränderungen und einem veränderten Aktinzytoskelett assoziiert, gekennzeichnet durch einen Anstieg in der Aktinstressfaserbildung. Die molekularen Mechanismen, welche diesen Änderungen des Zytoskeletts zugrunde liegen, sind höchstwahrscheinlich PKA-abhängig, da der Knockdown von GSKIP in den untersuchten Zellen weder die Rho-GTPasen- noch die p38 MAPK-vermittelte Phosphorylierung von Cofilin verändert. Zusammenfassend implizieren diese Beobachtungen, dass es sich bei GSKIP um einen Modulator der PKA-vermittelten Cofilin-regulierten Aktindynamik handelt.

Die Untersuchung von GSKIP-Knockdown-induzierten phänotypischen Veränderungen deckte einen Übergang der Zellen vom epithelialen hin zum mesenchymalen Phänotyp auf. Die Untersuchung assoziierter molekularer Mechanismen zeigte eine Herabregulation bekannter epithelialer Marker wie E-Cadherin und β-Catenin sowie eine Hochregulation von ZEB1, dem Vermittler der epithelial-mesenchymalen Transition (EMT), in A549 und HeLa-S3-

Zellen. Der GSKIP-Knockdown-vermittelte Verlust des epithelialen Phänotyps wurde durch die Untersuchung der Integrität wichtiger epithelialer Verbindungen, den Adhärenzverbindungen sowie den Desmosomen, bestätigt. Beide Verbindungen zeigten ausgeprägte Anomalien im Zuge eines Knockdowns von GSKIP. Dies suggeriert eine Abnahme ihrer Integrität und deckt die essentielle Rolle von GSKIP in der Aufrechterhaltung epithelialer Verbindungen auf.

9. Bibliography

Ab Naafs, M. (2017). "Second Messengers in Endocrinology: A Mini-Review of the Cyclic Nucleotides." J. Clin. Endocrinol. Metab 5(6).

Aberle, H., H. Schwartz & R. Kemler (1996). Cadherin-catenin complex: protein interactions and their implications for cadherin function. J Cell Biochem, 61, 514-23.

Agnew, B. J., L. S. Minamide and J. R. Bamburg (1995). "Reactivation of phosphorylated actin depolymerizing factor and identification of the regulatory site." J Biol Chem 270(29): 17582-17587.

Agustin, J. T., C. G. Wilkerson and G. B. Witman (2000). "The unique catalytic subunit of sperm cAMP-dependent protein kinase is the product of an alternative Calpha mRNA expressed specifically in spermatogenic cells." Mol Biol Cell 11(9): 3031-3044.

Albert, P. R. and L. Robillard (2002). "G protein specificity: traffic direction required." Cell Signal 14(5): 407-418.

Amano, M., M. Ito, K. Kimura, Y. Fukata, K. Chihara, T. Nakano, Y. Matsuura and K. Kaibuchi (1996). "Phosphorylation and activation of myosin by Rho-associated kinase (Rho-kinase)." J Biol Chem 271(34): 20246-20249.

Andrianantoandro, E. and T. D. Pollard (2006). "Mechanism of actin filament turnover by severing and nucleation at different concentrations of ADF/cofilin." Mol Cell 24(1): 13-23.

Asirvatham, A. L., S. G. Galligan, R. V. Schillace, M. P. Davey, V. Vasta, J. A. Beavo and D. W. Carr (2004). "A-kinase anchoring proteins interact with phosphodiesterases in T lymphocyte cell lines." J Immunol 173(8): 4806-4814.

Bamburg, J. R. and B. W. Bernstein (2008). "ADF/cofilin." Current Biology 18(7): R273-R275.

Bamburg, J. R. and B. W. Bernstein (2010). "Roles of ADF/cofilin in actin polymerization and beyond." F1000 Biol Rep 2: 62.

Bamburg, J. R., H. E. Harris and A. G. Weeds (1980). "Partial purification and characterization of an actin depolymerizing factor from brain." FEBS Lett 121(1): 178-182.

Bankston, J. R., H. A. DeBerg, S. Stoll and W. N. Zagotta (2017). "Mechanism for the inhibition of the cAMP dependence of HCN ion channels by the auxiliary subunit TRIP8b." J Biol Chem 292(43): 17794-17803.

Bastidas, A. C., M. S. Deal, J. M. Steichen, M. M. Keshwani, Y. Guo and S. S. Taylor (2012). "Role of N-terminal myristylation in the structure and regulation of cAMP-dependent protein kinase." J Mol Biol 422(2): 215-229.

Bhowmick, N. A., M. Ghiassi, A. Bakin, M. Aakre, C. A. Lundquist, M. E. Engel, C. L. Arteaga and H. L. Moses (2001). "Transforming growth factor-beta1 mediates epithelial to mesenchymal transdifferentiation through a RhoA-dependent mechanism." Mol Biol Cell 12(1): 27-36.

Brabletz, S. and T. Brabletz (2010). "The ZEB/miR-200 feedback loop--a motor of cellular plasticity in development and cancer?" EMBO Rep 11(9): 670-677.

Calejo, A. I. and K. Tasken (2015). "Targeting protein-protein interactions in complexes organized by A kinase anchoring proteins." Front Pharmacol 6: 192.

Caspi, M., A. Zilberberg, H. Eldar-Finkelman & R. Rosin-Arbesfeld (2008). Nuclear GSK-3beta inhibits the canonical Wnt signalling pathway in a beta-catenin phosphorylation-independent manner. Oncogene, 27, 3546-55.

Chang, C. J., C. H. Chao, W. Xia, J. Y. Yang, Y. Xiong, C. W. Li, W. H. Yu, S. K. Rehman, J. L. Hsu, H. H. Lee, M. Liu, C. T. Chen, D. Yu and M. C. Hung (2011). "p53 regulates epithelial-mesenchymal transition and stem cell properties through modulating miRNAs." Nat Cell Biol 13(3): 317-323.

Chang, C. W. and S. Kumar (2015). "Differential Contributions of Nonmuscle Myosin II Isoforms and Functional Domains to Stress Fiber Mechanics." Sci Rep 5: 13736.

Chen, X., J. C. Dai, S. A. Orellana and E. M. Greenfield (2005). "Endogenous protein kinase inhibitor gamma terminates immediate-early gene expression induced by cAMP-dependent protein kinase (PKA) signalling: termination depends on PKA inactivation rather than PKA export from the nucleus." J Biol Chem 280(4): 2700-2707.

Cho, J. H. and G. V. Johnson (2003). "Glycogen synthase kinase 3beta phosphorylates tau at both primed and unprimed sites. Differential impact on microtubule binding." J Biol Chem 278(1): 187-193.

Chou, H. Y., S. L. Howng, T. S. Cheng, Y. L. Hsiao, A. S. Lieu, J. K. Loh, S. L. Hwang, C. C. Lin, C. M. Hsu, C. Wang, C. I. Lee, P. J. Lu, C. K. Chou, C. Y. Huang and Y. R. Hong (2006). "GSKIP is homologous to the Axin GSK3beta interaction domain and functions as a negative regulator of GSK3beta." Biochemistry 45(38): 11379-11389.

Cieply, B., P. Riley, P. M. Pifer, J. Widmeyer, J. B. Addison, A. V. Ivanov, J. Denvir & S. M. Frisch (2012). Suppression of the epithelial-mesenchymal transition by Grainyhead-like-2. Cancer Res, 72, 2440-53.

Clapham, D. E. and E. J. Neer (1997). "G protein beta gamma subunits." Annu Rev Pharmacol Toxicol 37: 167-203.

Cohen, P. (1979). "The hormonal control of glycogen metabolism in mammalian muscle by multivalent phosphorylation." Biochem Soc Trans 7(3): 459-480.

Cole, K. A. and J. M. Maris (2012). "New strategies in refractory and recurrent neuroblastoma: translational opportunities to impact patient outcome." Clin Cancer Res 18(9): 2423-2428.

Colosimo, P. F., X. Liu, N. A. Kaplan & N. S. Tolwinski (2010). GSK3beta affects apical-basal polarity and cell-cell adhesion by regulating aPKC levels. Dev Dyn, 239, 115-25.

Corbin, J. D., P. H. Sugden, T. M. Lincoln and S. L. Keely (1977). "Compartmentalization of adenosine 3':5'-monophosphate and adenosine 3':5'-monophosphate-dependent protein kinase in heart tissue." J Biol Chem 252(11): 3854-3861.

Corbin, J. D., P. H. Sugden, L. West, D. A. Flockhart, T. M. Lincoln and D. McCarthy (1978). "Studies on the properties and mode of action of the purified regulatory subunit of bovine heart adenosine 3':5'-monophosphate-dependent protein kinase." J Biol Chem 253(11): 3997-4003.

Craven, K. B. and W. N. Zagotta (2006). "CNG and HCN channels: two peas, one pod." Annu Rev Physiol 68: 375-401.

Dan, C., A. Kelly, O. Bernard and A. Minden (2001). "Cytoskeletal changes regulated by the PAK4 serine/threonine kinase are mediated by LIM kinase 1 and cofilin." J Biol Chem 276(34): 32115-32121.

Deak, V. A., P. Skroblin, C. Dittmayer, K. P. Knobeloch, S. Bachmann and E. Klussmann (2016). "The A-kinase Anchoring Protein GSKIP Regulates GSK3beta Activity and Controls Palatal Shelf Fusion in Mice." J Biol Chem 291(2): 681-690.

Dema, A., M. F. Schroter, E. Perets, P. Skroblin, M. C. Moutty, V. A. Deak, W. Birchmeier and E. Klussmann (2016). "The A-Kinase Anchoring Protein (AKAP) Glycogen Synthase Kinase 3beta Interaction Protein (GSKIP) Regulates beta-Catenin through Its Interactions with Both Protein Kinase A (PKA) and GSK3beta." J Biol Chem 291(37): 19618-19630.

Denhardt, D. T. (1996). "Signal-transducing protein phosphorylation cascades mediated by Ras/Rho proteins in the mammalian cell: the potential for multiplex signalling." Biochem J 318(Pt 3): 729-747.

Di Benedetto, G., A. Zoccarato, V. Lissandron, A. Terrin, X. Li, M. D. Houslay, G. S. Baillie and M. Zaccolo (2008). "Protein kinase A type I and type II define distinct intracellular signalling compartments." Circ Res 103(8): 836-844.

Diehl, J. A., M. Cheng, M. F. Roussel and C. J. Sherr (1998). "Glycogen synthase kinase-3beta regulates cyclin D1 proteolysis and subcellular localization." Genes Dev 12(22): 3499-3511.

Diviani, D., J. Soderling and J. D. Scott (2001). "AKAP-Lbc anchors protein kinase A and nucleates Galpha 12-selective Rho-mediated stress fiber formation." J Biol Chem 276(47): 44247-44257.

Doherty, G. J. and H. T. McMahon (2008). "Mediation, modulation, and consequences of membrane-cytoskeleton interactions." Annu Rev Biophys 37: 65-95.

Dominguez, R. and K. C. Holmes (2011). "Actin structure and function." Annu Rev Biophys 40: 169-186.

Dovas, A. and J. R. Couchman (2005). "RhoGDI: multiple functions in the regulation of Rho family GTPase activities." Biochem J 390(Pt 1): 1-9.

Durfee, R. A., M. Mohammed and H. H. Luu (2016). "Review of Osteosarcoma and Current Management." Rheumatol Ther 3(2): 221-243.

Eccles, R. L., M. T. Czajkowski, C. Barth, P. M. Müller, E. McShane, S. Grunwald, P. Beaudette, N. Mecklenburg, R. Volkmer, K. Zühlke, G. Dittmar, M. Selbach, A. Hammes, O. Daumke, E. Klussmann, S. Urbé & O. Rocks (2016). Bimodal antagonism of PKA signalling by ARHGAP36. Nat Commun, 7, 12963.

Edwards, D. C., L. C. Sanders, G. M. Bokoch and G. N. Gill (1999). "Activation of LIM-kinase by Pak1 couples Rac/Cdc42 GTPase signalling to actin cytoskeletal dynamics." Nat Cell Biol 1(5): 253-259.

Embi, N., D. B. Rylatt and P. Cohen (1980). "Glycogen synthase kinase-3 from rabbit skeletal muscle. Separation from cyclic-AMP-dependent protein kinase and phosphorylase kinase." Eur J Biochem 107(2): 519-527.

Fang, X., S. X. Yu, Y. Lu, R. C. Bast, Jr., J. R. Woodgett and G. B. Mills (2000). "Phosphorylation and inactivation of glycogen synthase kinase 3 by protein kinase A." Proc Natl Acad Sci U S A 97(22): 11960-11965.

Fischer, E. H. and E. G. Krebs (1955). "Conversion of phosphorylase b to phosphorylase a in muscle extracts." J Biol Chem 216(1): 121-132.

Flynn, M. P., E. T. Maizels, A. B. Karlsson, T. McAvoy, J. H. Ahn, A. C. Nairn and M. Hunzicker-Dunn (2008). "Luteinizing hormone receptor activation in ovarian granulosa cells promotes protein kinase A-dependent dephosphorylation of microtubule-associated protein 2D." Mol Endocrinol 22(7): 1695-1710.

Gallicano, G. I., P. Kouklis, C. Bauer, M. Yin, V. Vasioukhin, L. Degenstein & E. Fuchs (1998). Desmoplakin is required early in development for assembly of desmosomes and cytoskeletal linkage. J Cell Biol, 143, 2009-22.

Garcia, M. A., W. J. Nelson and N. Chavez (2017). "Cell-Cell Junctions Organize Structural and Signalling Networks." Cold Spring Harb Perspect Biol.

Ghosh, M., X. Song, G. Mouneimne, M. Sidani, D. S. Lawrence and J. S. Condeelis (2004). "Cofilin promotes actin polymerization and defines the direction of cell motility." Science 304(5671): 743-746.

Giepmans, B. N. and S. C. van Ijzendoorn (2009). "Epithelial cell-cell junctions and plasma membrane domains." Biochim Biophys Acta 1788(4): 820-831.

Gloerich, M. and J. L. Bos (2010). "Epac: defining a new mechanism for cAMP action." Annu Rev Pharmacol Toxicol 50: 355-375.

Godsel, L. M., A. D. Dubash, A. E. Bass-Zubek, E. V. Amargo, J. L. Klessner, R. P. Hobbs, X. Chen & K. J. Green (2010). "Plakophilin 2 couples actomyosin remodeling to desmosomal plaque assembly via RhoA." Mol Biol Cell, 21, 2844-59.

Godsel, L. M., S. N. Hsieh, E. V. Amargo, A. E. Bass, L. T. Pascoe-McGillicuddy, A. C. Huen, M. E. Thorne, C. A. Gaudry, J. K. Park, K. Myung, R. D. Goldman, T. L. Chew & K. J. Green (2005). " Desmoplakin assembly dynamics in four dimensions: multiple phases differentially regulated by intermediate filaments and actin." J Cell Biol, 171, 1045-59.

Gohla, A., J. Birkenfeld and G. M. Bokoch (2005). "Chronophin, a novel HAD-type serine protein phosphatase, regulates cofilin-dependent actin dynamics." Nat Cell Biol 7(1): 21-29.

Gold, M. G., B. Lygren, P. Dokurno, N. Hoshi, G. McConnachie, K. Tasken, C. R. Carlson, J. D. Scott and D. Barford (2006). "Molecular basis of AKAP specificity for PKA regulatory subunits." Mol Cell 24(3): 383-395.

Gomez, E. W., Q. K. Chen, N. Gjorevski and C. M. Nelson (2010). "Tissue geometry patterns epithelial-mesenchymal transition via intercellular mechanotransduction." J Cell Biochem 110(1): 44-51.

Götz, F., Y. Roske, M. S. Schulz, K. Autenrieth, D. Bertinetti, K. Faelber, K. Zühlke, A. Kreuchwig, E. J. Kennedy, G. Krause, O. Daumke, F. W. Herberg, U. Heinemann & E. Klussmann (2016). "AKAP18:PKA-RIIα structure reveals crucial anchor points for recognition of regulatory subunits of PKA." *Biochem J,* 473**,** 1881-94.

Goyal, P., D. Pandey, A. Behring and W. Siess (2005). "Inhibition of Nuclear Import of LIMK2 in Endothelial Cells by Protein Kinase C-dependent Phosphorylation at Ser-283." J Biol Chem 280(30): 27569-27577.

Goyal, P., D. Pandey and W. Siess (2006). "Phosphorylation-dependent regulation of unique nuclear and nucleolar localization signals of LIM kinase 2 in endothelial cells." J Biol Chem 281(35): 25223-25230.

Gugnoni, M., V. Sancisi, G. Manzotti, G. Gandolfi and A. Ciarrocchi (2016). "Autophagy and epithelial-mesenchymal transition: an intricate interplay in cancer." Cell Death Dis 7(12): e2520.

Hall, A. (1998). "Rho GTPases and the Actin Cytoskeleton." Science 279(5350): 509.

Hart, M. J., R. de los Santos, I. N. Albert, B. Rubinfeld and P. Polakis (1998). "Downregulation of beta-catenin by human Axin and its association with the APC tumor suppressor, beta-catenin and GSK3 beta." Curr Biol 8(10): 573-581.

Hobbs, R. P. and K. J. Green (2012). "Desmoplakin regulates desmosome hyperadhesion." J Invest Dermatol 132(2): 482-485.

Hoeflich, K. P., J. Luo, E. A. Rubie, M. S. Tsao, O. Jin and J. R. Woodgett (2000). "Requirement for glycogen synthase kinase-3beta in cell survival and NF-kappaB activation." Nature 406(6791): 86-90.

Hoshi, M., A. Takashima, K. Noguchi, M. Murayama, M. Sato, S. Kondo, Y. Saitoh, K. Ishiguro, T. Hoshino and K. Imahori (1996). "Regulation of mitochondrial pyruvate dehydrogenase activity by tau protein kinase I/glycogen synthase kinase 3beta in brain." Proc Natl Acad Sci U S A 93(7): 2719-2723.

Hotulainen, P., E. Paunola, M. K. Vartiainen and P. Lappalainen (2005). "Actin-depolymerizing factor and cofilin-1 play overlapping roles in promoting rapid F-actin depolymerization in mammalian nonmuscle cells." Mol Biol Cell 16(2): 649-664.

Huang, T. Y., C. DerMardirossian and G. M. Bokoch (2006). "Cofilin phosphatases and regulation of actin dynamics." Curr Opin Cell Biol 18(1): 26-31.

Hundsrucker, C., P. Skroblin, F. Christian, H. M. Zenn, V. Popara, M. Joshi, J. Eichhorst, B. Wiesner, F. W. Herberg, B. Reif, W. Rosenthal and E. Klussmann (2010). "Glycogen synthase kinase 3beta interaction protein functions as an A-kinase anchoring protein." J Biol Chem 285(8): 5507-5521.

Hung, A. Y. and M. Sheng (2002). "PDZ domains: structural modules for protein complex assembly." J Biol Chem 277(8): 5699-5702.

Hurley, J. H. (1999). "Structure, mechanism, and regulation of mammalian adenylyl cyclase." J Biol Chem 274(12): 7599-7602.

Ikebe, M. and D. J. Hartshorne (1985). "Phosphorylation of smooth muscle myosin at two distinct sites by myosin light chain kinase." J Biol Chem 260(18): 10027-10031.

Ikebe, M., J. Koretz and D. J. Hartshorne (1988). "Effects of phosphorylation of light chain residues threonine 18 and serine 19 on the properties and conformation of smooth muscle myosin." J Biol Chem 263(13): 6432-6437.

Ilouz, R., N. Kowalsman, M. Eisenstein and H. Eldar-Finkelman (2006). "Identification of novel glycogen synthase kinase-3beta substrate-interacting residues suggests a common mechanism for substrate recognition." J Biol Chem 281(41): 30621-30630.

Jarnaess, E., A. Ruppelt, A. J. Stokka, B. Lygren, J. D. Scott and K. Tasken (2008). "Dual specificity A-kinase anchoring proteins (AKAPs) contain an additional binding region that enhances targeting of protein kinase A type I." J Biol Chem 283(48): 33708-33718.

Ji, W. K., A. L. Hatch, R. A. Merrill, S. Strack and H. N. Higgs (2015). "Actin filaments target the oligomeric maturation of the dynamin GTPase Drp1 to mitochondrial fission sites." Elife 4: e11553.

Jia, D., M. K. Jolly, S. C. Tripathi, P. Den Hollander, B. Huang, M. Lu, M. Celiktas, E. Ramirez-Peña, E. Ben-Jacob, J. N. Onuchic, S. M. Hanash, S. A. Mani and H. Levine (2017). "Distinguishing mechanisms underlying EMT tristability." Cancer Convergence 1(1): 2.

Jiang, W., M. Betson, R. Mulloy, R. Foster, M. Lévay, E. Ligeti & J. Settleman (2008) p190A. RhoGAP is a glycogen synthase kinase-3-beta substrate required for polarized cell migration. J Biol Chem, 283, 20978-88.

Jolly, M. K., M. Boareto, B. Huang, D. Jia, M. Lu, E. Ben-Jacob, J. N. Onuchic & H. Levine (2015). Implications of the Hybrid Epithelial/Mesenchymal Phenotype in Metastasis. Front Oncol, 5, 155.

Kanellos, G. and M. C. Frame (2016). "Cellular functions of the ADF/cofilin family at a glance." J Cell Sci 129(17): 3211-3218.

Kawano, Y., Y. Fukata, N. Oshiro, M. Amano, T. Nakamura, M. Ito, F. Matsumura, M. Inagaki and K. Kaibuchi (1999). "Phosphorylation of myosin-binding subunit (MBS) of myosin phosphatase by Rho-kinase in vivo." J Cell Biol 147(5): 1023-1038.

Kestler, C., G. Knobloch, I. Tessmer, E. Jeanclos, H. Schindelin and A. Gohla (2014). "Chronophin dimerization is required for proper positioning of its substrate specificity loop." J Biol Chem 289(5): 3094-3103.

Khurana, T., B. Khurana and A. A. Noegel (2002). "LIM proteins: association with the actin cytoskeleton." Protoplasma 219(1-2): 1-12.

Kim, Y. Y., S. H. Yun and J. Yun (2018). "Downregulation of Drp1, a fission regulator, is associated with human lung and colon cancers." Acta Biochim Biophys Sin (Shanghai) 50(2): 209-215.

Kim, D. H., T. Xing, Z. Yang, R. Dudek, Q. Lu & Y. H. Chen (2017). Epithelial Mesenchymal Transition in Embryonic Development, Tissue Repair and Cancer: A Comprehensive Overview. J Clin Med, 7.

Kinderman, F. S., C. Kim, S. von Daake, Y. Ma, B. Q. Pham, G. Spraggon, N.-H. Xuong, P. A. Jennings and S. S. Taylor (2006). "A Novel and Dynamic Mechanism for AKAP Binding to RII Isoforms of cAMP-dependent Protein Kinase." Molecular cell 24(3): 397-408.

Kinderman, F. S., C. Kim, S. von Daake, Y. Ma, B. Q. Pham, G. Spraggon, N. H. Xuong, P. A. Jennings and S. S. Taylor (2006). "A dynamic mechanism for AKAP binding to RII isoforms of cAMP-dependent protein kinase." Mol Cell 24(3): 397-408.

Knott, A. B., G. Perkins, R. Schwarzenbacher & E. Bossy-Wetzel (2008). Mitochondrial fragmentation in neurodegeneration. Nat Rev Neurosci, 9, 505-18.

Kobayashi, M., M. Nishita, T. Mishima, K. Ohashi and K. Mizuno (2006). "MAPKAPK-2-mediated LIM-kinase activation is critical for VEGF-induced actin remodeling and cell migration." EMBO J 25(4): 713-726.

Kowalczyk, A. P. and K. J. Green (2013). "Structure, function, and regulation of desmosomes." Prog Mol Biol Transl Sci 116: 95-118.

Kröger, C., F. Loschke, N. Schwarz, R. Windoffer, R. E. Leube and T. M. Magin (2013). "Keratins control intercellular adhesion involving PKC-α-mediated desmoplakin

phosphorylation." J Cell Biol 201(5): 681-692.

Kumar, S., A. Das and S. Sen (2014). "Extracellular matrix density promotes EMT by weakening cell-cell adhesions." Mol Biosyst 10(4): 838-850.

Lamouille, S., J. Xu and R. Derynck (2014). "Molecular mechanisms of epithelial-mesenchymal transition." Nat Rev Mol Cell Biol 15(3): 178-196.

Lang, P., F. Gesbert, M. Delespine-Carmagnat, R. Stancou, M. Pouchelet & J. Bertoglio (1996). Protein kinase A phosphorylation of RhoA mediates the morphological and functional effects of cyclic AMP in cytotoxic lymphocytes. EMBO J, 15, 510-9.

Larsen, J. E., V. Nathan, J. K. Osborne, R. K. Farrow, D. Deb, J. P. Sullivan, P. D. Dospoy, A. Augustyn, S. K. Hight, M. Sato, L. Girard, C. Behrens, I. I. Wistuba, A. F. Gazdar, N. K. Hayward and J. D. Minna (2016). "ZEB1 drives epithelial-to-mesenchymal transition in lung cancer." J Clin Invest 126(9): 3219-3235.

Lee, Y. J., S. Y. Jeong, M. Karbowski, C. L. Smith and R. J. Youle (2004). "Roles of the mammalian mitochondrial fission and fusion mediators Fis1, Drp1, and Opa1 in apoptosis." Mol Biol Cell 15(11): 5001-5011.

Li, G., J. Zhou, A. Budhraja, X. Hu, Y. Chen, Q. Cheng, L. Liu, T. Zhou, P. Li, E. Liu & N. Gao (2015). Mitochondrial translocation and interaction of cofilin and Drp1 are required for erucin-induced mitochondrial fission and apoptosis. Oncotarget, 6, 1834-49.

Li, M., X. Wang, M. K. Meintzer, T. Laessig, M. J. Birnbaum and K. A. Heidenreich (2000). "Cyclic AMP promotes neuronal survival by phosphorylation of glycogen synthase kinase 3beta." Mol Cell Biol 20(24): 9356-9363.

Li, S. and J. Yang (2014). "Ovol proteins: guardians against EMT during epithelial differentiation." Dev Cell 29(1): 1-2.

Liu, C., Y. Li, M. Semenov, C. Han, G. H. Baeg, Y. Tan, Z. Zhang, X. Lin and X. He (2002). "Control of beta-catenin phosphorylation/degradation by a dual-kinase mechanism." Cell 108(6): 837-847.

Lodish, H., A. Berk, P. Matsudaira, D. Baltimore, S. L. Zipursky and J. Darnell (1995). Molecular Cell Biology, W. H. Freeman.

Loh, J. K., C. C. Lin, M. C. Yang, C. H. Chou, W. S. Chen, M. C. Hong, C. L. Cho, C. M. Hsu, J. T. Cheng, A. K. Chou, C. H. Chang, C. N. Tseng, C. H. Wang, A. S. Lieu, S. L. Howng and Y. R. Hong (2015). "GSKIP- and GSK3-mediated anchoring strengthens cAMP/PKA/Drp1 axis signalling in the regulation of mitochondrial elongation." Biochim Biophys Acta 1853(8): 1796-1807.

Lowe, J. S. and P. G. Anderson (2015). Chapter 3 - Epithelial Cells. Stevens & Lowe's Human Histology (Fourth Edition) (Fourth Edition). Philadelphia, Mosby: 37-54.

Maciver, S. K. and P. J. Hussey (2002). "The ADF/cofilin family: actin-remodeling proteins." Genome Biol 3(5): reviews3007.

Maimaiti, Y., J. Tan, Z. Liu, Y. Guo, Y. Yan, X. Nie, B. Huang, J. Zhou and T. Huang (2017). "Overexpression of cofilin correlates with poor survival in breast cancer: A tissue microarray analysis." Oncol Lett 14(2): 2288-2294.

Manetti, F. (2012). "LIM kinases are attractive targets with many macromolecular partners and only a few small molecule regulators." Med Res Rev 32(5): 968-998.

Manning, G., D. B. Whyte, R. Martinez, T. Hunter and S. Sudarsanam (2002). "The protein kinase complement of the human genome." Science 298(5600): 1912-1934.

McCormick, K. and G. S. Baillie (2014). "Compartmentalisation of second messenger signalling pathways." Curr Opin Genet Dev 27: 20-25.

Mizuno, K. (2013). "Signalling mechanisms and functional roles of cofilin phosphorylation and dephosphorylation." Cell Signal 25(2): 457-469.

Moore, P. B., H. E. Huxley and D. J. DeRosier (1970). "Three-dimensional reconstruction of F-actin, thin filaments and decorated thin filaments." J Mol Biol 50(2): 279-295.

Moore, S. F., M. T. van den Bosch, R. W. Hunter, K. Sakamoto, A. W. Poole & I. Hers (2013). Dual regulation of glycogen synthase kinase 3 (GSK3)α/β by protein kinase C (PKC)α and Akt promotes thrombin-mediated integrin αIIbβ3 activation and granule secretion in platelets. J Biol Chem, 288, 3918-28.

Morfini, G., G. Szebenyi, R. Elluru, N. Ratner and S. T. Brady (2002). "Glycogen synthase kinase 3 phosphorylates kinesin light chains and negatively regulates kinesin-based motility." EMBO J 21(3): 281-293.

Moriyama, K., K. Iida and I. Yahara (1996). "Phosphorylation of Ser-3 of cofilin regulates its essential function on actin." Genes Cells 1(1): 73-86.

Motiani, R. K., J. Tanwar, D. A. Raja, A. Vashisht, S. Khanna, S. Sharma, S. Srivastava, S. Sivasubbu, V. T. Natarajan and R. S. Gokhale (2018). "STIM1 activation of adenylyl cyclase 6 connects Ca(2+) and cAMP signalling during melanogenesis." EMBO J 37(5).

Nadella, K. S., G. N. Jones, A. Trimboli, C. A. Stratakis, G. Leone & L. S. Kirschner (2008). Targeted deletion of Prkar1a reveals a role for protein kinase A in mesenchymal-to-epithelial transition. Cancer Res, 68, 2671-7.

Nadella, K. S., M. Saji, N. K. Jacob, E. Pavel, M. D. Ringel and L. S. Kirschner (2009). "Regulation of actin function by protein kinase A-mediated phosphorylation of Limk1." EMBO Rep 10(6): 599-605.

Nagata, K., K. Ohashi, N. Yang and K. Mizuno (1999). "The N-terminal LIM domain negatively regulates the kinase activity of LIM-kinase 1." Biochem J 343 Pt 1: 99-105.

Neuber, S., M. Muhmer, D. Wratten, P. J. Koch, R. Moll and A. Schmidt (2010). "The desmosomal plaque proteins of the plakophilin family." Dermatol Res Pract 2010: 101452.

Newlon, M. G., M. Roy, D. Morikis, D. W. Carr, R. Westphal, J. D. Scott and P. A. Jennings (2001). "A novel mechanism of PKA anchoring revealed by solution structures of anchoring complexes." EMBO J 20(7): 1651-1662.

Newlon, M. G., M. Roy, D. Morikis, Z. E. Hausken, V. Coghlan, J. D. Scott and P. A. Jennings (1999). "The molecular basis for protein kinase A anchoring revealed by solution NMR." Nat Struct Biol 6(3): 222-227.

Newton, A. C., M. D. Bootman and J. D. Scott (2016). "Second Messengers." Cold Spring Harb Perspect Biol 8(8).

Niessen, C. M. (2007). Tight junctions/adherens junctions: basic structure and function. J Invest Dermatol, 127, 2525-32.

Niwa, R., K. Nagata-Ohashi, M. Takeichi, K. Mizuno and T. Uemura (2002). "Control of Actin Reorganization by Slingshot, a Family of Phosphatases that Dephosphorylate ADF/cofilin." Cell 108(2): 233-246.

Ohashi, K. (2015). "Roles of cofilin in development and its mechanisms of regulation." Dev Growth Differ 57(4): 275-290.

Ohashi, K., K. Nagata, M. Maekawa, T. Ishizaki, S. Narumiya and K. Mizuno (2000). "Rho-associated Kinase ROCK Activates LIM-kinase 1 by Phosphorylation at Threonine 508 within the Activation Loop." J Biol Chem 275(5): 3577-3582.

Ohta, Y., K. Kousaka, K. Nagata-Ohashi, K. Ohashi, A. Muramoto, Y. Shima, R. Niwa, T. Uemura and K. Mizuno (2003). "Differential activities, subcellular distribution and tissue expression patterns of three members of Slingshot family phosphatases that dephosphorylate cofilin." Genes Cells 8(10): 811-824.

Okano, I., J. Hiraoka, H. Otera, K. Nunoue, K. Ohashi, S. Iwashita, M. Hirai and K. Mizuno (1995). "Identification and characterization of a novel family of serine/threonine kinases containing two N-terminal LIM motifs." J Biol Chem 270(52): 31321-31330.

Ono, S. (2007). "Mechanism of depolymerization and severing of actin filaments and its significance in cytoskeletal dynamics." Int Rev Cytol 258: 1-82.

Ono, S. (2007). "Mechanism of depolymerization and severing of actin filaments and its significance in cytoskeletal dynamics." Int Rev Cytol 258: 1-82.

Pandey, M. K. and T. R. DeGrado (2016). "Glycogen Synthase Kinase-3 (GSK-3)-Targeted Therapy and Imaging." Theranostics 6(4): 571-593.

Pasdar, M. & Z. Li (1993). Disorganization of microfilaments and intermediate filaments interferes with the assembly and stability of desmosomes in MDCK epithelial cells. Cell Motil Cytoskeleton, 26, 163-80.

Patel, T. B., Z. Du, S. Pierre, L. Cartin and K. Scholich (2001). "Molecular biological approaches to unravel adenylyl cyclase signalling and function." Gene 269(1-2): 13-25.

Perkins, G. A., L. Wang, L. J. Huang, K. Humphries, V. J. Yao, M. Martone, T. J. Deerinck, D. M. Barraclough, J. D. Violin, D. Smith, A. Newton, J. D. Scott, S. S. Taylor and M. H. Ellisman (2001). "PKA, PKC, and AKAP localization in and around the neuromuscular junction." BMC Neurosci 2: 17.

Pidoux, G. and K. Tasken (2010). "Specificity and spatial dynamics of protein kinase A signalling organized by A-kinase-anchoring proteins." J Mol Endocrinol 44(5): 271-284.

Qiao, J., F. Huang & H. Lum (2003). PKA inhibits RhoA activation: a protection mechanism against endothelial barrier dysfunction. Am J Physiol Lung Cell Mol Physiol, 284, L972-80.

Rall, T. W. and E. W. Sutherland (1958). "Formation of a cyclic adenine ribonucleotide by tissue particles." J Biol Chem 232(2): 1065-1076.

Rall, T. W. and E. W. Sutherland (1958). "Formation of a cyclic adenine ribonucleotide by tissue particles." J Biol Chem 232(2): 1065-1076.

Ramelot, T. A., J. R. Cort, S. Goldsmith-Fischman, G. J. Kornhaber, R. Xiao, R. Shastry, T. B. Acton, B. Honig, G. T. Montelione & M. A. Kennedy (2004). Solution NMR structure of the iron-sulfur cluster assembly protein U (IscU) with zinc bound at the active site. J Mol Biol, 344, 567-83.

Ray, H. J. & L. A. Niswander (2016). Dynamic behaviors of the non-neural ectoderm during mammalian cranial neural tube closure. Dev Biol, 416, 279-85.

Ray, H. J. & L. A. Niswander (2016). Grainyhead-like 2 downstream targets act to suppress epithelial-to-mesenchymal transition during neural tube closure. Development, 143, 1192-204.

Raya-Sandino, A., A. Castillo-Kauil, A. Dominguez-Calderon, L. Alarcon, D. Flores-Benitez, F. Cuellar-Perez, B. Lopez-Bayghen, B. Chavez-Munguia, J. Vazquez-Prado and L. Gonzalez-Mariscal (2017). "Zonula occludens-2 regulates Rho proteins activity and the development of epithelial cytoarchitecture and barrier function." Biochim Biophys Acta 1864(10): 1714-1733.

Rehklau, K., L. Hoffmann, C. B. Gurniak, M. Ott, W. Witke, L. Scorrano, C. Culmsee & M. B. Rust. (2017) Cofilin-1-dependent actin dynamics control DRP1-mediated mitochondrial fission. Cell Death Dis, 8, e3063.

Ringheim, G. E. and S. S. Taylor (1990). "Dissecting the domain structure of the regulatory subunit of cAMP-dependent protein kinase I and elucidating the role of MgATP." J Biol Chem 265(9): 4800-4808.

Rubinfeld, B., I. Albert, E. Porfiri, C. Fiol, S. Munemitsu and P. Polakis (1996). "Binding of GSK3beta to the APC-beta-catenin complex and regulation of complex assembly." Science 272(5264): 1023-1026.

Schillace, R. V., J. W. Voltz, A. T. Sim, S. Shenolikar and J. D. Scott (2001). "Multiple interactions within the AKAP220 signalling complex contribute to protein phosphatase 1 regulation." J Biol Chem 276(15): 12128-12134.

Schmidt, M., F. J. Dekker and H. Maarsingh (2013). "Exchange protein directly activated by cAMP (epac): a multidomain cAMP mediator in the regulation of diverse biological functions." Pharmacol Rev 65(2): 670-709.

Schrade K., Tröger J, Eldahshan A., Zühlke K., Abdul Azeez K., Elkins J., Neuenschwander M., Oder A., Elkewedi M., Jaksch S., Andrae K., et al., (2018). "An AKAP-Lbc-RhoA interaction inhibitor promotes the translocation of aquaporin-2 to the plasma membrane of renal collecting duct principal cells." PLoS ONE 13(1): e0191423.

Seino, S. and T. Shibasaki (2005). "PKA-dependent and PKA-independent pathways for cAMP-regulated exocytosis." Physiol Rev 85(4): 1303-1342.

Serrano-Gomez, S. J., M. Maziveyi and S. K. Alahari (2016). "Regulation of epithelial-mesenchymal transition through epigenetic and post-translational modifications." Molecular Cancer 15: 18.

Shankar, J. and I. R. Nabi (2015). "Actin Cytoskeleton Regulation of Epithelial Mesenchymal Transition in Metastatic Cancer Cells." PLoS One 10(7): e0132759.

Shin, K., V. C. Fogg and B. Margolis (2006). "Tight junctions and cell polarity." Annu Rev Cell Dev Biol 22: 207-235.

Siemens, H., R. Jackstadt, S. Hunten, M. Kaller, A. Menssen, U. Gotz and H. Hermeking (2011). "miR-34 and SNAIL form a double-negative feedback loop to regulate epithelial-mesenchymal transitions." Cell Cycle 10(24): 4256-4271.

Simpson, C. L., D. M. Patel & K. J. Green (2011). Deconstructing the skin: cytoarchitectural determinants of epidermal morphogenesis. Nat Rev Mol Cell Biol, 12, 565-80.

Skalhegg, B. S. and K. Tasken (2000). "Specificity in the cAMP/PKA signalling pathway. Differential expression,regulation, and subcellular localization of subunits of PKA." Front Biosci 5: D678-693.

Skroblin, P., S. Grossmann, G. Schafer, W. Rosenthal and E. Klussmann (2010). "Mechanisms of protein kinase A anchoring." Int Rev Cell Mol Biol 283: 235-330.

Somlyo, A. P. and A. V. Somlyo (2003). "Ca2+ sensitivity of smooth muscle and nonmuscle myosin II: modulated by G proteins, kinases, and myosin phosphatase." Physiol Rev 83(4): 1325-1358.

Soosairajah, J., S. Maiti, O. Wiggan, P. Sarmiere, N. Moussi, B. Sarcevic, R. Sampath, J. R. Bamburg and O. Bernard (2005). "Interplay between components of a novel LIM kinase-slingshot phosphatase complex regulates cofilin." EMBO J 24(3): 473-486.

Stamos, J. L. & W. I. Weis (2013). The β-catenin destruction complex. Cold Spring Harb Perspect Biol, 5, a007898.

Steed, E., M. S. Balda and K. Matter (2010). "Dynamics and functions of tight junctions." Trends Cell Biol 20(3): 142-149.

Stengel, K. and Y. Zheng (2011). "Cdc42 in oncogenic transformation, invasion, and tumorigenesis." Cell Signal 23(9): 1415-1423.

Sumi, T., K. Matsumoto and T. Nakamura (2001). "Specific activation of LIM kinase 2 via phosphorylation of threonine 505 by ROCK, a Rho-dependent protein kinase." J Biol Chem 276(1): 670-676.

Sutherland, C., I. A. Leighton and P. Cohen (1993). "Inactivation of glycogen synthase kinase-3 beta by phosphorylation: new kinase connections in insulin and growth-factor signalling." Biochem J 296 (Pt 1): 15-19.

Tanji, C., H. Yamamoto, N. Yorioka, N. Kohno, K. Kikuchi and A. Kikuchi (2002). "A-kinase anchoring protein AKAP220 binds to glycogen synthase kinase-3beta (GSK-3beta) and mediates protein kinase A-dependent inhibition of GSK-3beta." J Biol Chem 277(40): 36955-36961.

Taylor, S. S., R. Ilouz, P. Zhang and A. P. Kornev (2012). "Assembly of allosteric macromolecular switches: lessons from PKA." Nat Rev Mol Cell Biol 13(10): 646-658.

Thiery, J. P. (2002). "Epithelial-mesenchymal transitions in tumour progression." Nat Rev Cancer 2(6): 442-454.

Thiery, J. P. and J. P. Sleeman (2006). "Complex networks orchestrate epithelial-mesenchymal transitions." Nat Rev Mol Cell Biol 7(2): 131-142.

Thomas, G. M., S. Frame, M. Goedert, I. Nathke, P. Polakis and P. Cohen (1999). "A GSK3-binding peptide from FRAT1 selectively inhibits the GSK3-catalysed phosphorylation of axin and beta-catenin." FEBS Lett 458(2): 247-251.

Tian, X., Z. Liu, B. Niu, J. Zhang, T. K. Tan, S. R. Lee, Y. Zhao, D. C. Harris and G. Zheng (2011). "E-cadherin/beta-catenin complex and the epithelial barrier." J Biomed Biotechnol 2011: 567305.

Troger, J., M. C. Moutty, P. Skroblin and E. Klussmann (2012). "A-kinase anchoring proteins as potential drug targets." Br J Pharmacol 166(2): 420-433.

Tsai, C.-H. and Y.-J. Lee (2012). "Focus on ADF/cofilin: Beyond Actin Cytoskeletal Regulation." ISRN Cell Biology 2012: 1-7.

Turhani, D., K. Krapfenbauer, D. Thurnher, H. Langen and M. Fountoulakis (2006). "Identification of differentially expressed, tumor-associated proteins in oral squamous cell carcinoma by proteomic analysis." Electrophoresis 27(7): 1417-1423.

Turnham, R. E. and J. D. Scott (2016). "Protein kinase A catalytic subunit isoform PRKACA; History, function and physiology." Gene 577(2): 101-108.

Turnham, R. E. and J. D. Scott (2016). "Protein kinase A catalytic subunit isoform PRKACA; History, function and physiology." Gene 577(2): 101-108.

Ueda, K., M. Murata-Hori, M. Tatsuka and H. Hosoya (2002). "Rho-kinase contributes to diphosphorylation of myosin II regulatory light chain in nonmuscle cells." Oncogene 21(38): 5852-5860.

Valenta, T., G. Hausmann & K. Basler (2012). The many faces and functions of β-catenin. EMBO J, 31, 2714-36.

Van Aelst, L. & C. D'Souza-Schorey (1997). Rho GTPases and signalling networks. Genes Dev, 11, 2295-322.

Vartiainen, M. K., T. Mustonen, P. K. Mattila, P. J. Ojala, I. Thesleff, J. Partanen and P. Lappalainen (2002). "The three mouse actin-depolymerizing factor/cofilins evolved to fulfill cell-type-specific requirements for actin dynamics." Mol Biol Cell 13(1): 183-194.

Vasioukhin, V., C. Bauer, M. Yin & E. Fuchs (2000). Directed actin polymerization is the driving force for epithelial cell-cell adhesion. Cell, 100, 209-19.

Vezzosi, D. and J. Bertherat (2011). "Phosphodiesterases in endocrine physiology and disease." Eur J Endocrinol 165(2): 177-188.

Vigil, D., D. K. Blumenthal, W. T. Heller, S. Brown, J. M. Canaves, S. S. Taylor and J. Trewhella (2004). "Conformational differences among solution structures of the type Ialpha, IIalpha and IIbeta protein kinase A regulatory subunit homodimers: role of the linker regions." J Mol Biol 337(5): 1183-1194.

Wainger, B. J., M. DeGennaro, B. Santoro, S. A. Siegelbaum and G. R. Tibbs (2001). "Molecular mechanism of cAMP modulation of HCN pacemaker channels." Nature 411(6839): 805-810.

Wallace, D. C. (2012). Mitochondria and cancer. Nat Rev Cancer, 12, 685-98.

Walsh, D. A., J. P. Perkins and E. G. Krebs (1968). "An adenosine 3',5'-monophosphate-dependant protein kinase from rabbit skeletal muscle." J Biol Chem 243(13): 3763-3765.

Wang, H., L. Tao, F. Jin, H. Gu, X. Dai, T. Ni, J. Feng, Y. Ding, W. Xiao, Y. Qian and Y. Liu (2017). "Cofilin 1 induces the epithelial-mesenchymal transition of gastric cancer cells by promoting cytoskeletal rearrangement." Oncotarget 8(24): 39131-39142.

Wang, W., G. Mouneimne, M. Sidani, J. Wyckoff, X. Chen, A. Makris, S. Goswami, A. R. Bresnick and J. S. Condeelis (2006). "The activity status of cofilin is directly related to invasion, intravasation, and metastasis of mammary tumors." J Cell Biol 173(3): 395-404.

Watanabe, T., H. Hosoya and S. Yonemura (2007). "Regulation of myosin II dynamics by phosphorylation and dephosphorylation of its light chain in epithelial cells." Mol Biol Cell 18(2): 605-616.

Wennerberg, K. and C. J. Der (2004). "Rho-family GTPases: it's not only Rac and Rho (and I like it)." J Cell Sci 117(8): 1301-1312.

Whiting, J. L., P. J. Nygren, B. J. Tunquist, L. K. Langeberg, O. M. Seternes and J. D. Scott (2015). "Protein Kinase A Opposes the Phosphorylation-dependent Recruitment of Glycogen Synthase Kinase 3beta to A-kinase Anchoring Protein 220." J Biol Chem 290(32): 19445-19457.

Woodgett, J. R. (1990). "Molecular cloning and expression of glycogen synthase kinase-3/factor A." EMBO J 9(8): 2431-2438.

Xiao, J., Y. Lv, F. Jin, Y. Liu, Y. Ma, Y. Xiong, L. Liu, S. Zhang, Y. Sun, G. L. Tipoe, A. Hong, F. Xing and X. Wang (2017). "LncRNA HANR Promotes Tumorigenesis and Increase of Chemoresistance in Hepatocellular Carcinoma." Cell Physiol Biochem 43(5): 1926-1938.

Xu, Y. and S. Lu (2015). "Transforming growth factor-β1-induced epithelial to mesenchymal transition increases mitochondrial content in the A549 non-small cell lung cancer cell line." Mol Med Rep 11(1): 417-421.

Yonemura, S., Y. Wada, T. Watanabe, A. Nagafuchi and M. Shibata (2010). "alpha-Catenin as a tension transducer that induces adherens junction development." Nat Cell Biol 12(6): 533-542.

Yoon, C., S. J. Cho, K. K. Chang, D. J. Park, S. W. Ryeom and S. S. Yoon (2017). "Role of Rac1 Pathway in Epithelial-to-Mesenchymal Transition and Cancer Stem-like Cell Phenotypes in Gastric Adenocarcinoma." Mol Cancer Res 15(8): 1106-1116.

Yu, Y. and R. C. Elble (2016). "Homeostatic Signalling by Cell-Cell Junctions and Its Dysregulation during Cancer Progression." J Clin Med 5(2).

Zaravinos, A. (2015). "The Regulatory Role of MicroRNAs in EMT and Cancer." J Oncol 2015: 865816.

Zebda, N., O. Bernard, M. Bailly, S. Welti, D. S. Lawrence and J. S. Condeelis (2000). "Phosphorylation of ADF/cofilin abolishes EGF-induced actin nucleation at the leading edge and subsequent lamellipod extension." J Cell Biol 151(5): 1119-1128.

Zigmond, S. H. (1996). "Signal transduction and actin filament organization." Current Opinion in Cell Biology 8(1): 66-73.

Zoller, M. J., A. R. Kerlavage and S. S. Taylor (1979). "Structural comparisons of cAMP-dependent protein kinases I and II from porcine skeletal muscle." J Biol Chem 254(7): 2408-2412.

10. Publications

Schrade K., Tröger J, Eldahshan A., Zühlke K., Abdul Azeez K., Elkins J., Neuenschwander M., Oder A., Elkewedi M., Jaksch S., Andrae K., *et al.* (2018). An AKAP-Lbc-RhoA interaction inhibitor promotes the translocation of aquaporin-2 to the plasma membrane of renal collecting duct principal cells. PLoS ONE 13(1): e0191423.

Elucidation of the function of the AKAP GSKIP, Retreat of the "Cardiovascular and Metabolic Disease Program" of the MDC and DKFZ, TransCard Helmholtz Research School, November 26 – 28, 2014, Neuruppin, Germany. *Poster Presentation.*

The relationship between cleft palate and the AKAP GSKIP. MDC-FMP Retreat, October 15 - 17, 2015, Bad Saarow, Germany. *Poster Presentation.*

The AKAP GSKIP acts a potential regulator of the actin severing protein, cofilin. Retreat of the "Cardiovascular and Metabolic Disease Program" of the MDC and DKFZ, TransCard Helmholtz Research School, September 18 – 21, 2016, Bad Saarow, Germany. *Poster Presentation.*

Elucidation of functions of the AKAP GSKIP, TransCard Wollenberger Seminar. April 16, 2018, Berlin, Germany. *Oral Presentation.*

Elucidation of functions of the AKAP GSKIP, Retreat Havelboot 2018. August 28, 2018, Rathenow, Germany. *Oral Presentation.*

Elucidation of functions of the AKAP GSKIP, MDC evaluation 2018. September 18, 2018, Berlin, Germany. *Poster Presentation.*
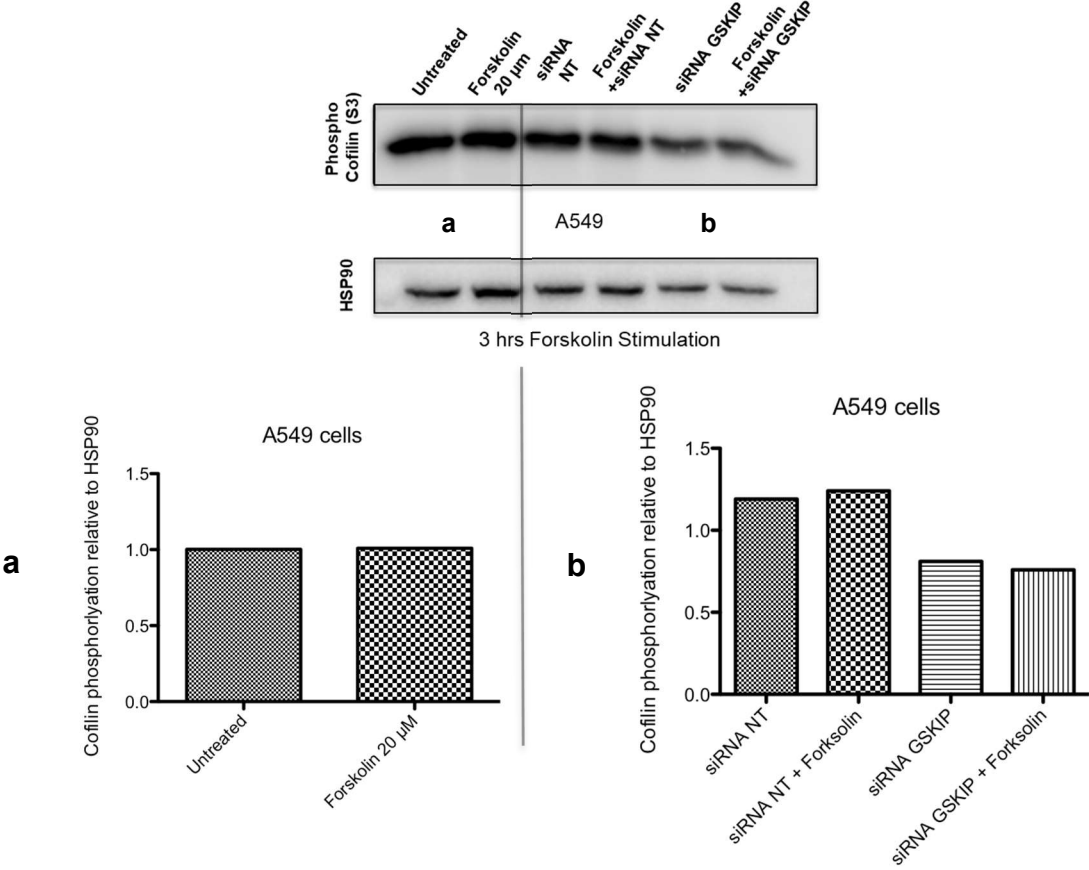
11. Supplementary Figures
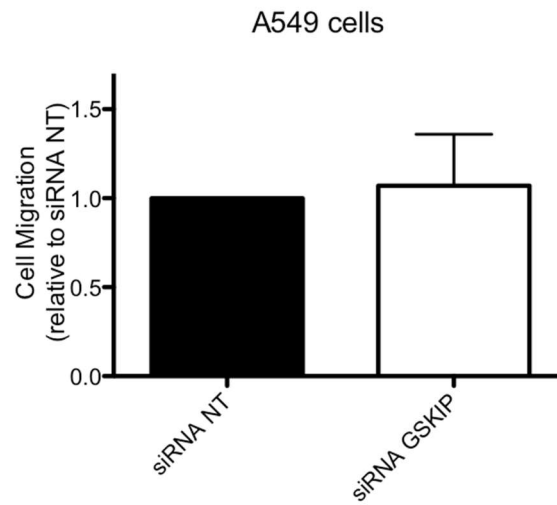
Supplementary figure 1 (S1). GSKIP KD does not alter the cellular migration in A549 cells. A549 cells were treated with siRNA to knock down the expression of GSKIP or with siRNA NT. The cellular migration was determined using the Transwell Migration Assay (section 3.2.1.7). Migration of the cells was determined relative to the NT control. n = 2, mean ± SEM.
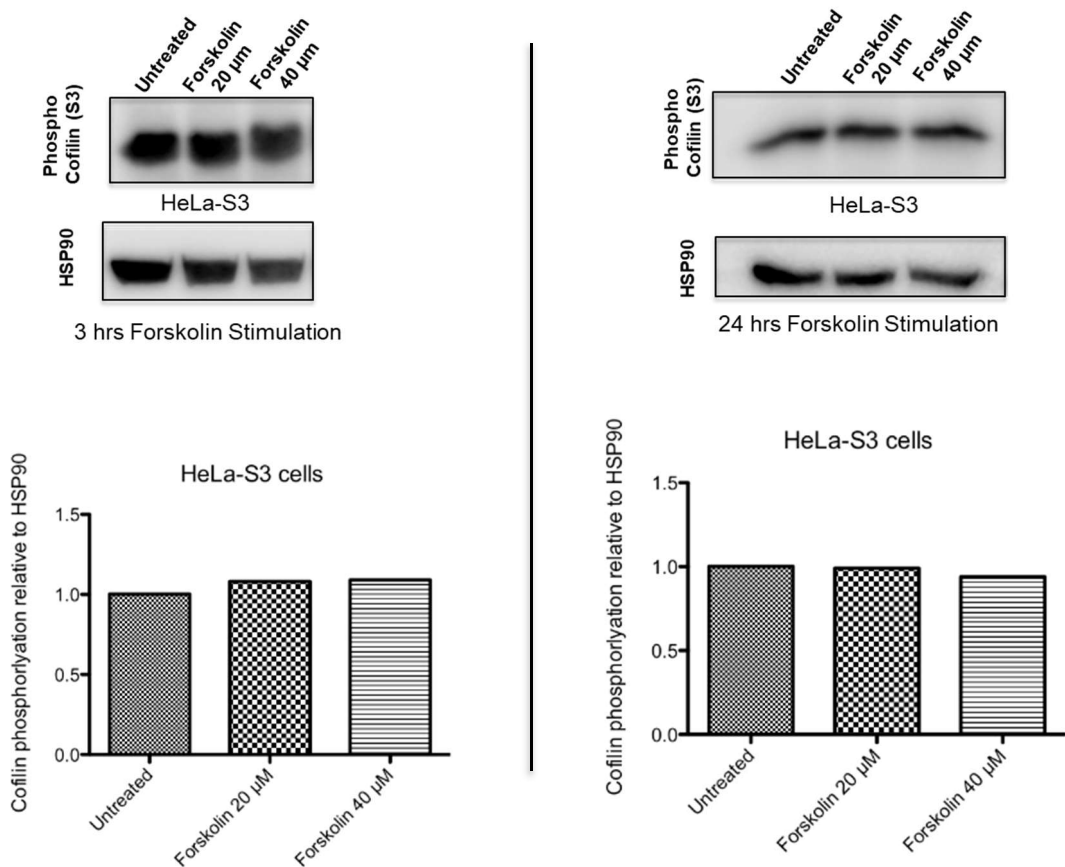
Supplementary figure 2 (S2). Forskolin stimulation does not alter CFL phosphorylation (S3) in HeLa-S3 cells. HeLa-S3 cells were treated with either 20 µM or 40 µM forskolin for 3 or 24 hrs. Phospho-CFL (S3) and HSP90 were detected by Western blotting. Signals were semi-quantitatively analysed by densitometry and the ratio of phospho-CFL to HSP90 calculated. n=1.

Supplementary figure 3 (S3). Forskolin stimulation does not alter CFL phosphorylation (S3) in A549 cells. S3 (a): A549 cells were treated with 20 µM for 3 hrs. Phospho-CFL (S3) and HSP90 were detected by Western blotting. Signals were semi-quantitatively analysed by densitometry and the ratio of phospho-CFL to HSP90 calculated. S3 (b): A549 cells were treated with siRNA to knock down the expression of GSKIP or with siRNA NT. 48 hrs post transfection, the cells were stimulated with 20 µM for 3 hrs. Phospho-CFL (S3) and HSP90 were detected by Western blotting. Signals were semi-quantitatively analysed by densitometry and the ratio of phospho-CFL to HSP90 calculated. n=1.
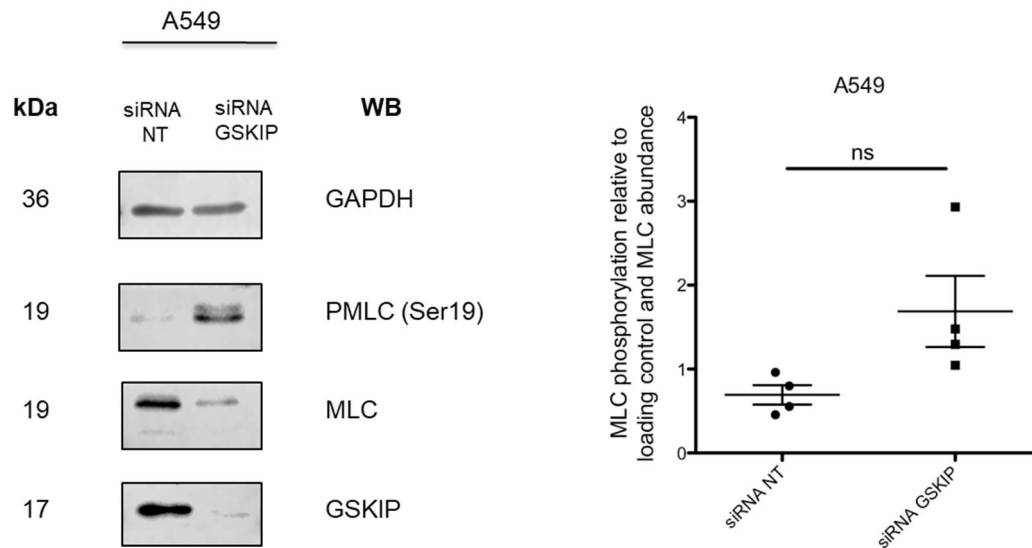
Supplementary figure 4 (S4). GSKIP KD does not modulate the mono-phosphorylation of MLC at serine 19 in A549 cells. A549 cells were treated with siRNA to knock down the expression of GSKIP or with siRNA NT. MLC, phospho-MLC (S19), and GAPDH were detected by Western blotting. Signals were semi-quantitatively analysed by densitometry and the ratio of phospho-MLC to normalised MLC calculated. n = 4, mean ± SEM, Paired T-test, *p < 0.05